Space-Time Diversity for CDMA Systems over Frequency-Selective Fading Channels

Ayman M. Assra

A Thesis

in

The Department

of

Eletrical and Computer Engineering

Presented in Partial Fulfillment of the Requirements
for the Degree of Doctor of Philosophy at
Concordia University
Montreal, Quebec, Canada

March 2010

Your file Votre référence
ISBN: 978-0-494-67325-6
Our file Notre référence
ISBN: 978-0-494-67325-6

Abstract

Space-Time Diversity for CDMA Systems over Frequency-Selective Fading Channels

Ayman M. Assra, PhD

Concordia University, 2010

Supporting the expected high data rates required by wireless Internet and high-speed multimedia services is one of the basic requirements in broadband mobile wireless systems. However, the achievable capacity and data rate of wireless communication systems are limited by the time-varying nature of the channel. Efficient techniques for combating the time-varying effects of wireless channels can be achieved by utilizing different forms of diversity. In recent years, transmit diversity based on space-time coding (STC) has received more attention as an effective technique for combating fading. On the other hand, most existing space-time diversity techniques have been developed for flat-fading channels. Given the fact that wireless channels are generally frequency-selective, in this thesis, we aim to investigate the performance of space-time diversity schemes for wideband code-division multiple-access (WCDMA) systems over frequency-selective fading channels. The proposed receiver in this case is a rake-type receiver, which exploits the path diversity inherent to multipath propagation. Then, a decorrelator detector is used to mitigate the multiple access interference (MAI) and the known near-far problem. We derive the bit error rate (BER) expression over frequency-selective fading channels considering both the fast and slow fading cases. Finally, we show that our proposed receiver achieves the full system diversity through simulation and analytical results.

Most of the work conducted in this area considers perfect knowledge of the channel at the receiver. Hence, channel identification brings significant challenges to multiple-input multiple-output (MIMO) CDMA systems. In light of this, we propose a channel estimation and data detection scheme based on the superimposed training-based approach. The proposed scheme enhances the performance by eliminating the MAI from both the channel and data estimates by employing two decorrelators; channel and data decorrelators. The performance of the proposed estimation technique is investigated over frequency-selective slow fading channels where we derived a closed-form expression for the BER as a function of the number of users, K, the number resolvable paths, L, and the number of receive antennas, V. Finally, our proposed scheme is shown to be more robust to channel estimation errors. Furthermore, both the analytical and simulation results indicate that the full system diversity is achieved.

Considering that training estimation techniques suffer either from low spectral efficiency (i.e., conventional training approach) or from high pilot power consumption (i.e., superimposed training-based approach), in the last part of the thesis, we present an iterative joint detection and estimation (JDE) using the expectation-maximization (EM) algorithm for MIMO CDMA systems over frequency-selective fading channels. We also derive a closed-form expression for the optimized weight coefficients of the EM algorithm, which was shown to provide significant performance enhancement relative to the conventional equal-weight EM-based signal decomposition. Finally, our simulation results illustrate that the proposed receiver achieves near-optimum performance with modest complexity using very few training symbols.

Acknowledgments

I owe my gratitude to all the people who have made this thesis possible and because of whom my graduate experience has been one that I will cherish forever.

First and foremost I would like to thank my advisors, Dr. Walaa Hamouda and Dr. Amr Youssef, for giving me an invaluable opportunity to work on challenging and extremely interesting research over the past four years. Without their broad visions and deep insights, valuable advices and strong encouragements, this thesis would have been a distant dream.

I would like also to express my thanks to Dr. M. Reza Soleymani, Dr. Yousef R. Shayan, and Dr. Ibrahim G. Hassan for agreeing to serve on my thesis committee and for sparing their invaluable time reviewing the manuscript.

Also, my most heartfelt gratitude to my beloved parents for their unfailing love and supports throughout the entire journey of this research study. " Dad and Mum, you are the best gift that I have from God". I am very grateful to my sister, Dalia, for believing in me. Her encouragement and support have made my life a lot more meaningful, colorful and joyful.

Finally, I would like to thank my big brother, Ehab, and my best friends: Ahmed Hassan, Karim Lotfy, Mabruk Gheryani, Faisal, and Sofian.

AYMAN M. ASSRA

To my parents for their love and patience

Contents

Abstract iii

Acknowledgments v

List of Figures xi

List of Acronyms xiv

List of Symbols xvi

Chapter 1 Introduction 1

1.1 An Overview of MIMO Systems 2

1.2 Motivation 4

1.3 Thesis Contributions 6

1.4 Outline of the Thesis 7

Chapter 2 Literature Review 9

2.1 Transmit Diversity for Wideband CDMA (WCDMA) Systems 10

2.2 Channel Modeling 12

2.2.1 Multipath Propagation 12

2.2.2 Doppler Shift 13

2.2.3 Fading Channels 14

2.3 Channel Estimation Techniques 16
2.3.1 Training-Based Channel Estimation 18
2.3.2 Blind Channel Estimation 19
2.3.3 Semi-blind Channel Estimation 21
2.3.4 Iterative joint channel estimation and data detection 22
2.4 Channel Estimation For MIMO CDMA systems 24
2.5 Conclusions 25

Chapter 3 Performance Analysis of Space-Time Diversity in CDMA Systems **26**

3.1 Introduction 26
3.2 Multiuser System Model 27
3.3 Performance Analysis 32
3.3.1 Fast Fading 33
3.3.2 Slow Fading 37
3.4 Probability of Bit Error 38
3.5 Numerical and Simulation Results 40
3.6 Conclusions 43

Chapter 4 A Channel Estimation and Data Detection Scheme for Multiuser MIMO-CDMA Systems in Fading Channels **45**

4.1 Introduction 45
4.2 System Model 46
4.3 Channel Estimation 49
4.4 Data Detection 52
4.5 Performance Analysis 56
4.5.1 BER Analysis 57
4.5.2 Asymptotic Performance and Diversity 64

4.6 Simulation Results 66
4.7 Conclusions 69

Chapter 5 EM-Based Joint Channel Estimation and Data Detection for MIMO-CDMA Systems **73**

5.1 Introduction 73
5.2 System Model 74
5.3 EM-Based ST Receiver 76
5.4 EM Optimized Weights and Initialization 82
5.4.1 Optimized Weights (β_k^v) 83
5.4.2 EM Initialization 90
5.5 Cramér-Rao Lower Bound (CRLB) on Channel Estimates 91
5.6 Simulation Results 93
5.7 Conclusions 97

Chapter 6 Conclusions and Future Works **99**

6.1 Summary and Conclusions 99
6.2 Future Works 101

Appendix A **102**

A.1 Definition of Pilot and Data Code Matrices 102
A.2 Covariance Matrix of $\mathbf{X}^v$ 105
A.3 Coefficient Matrices $\mathbf{S}_1$ and $\mathbf{S}_2$ 106

Appendix B **109**

B.1 Estimation of $\mathcal{Q}_k(\mathbf{b}_k|\mathbf{b}^i)$ 109
B.2 Derivation of $E\left[\| E_g \|^2\right]$ 115
B.3 Distribution of $\mathbf{h}^v|\mathbf{y}_w, \mathbf{b}^i$: 119
B.4 Consistency of Channel Estimates 122

Bibliography 124

List of Figures

2.1 STS scheme [16]. 10

3.1 Received signal for K-user system considering single receive antenna. . . . 28

3.2 Multiuser receiver structure in case of single receive antenna. 30

3.3 BER performance for asynchronous DS-CDMA systems with two transmit and one receive antenna over frequency-selective fast fading channels with L=2 paths. 41

3.4 BER performance for a 3-user system as a function of the number of paths, L=2,3, over frequency-selective fast fading channels. 42

3.5 BER performance for a multiuser system with two transmit and two receive antennas over frequency-selective fast fading channels with L=2 paths. . . 43

3.6 BER performance for asynchronous DS-CDMA systems with two transmit and one receive antenna over frequency-selective slow fading channels with $L = 2$ paths. 44

4.1 Block diagram of pilot-sequence-assisted STS transmission system corresponding to a single receive antenna. 46

4.2 Asynchronous transmission of K code sequences, each has a period $T_s = 2N$ chips, over frequency selective fading channel with L resolvable paths. The estimation interval is $T_s + \tau_K + (L-1)T_c$. 47

4.3 The indented contour C. 60

4.4 Asymptotic nonzero eigenvalues of 5-user STS system with L=2,3 paths, two antennas at the transmitter and one antenna at the receiver side. . . 66

4.5 Comparison between different channel estimation and data detection techniques for the 5-user STS system with L=2 paths, PNR=5dB, two antennas at the transmitter and one antenna at the receiver side. 67

4.6 Effect of different PNR values on the BER performance of the proposed estimation technique for a 5-user STS system with L=2 paths, two antennas at the transmitter and one antenna at the receiver side. 69

4.7 BER performance of the proposed estimation technique for a 5-user STS system with L=3 paths and PNR=5dB, two antennas at the transmitter and one antenna at the receiver side. 70

4.8 BER performance of the proposed estimation technique for the multiuser STS system with L=2 paths and PNR=5dB. The STS system employs two transmit antennas and V=3 antennas at the receiver side. 71

4.9 BER performance of the proposed system considering different channel delay profiles. The STS system employs two transmit and one receive antenna with L= 2 paths and PNR=5dB. 72

5.1 ST JDE receiver based on the EM algorithm. 83

5.2 The behavior of the optimized weight coefficients for 2-user STS system assuming AWGN channel. 90

5.3 BER performance of the first user considering ST EM-JDE receiver with two transmit and one receive antenna over frequency-selective fading channels. The channel coefficients are assumed unknown at the receiver (M = 40, p'=8, L = 2, 2-iteration). 94

5.4 BER performance of the first user considering ST EM-JDE receiver with V=2 receive antennas, $M = 40, p' = 8, L = 2$, 2 iterations. 95

5.5 BER behavior of the first user as a function of the MAI level with V=1 receive antenna over frequency-selective fading channels, $M = 40, p' = 8, L = 2, \gamma_1$=15dB. 96

5.6 BER behavior of the first user as a function of the MAI level for V=2 receive antennas over flat fading channels, $M = 20, p' = 1, L = 1, \gamma_1$=8dB. 97

5.7 MSE of channel estimates in MIMO CDMA system with V=2 receive antennas considering flat fading channel, $M = 20, p' = 1$,2 iterations. 98

List of Acronyms

AWGN	additive white Gaussian noise
BER	bit error rate
BPSK	binary phase-shift keying
CDMA	code-division multiple-access
CRLB	Cramér-Rao Lower Bound
CSI	channel state information
DS	direct sequence
EM	expectation-maximization
ICI	interchip interference
ISI	intersymbol interference
JDE	joint detection and estimation
MIMO	multiple-input multiple-output
MAI	multiple access interference
ML	Maximum-Likelihood
MMSE	minimum mean-square error
MRC	maximal-ratio-combiner
MIP	multipath intensity profile
MVUE	minimum variance unbiased estimators
MSE	mean-square error
pdf	probability density function

PIC	parallel interference cancellation
rms	root mean-square
SISO	single-input single-output
STC	space-time coding
SIC	successive interference cancellation
STTC	space-time trellis coding
STBC	space-time block coding
STS	space-time spreading
SNR	signal to noise ratio
SIMO	single-input multiple-output
ST-block	space-time-block
SU	single-user
WCDMA	Wideband CDMA
3G	third-generation

List of Symbols

b_1	odd data symbol
b_2	even data symbol
$\boldsymbol{t_q}$	STS signal transmitted from the q^{th} transmit antenna
$\mathcal{P}$	processing gain
$\boldsymbol{c}$	unit-norm spreading sequence with processing gain $\mathcal{P}$
$\boldsymbol{c_q}$	q^{th} data spreading sequence with processing gain $2\mathcal{P}$
h_q	complex channel coefficient from the q^{th} transmit antenna to the receive antenna
d_q	received signal after despreading with $\boldsymbol{c_q}$
H	Hermitian transpose
$\boldsymbol{d}$	despreader output vector
$\boldsymbol{\mathcal{H}}$	channel matrix of STS system with two transmit and one receive antenna
$\boldsymbol{b}$	data vector
$\boldsymbol{h_q}$	qth column of the channel matrix $\boldsymbol{\mathcal{H}}$
$Re\{\cdot\}$	real part
f_c	carrier frequency
θ	incident angle
f_d	Doppler shift

u'	vehicle speed
c	speed of light
f_{dmax}	maximum Doppler shift
$\phi_d(f')$	Doppler power spectrum of the channel
B_d	Doppler spread of the channel
Δt_c	coherence time of the channel
$f(a)$	probability density function of Rayleigh distribution
m_a	mean value of Rayleigh distributed random variable
σ_a^2	variance of Rayleigh distributed random variable
L	Number of resolvable paths
$h(t;\tau)$	time-variant impulse response at time t to an impulse applied at time $t-\tau$
$\tilde{\tau}_l$	time delay of the l^{th} path
$h^{t,l}$	complex amplitude of the l^{th} path
$\delta(\cdot)$	Delta function
$\phi'_h(\Delta t;\tilde{\tau}_i,\tilde{\tau}_j)$	autocorrelation function of $h(t;\tau)$
$E[\cdot]$	Expectation
$\phi'_h(\tilde{\tau}_i)$	average channel output power
$P'(\tilde{\tau}_l)$	power delay profile of the channel
τ_{rms}	root mean-square delay spread of the channel
$b[m]$	m^{th} information symbol
R_s	number of received samples per symbol duration
$\bar{r}[m']$	sampled received vector during the m'^{th} symbol duration
$\bar{h}[m]$	sampled channel fading vector during the m^{th} symbol duration
$\mathcal{N}$	length of channel estimation interval
$\bar{r}$	received signal vector within the channel estimation interval

$\Omega(\bar{b})$	data symbol matrix within the estimation interval
I_{R_s}	$R_s \times R_s$ identity matrix
$\bar{h}$	channel parameter vector
$\hat{\bar{h}}$	estimated channel parameter vector
$\dagger$	pseudo-inverse
$f(\bar{r};\bar{h})$	likelihood function of the unknown parameter $\bar{h}$
$f(\bar{r}\|\bar{b};\bar{h})$	likelihood function when $\bar{b}$ is known
$f(\bar{b})$	marginal probability density function of $\bar{b}$
$\hat{\bar{b}}$	estimated data vector
$\mathcal{T}(\bar{h})$	filtering matrix
$Pr(\bar{h})$	projection transform of $\bar{r}$ into the noise subspace of the observation
$\mathcal{B}$	vector-valued parameter to be estimated
$\mathcal{Y}$	vector-valued observation
$\hat{\mathcal{B}}$	ML estimate of $\mathcal{B}$
$\mathcal{X}$	complete unobservable data
$\Phi(\mathcal{X}\|\mathcal{B})$	complete log-likelihood function
$\mathcal{B}^i$	EM estimate of $\mathcal{B}$ at the i^{th} iteration
$\mathcal{Q}(\mathcal{B}\|\mathcal{B}^i)$	conditional expectation of $\Phi(\mathcal{X}\|\mathcal{B})$ given $\mathcal{Y}$ and $\mathcal{B}^i$
V	number of receive antennas
$r^v(t)$	received complex low-pass equivalent signal at the v^{th} receive antenna
b_1^k	odd data bit of the k^{th} user
b_2^k	even data bit of the k^{th} user
$c_q^k(t)$	q^{th} data spreading code of the k^{th} user
E_s	received signal energy
T_b	bit period
T_c	chip period

τ_k	transmit delay of the k^{th} user
$h_{ql,v}^{k,t}$	fading channel coefficient of the k^{th} user, l^{th} path from the q^{th} transmit antenna to the v^{th} receive antenna at time t
$h_{ql,v}^{k,t+T_b}$	fading channel coefficient of the k^{th} user, l^{th} path from the q^{th} transmit antenna to the v^{th} receive antenna at time $t+T_b$
σ_n^2	noise variance
$n^v(t)$	Gaussian with zero mean and variance σ_n^2
P	space-time block code interval
Nc($\mathbf{0}$,$\boldsymbol{V}$)	zero mean complex Gaussian vector with covariance matrix $\boldsymbol{V}$
K	number of users
$\boldsymbol{Y}_v$	matched filter output vector at the v^{th} receive antenna
$\boldsymbol{R}$	cross-correlation matrix
$\boldsymbol{N}_v$	Gaussian noise at the v^{th} matched filter bank
$\boldsymbol{U}_v$	faded data vector transmitted by the K-user system at the v^{th} receive antenna
D	diversity order
$\boldsymbol{Z}_v$	decorrelator output vector at the v^{th} receive antenna
T	transpose
$\hat{b}_q^k$	decision variable of the q^{th} bit transmitted by the k^{th} user
$Q(x)$	Gaussian Q-function
$\sigma_{\tilde{x}}^2$	variance of noise term in $\hat{x}_q^k$
α	siganl to interfernce and noise ratio
$\phi_{A,B}(\omega_1,\omega_2)$	joint characteristic function of A and B
$f_{A,B}$	joint probability density function of A and B

f_α	probability density function of the output SNR of the decorrelator detector
$M(.,.,.)$	WhittakerM function
${}_1F_1(.;.;.)$	confluent hypergeometric function
P_b	average probability of bit error
${}_2F_1(.,.;.;.)$	special case of the generalized hypergeometric function
$\overline{\gamma}$	average received SNR
U	number of transmit antennas
ρ_p	pilot signal to noise ratio
ρ_d	data signal to noise ratio
M	number of symbols in each transmitted data block
T_s	symbol duration
$P_{k1}(t)$	first pilot sequence of the k^{th} user
$P_{k2}(t)$	second pilot sequence of the k^{th} user
$c_{k1}(t)$	first data sequence of the k^{th} user
$c_{k2}(t)$	second data sequence of the k^{th} user
N	coding gain
$b_{k1}[m]$	odd bit of the k^{th} user within the m^{th} symbol duration
$b_{k2}[m]$	even bit of the k^{th} user within the m^{th} symbol duration
$h_{ql}^{k,v}$	the channel coefficient corresponding to the k^{th} user, l^{th} path from the q^{th} transmit antenna to v^{th} receive antenna
σ_h^2	variance of channel coefficient
τ_{max}	maximum user delay
$\mathbf{y}^v[0]$	chip matched filter output vector at the v^{th} receive antenna within the channel estimation interval
$\mathbf{H}^v$	channel impulse response of the K-user system at the v^{th} receive antenna

$\mathbf{C}[0]$	code matrix of the K users corresponding to the current received symbols within the observation interval
$\mathbf{C}_k[0]$	pilot and data code sequences of user k associated with the current STS symbol within the observation window
$\mathbf{C}[1]$	code matrix of the K users corresponding to the following received symbols within the observation interval
$\mathbf{C}_k[1]$	pilot and data code sequences of user k associated with the following STS symbol within the observation window
$\mathbf{b}[m]$	transmitted data vector of K-user system during the m^{th} symbol duration
$\mathbf{b}_k[m]$	transmitted data vector by the k^{th} users during the m^{th} symbol duration
$\mathbf{C}_p$	pilot-data code matrix during the observation interval
$\mathbf{b}$	data vector of the K-user system within the observation interval
$\otimes$	*Kronecker product* operation
$\mathbf{y}_c^v[0]$	channel despreader output at the v^{th} receive antenna
$\mathbf{R}_p$	pilot-data cross-correlation matrix
$\mathbf{N}_{cc}^v[0]$	noise at the channel despreader output of the v^{th} receive antenna
$\mathbf{y}_d^v[0]$	channel decorrelator output at the v^{th} receive antenna
$\mathbf{N}_{cd}^v[0]$	noise at the channel decorrelator output of the v^{th} receive antenna
$O(\cdot)$	big O notation
$\hat{h}_{ql}^{k,v}$	estimated channel coefficient of the k^{th} user, l^{th} path from the q^{th} transmit antenna to the v^{th} receive antenna
$e_{ql}^{k,v}$	channel estimation error of the k^{th} user, l^{th} path from the q^{th} transmit antenna to the v^{th} receive antenna

$\mathbf{g}^{v}[m]$ data chip-matched filter output at the v^{th} receive antenna during the m^{th} symbol interval

$\mathbf{C}'[0]$ data matrix corresponding to the current STS symbols of the K-user system within the observation interval

$\mathbf{C}'[1]$ data matrix corresponding to the following STS symbols of the K-user system within the observation interval

$\mathbf{C}'[-1]$ data matrix corresponding to the previous STS symbols of the K-user system within the observation interval

$\mathbf{E}^{v'}$ channel estimation error vector of the K users at the v^{th} receive antenna

$\mathbf{E}_k^{v'}$ channel estimation error vector of the k^{th} user at the v^{th} receive antenna

$\mathbf{C}_d$ data code matrix during the data estimation interval

$\mathbf{H}_d^v$ channel impulse response of the K-user system at the v^{th} receive antenna during the data estimation interval

$\mathbf{g}_c^v[m]$ data matched filter output of the v^{th} receive antenna at the m^{th} symbol interval

$\mathbf{R}_d$ data cross-correlation matrix

$\mathbf{N}_{dc}^v[m]$ noise vector with $N_c(\mathbf{0}, \mathbf{R}_d)$

$\mathbf{g}_d^v[m]$ data decorrelator output of the v^{th} receive antenna at the m^{th} symbol interval

$\mathbf{N}_{dd}^v[m]$ noise vector with $N_c(\mathbf{0}, \mathbf{R}_d^{-H})$

$\hat{b}_{11}[m]$ estimated odd bit of the first user within the m^{th} symbol duration

$\hat{b}_{12}[m]$ estimated even bit of the first user within the m^{th} symbol duration

$\mathcal{Z}_1$ decision variable of $b_{11}[m]$ when $b_{12}[m] = +1$

$\mathcal{Z}_2$ decision variable of $b_{11}[m]$ when $b_{12}[m] = -1$

Z_{1v}	quadratic form related to the v^{th} receive antenna when $b_{12}[m] = +1$
Z_{2v}	quadratic form related to the v^{th} receive antenna when $b_{12}[m] = -1$
$\mathbf{S}_1$	coefficient matrix
$\mathbf{S}_2$	coefficient matrix
$\mathbf{X}^v$	vector includes the variables of Z_{1v} and Z_{2v}
$\mathbf{R}_x$	covariance matrix of $\mathbf{X}^v$
$\Phi_{Z_1}(\omega)$	characteristic function of Z_1
$\phi_{Z_{1v}}(\omega)$	characteristic function of Z_{1v}
$\{\lambda_n\}$	eigenvalues of $\mathbf{S}_1\mathbf{R}_x$
N'	number of eigenvalues of $\mathbf{S}_1\mathbf{R}_x$
n_1	number of negative eigenvalues of $\mathbf{S}_1\mathbf{R}_x$
f_{Z_1}	probability density function of Z_1
$Res(f(z), z_o)$	residue of $f(z)$ at the pole $z = z_o$
$\{\beta_n\}$	eigenvalues of $\mathbf{S}_2\mathbf{R}_x$
n_2	number of negative eigenvalues of $\mathbf{S}_2\mathbf{R}_x$
σ_{hl}^2	variance of the channel coefficient of the l^{th} path
σ_o^2	average power of the initial path
κ	normalized decay factor
E_k	k^{th} user transmit energy
σ_k^2	variance of attenuation coefficients of k^{th} user
$\mathbf{B}(m)$	data matrix of K-user STS system within the m^{th} period
$\mathbf{B}_k(m)$	data matrix of k^{th} user of STS system within the m^{th} period
$\mathbf{h}^v$	channel vector of K-user STS system at the v^{th} receive antenna

$\mathbf{h}_k^v$	channel vector of the k^{th} user of STS system at the v^{th} receive antenna
$\mathbf{R}[0]$	cross-correlation matrix of the codes corresponding to the current STS symbols
$\mathbf{R}[-1]$	cross-correlation matrix between the codes corresponding to the current STS symbols and the codes corresponding to the previous STS symbols
$\mathbf{R}[1]$	cross-correlation matrix between the codes corresponding to the current STS symbols and the codes corresponding to the following STS symbols
$\mathbf{n}_c^v[m]$	noise vector modelled as $N_c(\mathbf{0}, \mathbf{R}[0])$
$\mathbf{F}[0]$	lower triangular matrix
$\mathbf{F}[1]$	upper right triangular matrix with zero diagonal
$\mathbf{y}_w^v[m]$	output of the whitening filter of the v^{th} receive antenna during the m^{th} symbol interval
$\mathbf{n}_w^v[m]$	noise vector modelled as $N_c(\mathbf{0}, N_o\mathbf{I}_{2LK})$
$\mathbf{g}_k^v(m)$	contribution of the k^{th} user signal in $\mathbf{y}_w^v[m]$ during the m^{th} symbol interval
Δm	time delay
$\mathbf{F}_k[\Delta m]$	matrix including the $2L$ columns corresponding to the k^{th} user in $\mathbf{F}[\Delta m]$
β_k^v	optimized weight coefficient of the k^{th} user at the v^{th} receive antenna
$\mathbf{n}_{wk}^v[m]$	noise vector modelled as $N_c(\mathbf{0}, \beta_k^v N_o\mathbf{I}_{2LK})$
$\mathbf{y}_w$	output of the V whitening matched filters within a frame of M codes
$\mathbf{b}$	transmitted data bits from the K users within a frame of M codes

$\mathbf{G}$	complete data within a frame of M codewords
$\Phi(\mathbf{G}\|\mathbf{b})$	complete log-likelihood function
$\Phi(\mathbf{g}_k^v, \mathbf{h}_k^v\|\mathbf{b}_k)$	individual complete log-likelihood function
$\mathbf{R}_{kj}[0]$	cross-correlation between the codes of k^{th} and j^{th} user in $\mathbf{R}[0]$
$\mathbf{R}_{kj}[-1]$	cross-correlation between the codes of k^{th} and j^{th} user in $\mathbf{R}[-1]$
$\mathbf{b}^i$	EM data estimate at the i^{th} iteration
$\mathcal{Q}(\mathbf{b}\|\mathbf{b}^i)$	conditional expectation of $\Phi(\mathbf{G}\|\mathbf{b})$ given $\mathbf{y}_w$ and $\mathbf{b}^i$
$\mathcal{Q}_k(\mathbf{b}_k\|\mathbf{b}^i)$	conditional expectation of $\Phi(\mathbf{g}_k^v, \mathbf{h}_k^v\|\mathbf{b}_k)$ given $\mathbf{y}_w$ and $\mathbf{b}^i$
$\mathbf{h}$	channel vector of K-user STS system with V receive antennas
$\rho_{1,ll',m}^{kj^i}(m_p)$	coefficient defined in terms of the cross-correlation between the codes of k^{th} and j^{th} user, and the current and following data estimates
$\mathbf{y}_{c,k}^v[m]$	vector includes the outputs corresponding to the k^{th} user at the v^{th} despreader output
$(h_{ql}^{k,v})^i$	EM channel estimate of the k^{th} user, l^{th} path from the q^{th} transmit antenna to the v^{th} receive antenna at the i^{th} iteration
$\mathbf{\Omega}_{hh}^i$	error covariance matrix of the EM channel estimates at the i^{th} iteration
Σ_{hh}	covariance matrix of the channel coefficients of the K users STS system at the v^{th} receive antenna
Σ_{hk}	covariance matrix of the channel coefficients of the k^{th} user of STS system at the v^{th} receive antenna
$\|\cdot\|$	vector norm

E_g	error between the true signal vector, $\mathbf{g}_k^v(m_s)$, and its estimate $(\mathbf{g}_k^v(m_s))^i$, $m_s \in \{m, m+1\}$, after being projected on $\mathbf{F}_k[0]$ and $\mathbf{F}_k[1]$ respectively
$\mathbf{n}_{c,k}^v[m]$	noise vector of the k^{th} user at the v^{th} despreader output during the m^{th} symbol interval
$R_{kk,\zeta\zeta}[0]$	ζ^{th} diagonal element of $\mathbf{R}_{kk}[0]$
$r_{jj,m_p}(\zeta,\zeta)$	ζ^{th} diagonal element of $\mathbf{R}_{jj}[m_p]^T\mathbf{R}_{jj}[m_p]$
$P_{e_{jq}}^{v,i}$	probability of the error of the i^{th} iteration at the v^{th} receive antenna
$\mathbf{s}_1$	multipath code matrix
$\mathbf{s}_2$	multipath code matrix
$\mathbf{ch}_q$	multipath channel vector
γ_k	k^{th} user SNR
p'	length of training sequence
$\mathbf{z}_{p'}^v$	output of the v^{th} matched filter bank within a frame of p' codewords
$\mathbf{h}_{mmse}^v$	MMSE channel estimate vector at the v^{th} receive antenna
$\mathbf{z}^V$	output of the V matched filter banks within a frame of M codewords

Chapter 1

Introduction

With the rapid growth of mobile communication and mobile computing, wireless transmission technology has evolved intensively over the last two decades. Recently, there has been a tremendous growth in the market of mobile communication and Internet services. Future wireless systems are expected not only to provide broadband communication but also to provide a variety of high data rate multimedia services. In addition, they must operate reliably in different types of environments: urban, suburban, and rural; indoor and outdoor. In order to achieve the above objectives, very high capacity and more efficient use of the available frequency spectrum are the most dominant factors in the design of any wireless communication system. However, the physical limitations of the wireless channel pose a fundamental challenge for a reliable communication. These limitations , which take a form of multipath propagation loss, time variation of the channel characteristic, noise, and other interferences, reduce the wireless channel into a 'narrow pipe', which does not easily accommodate wideband data transmission over traditional single-input single-output (SISO) wireless communication systems.

Recent research in multiple-input multiple-output (MIMO) systems has provided significant technical breakthroughs in the feasibility of high data rate wireless systems. Together with intelligent space-time signal processing and detection techniques, MIMO sys-

tems achieve higher capacity and higher spectral efficiency compared to conventional communication systems. With MIMO technology, the data rates provided by third-generation (3G) mobile wireless networks can be potentially increased from the current 2Mbit/sec up to 14.4Mbits/sec and higher [1]. Furthermore, MIMO systems can achieve higher spectral efficiencies of 20 - 40 bits/sec/Hz compared to SISO ones, where only around of 1-5 bits/sec/Hz is achieved [2].

1.1 An Overview of MIMO Systems

A good introduction to MIMO systems can be found in [3]. In short, MIMO systems achieve enormous gains in spectral efficiency and system capacity by multiple parallel transmissions of space-time signals using the same frequency band and careful exploitation of the multipath information, which is induced by the rich scattering MIMO wireless channels [1],[4]. Furthermore, the effective transmission rate of MIMO systems is increased linearly proportional to the smaller of the number of transmit and receive antennas [5],[6].

The original approach to using MIMO was proposed by Foschini *et al.* and is known as the Bell Laboratories Layered Space Time Architecture (BLAST) [7]. Together with Vertical-BLAST (VBLAST) [8], a simplified version of BLAST, such schemes are designed to maximize the system throughput. Specifically they seek to improve the spectral efficiency by transmitting independent signals from multiple transmit antennas. A BLAST scheme typically relies on successive interference cancellation (SIC) [7] at the receiver to detect the signals. In doing so, however, it loses diversity gain due to the interference cancellation process. Moreover the scheme requires at least the same number of receive antennas as transmit antennas. This constraint is relaxed by proposing a new approach, known as space-time coding (STC), that uses multiple transmit antennas and optionally multiple receive antennas [9]−[12]. One form of STC is known as space-time trellis coding

(STTC) [9] and it is shown to achieve maximum diversity gain at the expense of increased complexity of optimal decoding at the receiver. To reduce this decoding complexity, sub-optimal approaches have been developed including multistage decoding [9] and antenna partitioning [13]. A second class of STC, known as space-time block coding (STBC), has also been introduced in [10],[12] to overcome the computational complexity of STTC. It is known that, for the same number of transmit and receive antennas, both STTC and STBC normally achieve the same spatial diversity. However, despite the low complexity they offer, STBCs do not offer any coding gain [11],[14].

While code-division multiple-access (CDMA) is considered as one of the generic multiple-access schemes in the second and third generation wireless systems [15], CDMA systems have fundamental difficulties when utilized in wideband wireless communications. As the system bandwidth increases, there are more resolvable paths with different delays. Hence, the received CDMA signals suffer from interchip interference (ICI), which causes significant cross-correlation among users signature waveforms. In other words, the multi-path fading and multi-access interference (MAI) induced by the wideband transmissions degrades the overall system throughput. Therefore, the integration of CDMA with MIMO techniques, forming space-time spreading (STS) systems, has become an active area of research. One of the first STS systems was introduced in [16], where the proposed scheme is shown to achieve full spatial diversity and maintain high spectral efficiency without any wastage of system resources. Given these advantages it has become a strong candidate for next-generation wireless networks, where it has been considered as part of the IS-2000 wideband CDMA standard [17]. The success of MIMO CDMA systems is also dependent on the channel characteristics and in particular the perfect knowledge of the channel state information (CSI). Furthermore, STC systems are sensitive to the channel matrix properties. Consequently, current research works in MIMO CDMA are focused on channel modeling and development of efficient channel estimation techniques.

1.2 Motivation

In wireless communications, fading is a major obstacle towards achieving higher data rates and reliable communications. Diversity is a known technique to combat fading effects [18] by providing multiple copies of the transmitted signal over several frequency slots (frequency diversity), different time slots (temporal diversity), or multiple antennas (spatial diversity). Thus, the probability that all copies simultaneously encounter severe attenuation is reduced.

In MIMO CDMA systems, the overall system performance is enhanced by achieving spatial diversity gain. However, considering wideband transmission, the multipath signals violate the orthogonal property of the codes assigned to different users. Consequently, the MAI caused by the non-zero cross-correlation among different spreading codes results in a severe degradation in the diversity gain provided by the MIMO transmission [19]. To that end, multiuser detection techniques have been proposed to eliminate the effect of MAI, and thus improving the system performance [20]. As the use of optimum maximum likelihood (ML) detection is impractical due to the large computational complexity, which grows exponentially with the number of users and antennas, several suboptimal detection schemes have been developed, e.g., decorrelator and minimum mean-square error (MMSE) receivers [15]. Most of the works conducted in this area assume perfect channel estimation, and relatively few researchers have investigated the effect of channel estimation errors and possible estimation techniques.

In MIMO CDMA systems, channel estimation plays a crucial role on determining the system performance (e.g., [21]−[25] and references therein). In order to achieve the promised performance gain of MIMO systems, the channel coefficients must be known or estimated perfectly at the receiver [5]. Commonly used channel estimation techniques either reduce the effective data rate as in training-based channel estimation [19],[21], or increase the computational complexity of the system as in blind-based channel estimation techniques [26]−[28]. The former channel estimation is performed by periodically inserting

known training bits among the data frames, where in the latter, channel estimation is implemented by exploiting the statistical characteristics of the transmitted signals. As a remedy to the poor spectral efficiency of the conventional training approach, superimposed training-based techniques [22] have been considered where a distinct training sequence is added to the data sequence. This estimation technique is known to offer relatively large bandwidth utilization [29]. Also, as a solution to the complexity problem of blind systems, one can employ semi-blind channel estimation techniques. In this case, the channel estimation is carried out not only using unknown data but also through the observation corresponding to known training sequence [23].

Recently, there has been an increasing interest in iterative joint channel estimation and data detection techniques [30], [31]. These iterative receivers have shown enhanced performance with reasonable convergence rates using very short training sequences. Among these iterative techniques, the expectation-maximization (EM) [32] has been considered for its attractive features. The EM algorithm has the advantage of attaining the ML solution iteratively with reduced complexity [33]. In the past, an extensive effort has been focused on employing the EM algorithm in joint detection and estimation (JDE) techniques for SISO systems [34]−[37]. Recently, there has been an interest in applying the EM algorithm in MIMO systems. For example, Cozzo and Hughes [38] have proposed a JDE technique based on the EM algorithm in flat fading channels with multiple antennas at both the transmitter and receiver. Chun and Ching [31] have also proposed an iterative receiver for a space-time trellis coded system in frequency-selective fading channels, where channel estimation and data detection are performed using the EM algorithm.

In this thesis, we investigate the performance of MIMO CDMA systems over frequency-selective fading channels. Given the wideband nature of CDMA, in this thesis, we present a design for a space-time detection scheme for MIMO CDMA, which is capable of mitigating the effect of MAI as well as exploiting the diversity gain provided by STC. In this part, we study the performance of MIMO CDMA in fast fading channels, where

we assume that the CSI is available at the receiver side. Later, we investigate the effect of channel estimation error on the system performance. In addition, we devise possible approaches to the problem of channel estimation in MIMO CDMA systems.

1.3 Thesis Contributions

The contribution of this thesis can be summarized as follows:

1. In Chapter 3, we investigate the performance of direct sequence (DS)-CDMA using STS over frequency-selective fading channels. Considering fast fading channels, we show that the received signal quality can be improved by utilizing the spatial and temporal diversities at the receiver side. We also study the problem of multiuser interference in asynchronous CDMA systems that employ transmit/receive diversity using STS. To overcome the effects of interference, a decorrelator detector is used at the base station. Considering binary phase-shift keying (BPSK) transmission, we analyze the system performance in terms of its probability of bit error. For the fast fading channel, both simulations and analytical results show that the full system diversity is achieved. On the other hand, when considering a slow fading channel, we show that the scheme reduces to conventional STS schemes where the diversity order is half of that of fast fading.

2. In Chapter 4, we examine the effect of channel estimation errors on the performance of MIMO CDMA systems. We propose a channel estimation and data detection scheme based on the superimposed training technique for STS systems. The proposed scheme enhances the performance of the STS system by eliminating the interference effect from both the channel and data estimates using two decorrelators. We investigate the performance of the proposed estimation technique considering an asynchronous CDMA uplink transmission over frequency-selective channels. Compared with other conventional estimation techniques, our results show that the

proposed estimation technique is more robust to channel estimation errors. Furthermore, both simulations and analytical results are provided, where they indicate that full system diversity is achieved.

3. In chapter 5, we present an iterative joint channel estimation and data detection technique based on the EM algorithm for MIMO CDMA systems over frequency-selective fading channels. We derive a closed-form expression for the optimized weight coefficients of the EM algorithm, which is shown to provide large performance improvement relative to the conventional equal weight EM-based signal decomposition. Our results show that the receiver can achieve near-optimum performance with modest complexity using very few training symbols. We also show that the proposed receiver attains the full system diversity through accurate channel estimates.

The above contributions have resulted in the list of publications in [39]−[46].

1.4 Outline of the Thesis

The rest of the thesis is organized as follows: Chapter 2 is an introductory chapter which provides some of the relevant fundamentals of MIMO CDMA systems. It begins with a description of the standard STS scheme employed in the thesis. Also, we present a survey on channel estimation techniques which can be implemented in MIMO CDMA systems. Finally, we present a literature review of existing works related to channel estimation and data detection for MIMO systems.

In Chapter 3, we introduce a space-time detection scheme based on the decorrelator detector of MIMO CDMA systems over frequency-selective fading channels. We analyze the proposed scheme considering slow and fast fading channels. In our analysis, we obtain the probability density function (pdf) of the signal to noise ratio (SNR) at the decorrelator output and after signal combining. This pdf is then used to evaluate the probability of bit error as a function of the system parameters for the two transmit and V receive antenna

configuration and a multipath channel with L resolvable paths.

In Chapter 4, we propose a channel estimation and data detection scheme based on the superimposed training technique for STS systems. We analyze the bit error rate (BER) performance of the proposed scheme with two transmit and V receive antenna configuration over frequency-selective channels. Our analytical results, supported by simulation results, show that the proposed scheme attains the full system diversity. We also derive an asymptotic form for the average BER in terms of the received signal parameters to provide further insights on the proposed system performance.

In chapter 5, we introduce an EM-based joint channel estimation and data detection for MIMO CDMA systems over frequency-selective fading channels. The proposed JDE receiver structure is derived, where we show that it can bring an optimum balance between the single-user matched filter detector and the parallel interference cancellation (PIC) based detector. A closed form of the optimum weight is derived based on MMSE criterion. We also prove that the estimator is asymptotically efficient where it converges to the Cramér-Rao lower bound (CRLB) at high SNR.

Chapter 6 provides a brief summary of the work accomplished throughout this thesis and some important conclusions. Recommendations for future areas of investigation related to this research are also presented.

Chapter 2

Literature Review

In our research, we study the performance of MIMO CDMA systems over frequency-selective fading channels. Our goal is to exploit the temporal and spatial diversity gains provided by the time-variant multipath fading channels. At the earlier stage of our research, we assumed a perfect knowledge of the channel at the receiver. Later on, we investigated the effect of imperfect channel estimation on the system performance and the implementation of joint channel and data estimation techniques for STS systems. Accordingly, in this chapter, we first discuss the basic concepts of STS systems. Then, we present a brief description of different channel models and possible channel estimation techniques. Finally, we present the recent works that are related to the above mentioned problems, which will be investigated in this thesis. Our objective is to make the reader aware of many considerations involved, highlight the particular scenarios that we study throughout the thesis, and encourage future work in the area.

2.1 Transmit Diversity for Wideband CDMA (WCDMA) Systems

In [16], a transmit diversity scheme known as STS, inspired by Alamouti scheme [12], was proposed. Considering a DS-CDMA system with two transmit and one receive antenna, the STS scheme can be summarized as follows: Assume b_1,b_2 are data symbols assigned to each user in two consecutive symbol intervals. Hence, the signal transmitted from the first antenna, according to Fig. 2.1, is given by

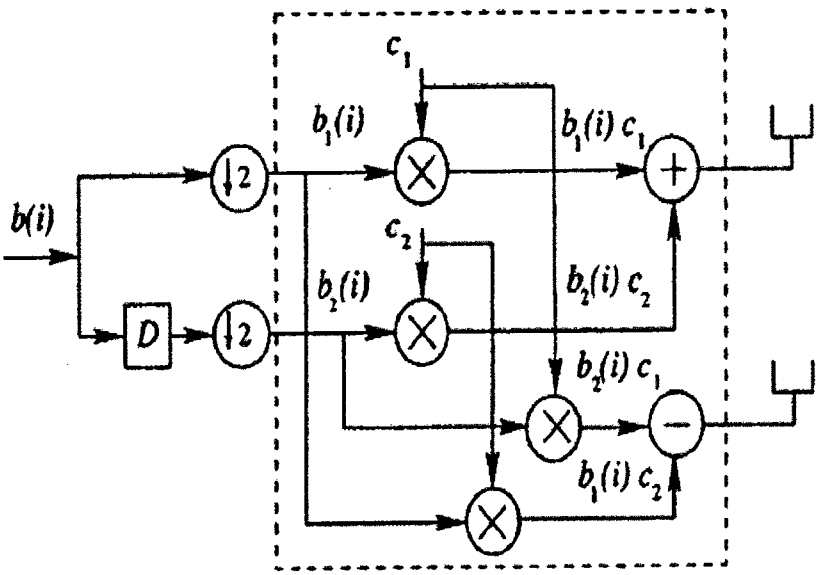

Figure 2.1: STS scheme [16].

$$t_1 = (1/\sqrt{2})(b_1c_1 + b_2c_2)$$

and the signal transmitted from the second antenna takes the form

$$t_2 = (1/\sqrt{2})(b_2c_1 - b_1c_2)$$

where

$$\boldsymbol{c}_1 = \begin{bmatrix} \boldsymbol{c} \\ \boldsymbol{0}_{\mathcal{P}\times 1} \end{bmatrix}, \quad \boldsymbol{c}_2 = \begin{bmatrix} \boldsymbol{0}_{\mathcal{P}\times 1} \\ \boldsymbol{c} \end{bmatrix},$$

and $\boldsymbol{c}$ is a unit-norm spreading sequence with processing gain $\mathcal{P}$. The vector $\boldsymbol{0}_{\mathcal{P}\times 1}$ represents a zero vector with $\mathcal{P}$-dimension. Hence, $\boldsymbol{c}_1$,$\boldsymbol{c}_2$ are orthogonal $2\mathcal{P} \times 1$ unit-norm spreading sequences. The received signals after despreading with $\boldsymbol{c}_1$ and $\boldsymbol{c}_2$ are then given respectively by

$$d_1 = (1/\sqrt{2})(h_1 b_1 + h_2 b_2) + \boldsymbol{c}_1^H \boldsymbol{n},$$

$$d_2 = (1/\sqrt{2})(-h_2 b_1 + h_1 b_2) + \boldsymbol{c}_2^H \boldsymbol{n},$$

where $h_q, q = 1, 2$, is the complex channel coefficient between the q^{th} transmit antenna and the receive antenna, and the superscript H denotes Hermitian transpose. $\boldsymbol{n}$ represents the received noise samples. Let $\boldsymbol{d} = [d_1\ d_2]^T$, then we have

$$\boldsymbol{d} = \frac{1}{\sqrt{2}} \mathcal{H} \boldsymbol{b} + \boldsymbol{\nu}' \tag{2.1}$$

where

$$\mathcal{H} = \begin{bmatrix} h_1 & h_2 \\ -h_2 & h_1 \end{bmatrix}, \ \boldsymbol{b} = \begin{bmatrix} b_1 \\ b_2 \end{bmatrix}, \ \boldsymbol{\nu}' = \begin{bmatrix} \boldsymbol{c}_1^H \boldsymbol{n} \\ \boldsymbol{c}_2^H \boldsymbol{n} \end{bmatrix}.$$

Let $\boldsymbol{h_q}$ denote the q^{th} column of $\mathcal{H}$, then by multiplying the vector $\boldsymbol{d}$ in (2.1) by $\boldsymbol{h_q}^H$, we have

$$Re\{\boldsymbol{h_q}^H \boldsymbol{d}\} = (1/\sqrt{2})(|h_1|^2 + |h_2|^2) b_q + Re\{\boldsymbol{h_q}^H \boldsymbol{\nu}'\} \tag{2.2}$$

where $Re\{\cdot\}$ denotes the real part of the enclosed argument. Eq. (2.2) shows a two-fold diversity gain. This transmit scheme is called STS since each user's data are spread in a different fashion on each transmit antenna. Recently, STS schemes have attracted research interests over CDMA systems [47], [48]. For example, the downlink performance of CDMA systems using the above STS scheme has been investigated in [16], where the channel is

modeled as either flat or frequency-selective Rayleigh-fading in the absence of multiuser interference. In [47], the performance of the proposed STS scheme has been investigated with various detection schemes for the case of independent flat-fading channels. Given the fact that STS was initially designed for slow fading channels, the system performance degrades when employed over fast time-variant channels [16]. In light of this, the authors in [49] introduced a DS-CDMA system that employs a STBC scheme over fast fading channels. In this scheme, orthogonal spreading codes are employed to exploit the time diversity introduced by the channel, and hence a two-fold of the diversity order obtained using the STS scheme in [16]. For the general multiuser case, the performance for both the decorrelator and the MMSE multiuser detectors was presented in [50], [51].

Most of the work done in STS systems assumes perfect knowledge of the channel at the receiver. Hence, channel identification brings significant challenges to STS systems. In what follows, we present a summary of the recent research development on channel modelling and channel estimation techniques. Then we introduce the research efforts for employing these techniques in MIMO CDMA systems.

2.2 Channel Modeling

For many real links such as radio, satellite and mobile channels, received signals experience fading [52], which severely degrades the system performance. In this part, we discuss the basic concepts of fading channel models.

2.2.1 Multipath Propagation

In a cellular mobile radio environment, the surrounding objects such as houses, buildings, or trees act as reflectors of radio waves. When a modulated signal is transmitted, multiple reflected waves of the transmitted signal will arrive at the receiving antenna from different directions with different propagation delays. These reflected waves are known

as multipath signals [53]. Due to the different arrival angles and times, the multipath signals at the receiver site have different phases. Thus, these signals may combine either in a constructive or a destructive way, depending on the random phases. The sum of these multipath components forms a spatially varying standing wave field. Hence, the mobile unit moving through the multipath field will receive a signal which can vary widely in amplitude and phase. On the other hand, when the mobile unit is stationary, the amplitude variations in the received signal are due to the movement of surrounding objects in the radio channel. The amplitude fluctuation of the received signal, known as signal fading, is caused by the time variant multipath characteristics of the channel [52].

2.2.2 Doppler Shift

Due to the relative motion between the transmitter and the receiver, transmitted waves are subject to a shift in frequency, a phenomena known as Doppler shift [53]. Consider a transmission of a single tone of frequency f_c and an arrival of one wave at the receiver, which has an incident angle θ with respect to the direction of the vehicle motion. Then, the Doppler shift of the received signal, denoted by f_d, is given by

$$f_d = \frac{u' f_c}{c} \cos\theta, \tag{2.3}$$

where u' is the vehicle speed and c is the speed of light. The Doppler shift in a multipath propagation environment spreads the bandwidth of the multipath waves within the range of $f_c \pm f_{dmax}$, where f_{dmax} is the maximum Doppler shift, given by $f_{dmax} = \frac{u' f_c}{c}$. f_{dmax} is also referred as the maximum fade rate. As a result, a transmission of single tone gives rise to a received signal with a spectrum of nonzero width. This phenomenon is known as frequency dispersion of the channel. Let $\phi_d(f')$ denote the Doppler power spectrum of the channel. The range of f' over which $\phi_d(f')$ is essentially nonzero is called the Doppler spread of the channel, $B_d = 2f_d$, and its reciprocal reflects the coherence time of the

channel, Δt_c. Clearly, a slowly fading channel has a large Δt_c or, equivalently, a small B_d.

2.2.3 Fading Channels

Because of the multiplicity of factors involved in propagation in a cellular mobile environment, it is convenient to apply statistical techniques to describe signal variations. In a narrowband system, the transmitted signals usually occupy a bandwidth smaller than the channel coherence bandwidth, which is defined as the frequency range over which the channel fading process is correlated. That is, all spectral components of the transmitted signal are subject to the same fading attenuation. This type of fading is referred to as frequency nonselective or frequency flat fading. On the other hand, if the transmitted signal bandwidth is greater than the channel coherence bandwidth, the spectral components of the transmitted signal with a frequency separation larger than the coherence bandwidth are faded independently. In this case, the received signal spectrum becomes distorted, since the relationships between various spectral components are not the same as in the transmitted signal. This phenomenon is known as frequency-selective fading [52]. In wideband systems, the transmitted signals usually undergo frequency-selective fading. In this section, we introduce a brief description of the Rayleigh fading model and frequency-selective fading channels.

Rayleigh Fading

We consider the transmission of a single tone with a constant amplitude. In a typical land mobile radio channel, we may assume that the direct wave is obstructed and the mobile unit receives only reflected waves. When the number of reflected waves is large, according to the central limit theorem, the two quadrature components of the received signal are uncorrelated Gaussian random processes with a zero mean and variance σ_s^2. As a result, the envelope of the received signal at any time instant follows a Rayleigh probability distribution and its phase follows a uniform distribution between $-\pi$ and π

[53]. The pdf of the Rayleigh distribution is given by

$$f(a) = \begin{cases} \frac{a}{\sigma_s^2} e^{-\frac{a^2}{2\sigma_s^2}}, & \text{a}\geq 0 \\ 0, & \text{a}<0. \end{cases} \tag{2.4}$$

The Rayleigh distributed random variable, a, has a mean value m_a and a variance σ_a^2, which are defined as follows

$$\begin{aligned} m_a &= \sqrt{\frac{\pi}{2}}\sigma_s \\ \sigma_a^2 &= \left(2 - \frac{\pi}{2}\right)\sigma_s^2. \end{aligned} \tag{2.5}$$

Frequency-Selective Fading

In a multipath fading channel with L paths, the time-variant impulse response at time t to an impulse applied at time $t - \tau$ is expressed as [53]

$$h(t;\tau) = \sum_{l=1}^{L} h^{t,l}\delta(\tau - \tilde{\tau}_l), \tag{2.6}$$

where $\tilde{\tau}_l$ and $h^{t,l}$ represent the time delay and the complex amplitude of the l^{th} path respectively. In (2.6), $\delta(\cdot)$ represents the delta function. Without loss of generality, we assume that $h(t;\tau)$ is wide-sense stationary, which means that the mean value of the channel random process is independent of time and the autocorrelation of the random process depends only on the time difference [53]. Then, $h^{t,l}$ can be modeled by narrowband complex Gaussian processes, which are independent for different paths. The autocorrelation function of $h(t;\tau)$ is given by

$$\phi_h'(\Delta t;\tilde{\tau}_i,\tilde{\tau}_j) = \frac{1}{2}E\left[h^*(t,\tilde{\tau}_i)h(t+\Delta t,\tilde{\tau}_j)\right], \tag{2.7}$$

where Δt denotes the observation time difference and * denotes complex conjugate. If we assume $\Delta t = 0$, the resulting autocorrelation function, denoted by $\phi'_h(\tilde{\tau}_i, \tilde{\tau}_j)$, is only function of the time delays $\tilde{\tau}_i$ and $\tilde{\tau}_j$. Due to the fact that scattering at two different paths is uncorrelated in most radio transmissions, we have

$$\phi'_h(\tilde{\tau}_i, \tilde{\tau}_j) = \phi'_h(\tilde{\tau}_i)\,\delta(\tilde{\tau}_i - \tilde{\tau}_j), \tag{2.8}$$

where $\phi'_h(\tilde{\tau}_i)$ represents the average channel output power , which is given by $\phi'_h(\tilde{\tau}_i) = \frac{1}{2}E[h^*(t,\tilde{\tau}_i)h(t,\tilde{\tau}_i)]$. We can further assume that the L different paths have the same normalized autocorrelation function, but different average powers. Let us denote the average power for the l^{th} path by $P'(\tilde{\tau}_l)$, then we have $P'(\tilde{\tau}_l) = \phi'_h(\tilde{\tau}_l)$. Let, $P'(\tilde{\tau}_l), l = 1, \ldots, L$, represent the power delay profile of the channel. The root mean-square (rms) delay spread of the channel, τ_{rms}, is defined as [54]

$$\tau_{rms} = \sqrt{\frac{\sum_{l=1}^{L} P'(\tilde{\tau}_l)\tilde{\tau}_l^2}{\sum_{l=1}^{L} P'(\tilde{\tau}_l)} - \left[\frac{\sum_{l=1}^{L} P'(\tilde{\tau}_l)\tilde{\tau}_l}{\sum_{l=1}^{L} P'(\tilde{\tau}_l)}\right]^2}. \tag{2.9}$$

In wireless communication environments, the channel power delay profile can be Gaussian, exponential or two-ray equal-gain [55]. For example, the two-ray equal-gain profile can be represented by

$$P'(\tau) = \frac{1}{2}\left(\delta(\tau) + \delta(\tau - 2\tau_{rms})\right), \tag{2.10}$$

where $2\tau_{rms}$ is the delay difference between the two paths.

2.3 Channel Estimation Techniques

In this section, we present a brief discussion of various channel estimators introduced in the literature. The propagation of signals through wireless channels results in the transmitted signal arriving at the receiver through multiple paths. This multipath propagation results in a received signal that is a superposition of several delayed and

scaled copies of the transmitted signal giving rise to signal fading. At the receiver, after processing (matched filtering, etc.), the continuous-time received signals are sampled at the baud (symbol) or higher rate before channel estimation takes place [53]. It is therefore convenient to work with a baseband-equivalent discrete-time channel model.

Let $b[m]$ denote the m^{th} information symbol, and $\bar{r}[m']$ be the received vector which groups R_s consecutive received samples during the m'^{th} symbol duration (sampling rate is typically a multiple, R_s, of baud rate). Considering slowly time-varying channel, the received signal vector $\bar{r}[m']$ can be expressed as [56]

$$\bar{r}[m'] = \sum_{m} \bar{h}[m]b[m' - m] + \bar{w}[m'], \tag{2.11}$$

where $\bar{h}[m]$ is $(R_s \times 1)$ channel response vector and $\bar{w}[m']$ represents the additive noise at the receiver. In (2.11), m is limited by the number of resolvable paths in the channel.

One of the objectives of receiver design is to minimize the detector error. In general, the design of the optimal detector requires the knowledge of the channel [20]. In this section, we consider four types of channel estimators based on the framework of maximizing the likelihood function: (i) training-based channel estimation [22]; (ii) blind channel estimation [24]; (iii) semi-blind channel estimation [23]; and (iv) iterative joint channel estimation and data detection algorithms [31]. One of the most popular parameter estimation algorithms is the ML method. These ML estimators can be derived in a systematic way. Consider the R_s-vector channel model given in (2.11) with L multiple paths. Assuming channel estimation interval of $\mathcal{N}$ symbols, then the received signal vector can be

expressed as

$$\begin{aligned}\bar{r} &= \begin{bmatrix} b[\mathcal{N}-1]I_{R_s} & b[\mathcal{N}-2]I_{R_s} & \cdots & b[\mathcal{N}-L]I_{R_s} \\ \vdots & \cdots & \cdots & \vdots \\ b[0]I_{R_s} & b[-1]I_{R_s} & \cdots & b[-L+1]I_{R_s} \end{bmatrix} \begin{bmatrix} \bar{h}[0] \\ \vdots \\ \bar{h}[L-1] \end{bmatrix} \\ &+ \begin{bmatrix} \bar{w}[\mathcal{N}-1] \\ \vdots \\ \bar{w}[0] \end{bmatrix} \\ &= \Omega(\bar{b})\bar{h} + \bar{w} \end{aligned} \tag{2.12}$$

where $\Omega(\bar{b})$ is $(\mathcal{N}R_s \times LR_s)$ matrix including the data symbols within the estimation interval. In (2.12), I_{R_s} represents $R_s \times R_s$ identity matrix, $\bar{h}$ is the vector of the channel parameters, and $\bar{w}$ includes the noise samples within the estimation interval. In what follows, we describe the above mentioned estimation techniques in more details.

2.3.1 Training-Based Channel Estimation

The training-based channel estimation assumes the availability of the input vector $\bar{b}$ (as training symbols) and its corresponding observation vector $\bar{r}$. When the noise samples in $\bar{w}$ are modeled as Gaussian variables with zero mean and variance σ^2, then the ML estimator is defined by [57]

$$\hat{\bar{h}} = \arg\min_{\bar{h}} \|\bar{r} - \Omega(\bar{b})\bar{h}\|^2 = \Omega^{\dagger}(\bar{b})\bar{r}, \tag{2.13}$$

where $\Omega^{\dagger}(\bar{b})$ is the pseudo-inverse of the $\Omega(\bar{b})$ defined in (2.12) and $\|\cdot\|$ denotes the Ecludian vector norm. This estimation technique suffers from high computational complexity. Hence, various adaptive implementations of such estimator are proposed in [57].

In conventional training-based approach, a distinct training sequence, known to

the receiver, is time-multiplexed with the data sequence before transmission from the corresponding antenna. This technique is known as pilot-aided channel estimation. Although this channel estimation approach provides accurate channel estimates, it limits the spectral efficiency of the system, especially when the time variations of the channel are fast [15]. Recently, a superimposed training-based approach has been explored where a distinct training sequence is added (superimposed) to the data sequence before modulation and transmission from the corresponding antenna [22]. This estimation technique is known to offer relatively large bandwidth utilization [29].

2.3.2 Blind Channel Estimation

Suppose that both the input vector $\bar{b}$ and the channel vector $\bar{h}$ are unknown. Then, the simultaneous estimation of $\bar{b}$ and $\bar{h}$ appears to be ill-posed. This kind of estimation problem can be solved using blind channel estimation techniques [23],[24]. The key in blind channel estimation is the utilization of qualitative information about the channel and the input. In this case, we consider two different types of ML techniques based on different models of the input sequence [24].

Stochastic ML Estimation

While $\bar{b}$ is unknown, it may be modeled as a random vector with a known distribution. In such a case, the likelihood function of $\bar{h}$ can be obtained by

$$f(\bar{r};\bar{h}) = \int f(\bar{r}|\bar{b};\bar{h}) f(\bar{b}) d\bar{b} \tag{2.14}$$

where $f(\bar{b})$ is the marginal pdf of $\bar{b}$, and $f(\bar{r}|\bar{b};\bar{h})$ is the likelihood function when $\bar{b}$ is known. The integration limits of $\bar{b}$ in (2.14) is determined according to its statistical distribution. Assume, for example, that $b[m]$ takes, with equal probability, a finite number of values

(K_1). Then, the likelihood function of the channel parameter is given by

$$f(\bar{r};\bar{h}) = \sum_{s=1}^{K_1} f(\bar{r}|\bar{b};\bar{h}) f(\bar{b}=\bar{b}_s)$$

$$= C \sum_{s=1}^{K_1} \exp\left(-\frac{\|\bar{r}-\Omega(\bar{b}_s)\bar{h}\|^2}{2\sigma^2}\right), \tag{2.15}$$

where C is constant. Hence, the stochastic ML estimator is defined by

$$\hat{\bar{h}} = \arg\min_{\bar{h}} \sum_{s=1}^{K_1} \exp\left(-\frac{\|\bar{r}-\Omega(\bar{b}_s)\bar{h}\|^2}{2\sigma^2}\right). \tag{2.16}$$

In general, the maximization of the likelihood function defined in (2.14) is difficult since $f(\bar{r};\bar{h})$ is nonconvex [58]. However, this optimization can be implemented using the EM algorithm as shown in [33].

Deterministic ML Estimation

The deterministic ML approach assumes no statistical model for $b[m]$. In other words, both $\bar{h}$ and $\bar{b}$ are parameters to be estimated. The ML estimates can be found in this case by a nonlinear least-squares optimization [59]

$$\{\hat{\bar{h}}, \hat{\bar{b}}\} = \arg\min_{\bar{h},\bar{b}} \|\bar{r}-\Omega(\bar{b})\bar{h}\|^2. \tag{2.17}$$

The joint minimization of the likelihood function with respect to both the channel and the source parameters spaces is known to be difficult. Fortunately, the observation vector $\bar{r}$ is linear in both the channel and the input parameters spaces individually. In particular, we have

$$\bar{r} = \Omega(\bar{b})\bar{h} + \bar{w} = \mathcal{T}(\bar{h})\bar{b} + \bar{w}, \tag{2.18}$$

where

$$\mathcal{T}(\bar{h}) = \begin{bmatrix} \bar{h}[0] & \cdots & \bar{h}[L] & & \\ & \ddots & & \ddots & \\ & & \bar{h}[0] & \cdots & \bar{h}[L] \end{bmatrix}$$

is the so-called filtering matrix. We therefore have a separable nonlinear least-squares problem that can be solved sequentially [60]

$$\begin{aligned} \{\hat{\bar{h}}, \hat{\bar{b}}\} &= \arg\min_{\bar{b}} \{\min_{\bar{h}} \|\bar{r} - \Omega(\bar{b})\bar{h}\|^2\} \\ &= \arg\min_{\bar{h}} \{\min_{\bar{b}} \|\bar{r} - \mathcal{T}(\bar{h})\bar{b}\|^2\}. \end{aligned} \tag{2.19}$$

If we are only interested in estimating the channel, the above minimization can be rewritten as

$$\hat{\bar{h}} = \arg\min_{\bar{h}} \| \underbrace{(I - \mathcal{T}(\bar{h})\mathcal{T}^{\dagger}(\bar{h}))}_{Pr(\bar{h})} \bar{r}\|^2 = \arg\min_{\bar{h}} \|Pr(\bar{h})\bar{r}\|^2, \tag{2.20}$$

where $Pr(\bar{h})$ represents the projection transform of $\bar{r}$ onto the orthogonal complement of the range space of $\mathcal{T}(\bar{h})$, or the noise subspace of the observation. A discussion of algorithms of this type can be found in [60].

2.3.3 Semi-blind Channel Estimation

Semi-blind channel estimation has attracted more attention recently due to the need for fast and robust channel estimation. This technique assumes additional knowledge of the input sequence. Both the stochastic and deterministic ML estimators remain the same except that the likelihood functions need to be modified to incorporate the knowledge of the input [26]. Semi-blind channel estimation may offer significant performance improvement over both the blind and the training-based methods as demonstrated in the evaluation of Cramér-Rao lower bound in [27].

2.3.4 Iterative joint channel estimation and data detection

Recently, iterative joint channel estimation and data detection techniques have shown significant improvement over conventional estimation techniques [30]. Since the detected data symbols are iteratively employed to improve the quality of the channel estimates, the iterative JDE techniques have shown performance enhancement with reasonable convergence rates using very short training sequences [31]. Among these iterative techniques, the EM algorithm has been considered for its attractive features [32]. The main feature of the EM algorithm is that it attains the ML solution iteratively with reduced complexity [33]. In what follows, we briefly describe some of the relevant details of the EM algorithm.

EM algorithm

Let $\mathcal{B}$ denote a vector-valued parameter to be estimated from a vector-valued observation $\mathcal{Y}$ with probability density $f(\mathcal{Y}|\mathcal{B})$, then the ML estimate of $\mathcal{B}$ is given by

$$\hat{\mathcal{B}} = \arg \max_{\mathcal{B}} f(\mathcal{Y}|\mathcal{B}). \tag{2.21}$$

The EM algorithm provides an iterative scheme to approach the ML estimate in cases where a direct computation of $\hat{\mathcal{B}}$ is prohibitive. The derivation of the EM algorithm relies on a complete unobservable data $\mathcal{X}$ which, if it could be observed, would ease the estimation of $\mathcal{B}$. The observed random variable $\mathcal{Y}$ which is referred to as the incomplete data within the EM framework, is related to $\mathcal{X}$ by a mapping $\mathcal{X} \mapsto \mathcal{Y}(\mathcal{X})$. Since $\mathcal{X}$ is not observable, at the i^{th} iteration the EM algorithm computes in a first step, called the expectation step (E-step), the estimate

$$\mathcal{Q}\left(\mathcal{B}|\mathcal{B}^i\right) = E\left[\Phi\left(\mathcal{X}|\mathcal{B}\right)|\mathcal{Y}, \mathcal{B}^i\right], \tag{2.22}$$

of the log-likelihood function $\Phi(\mathcal{X}|\mathcal{B}) = \log f(\mathcal{X}|\mathcal{B})$. The conditional expectation in (2.22) is evaluated given $\mathcal{Y}$ and the data estimate at the i^{th} iteration, $\mathcal{B}^i$. In a second step, called the maximization step (M-step), the parameter vector is updated according to

$$\mathcal{B}^{i+1} = \arg\max_{\mathcal{B}} \mathcal{Q}\left(\mathcal{B}|\mathcal{B}^i\right). \tag{2.23}$$

If $\{\mathcal{B}^i\}_{i=0}^{\infty}$ is a sequence of estimates generated by the EM algorithm starting from an initial value $\mathcal{B}^0$, then the sequence $\{\Phi(\mathcal{Y}|\mathcal{B}^i)\}_{i=0}^{\infty}$ is nondecreasing (monotonicity property). Provided that the function $\mathcal{Q}(\mathcal{B}|\mathcal{B}^i)$ fulfills the mild regularity conditions [33], $\{\Phi(\mathcal{Y}|\mathcal{B}^i)\}_{i=0}^{\infty}$ converges to a fixed point of $\Phi(\mathcal{Y}|\mathcal{B})$ [33], [61]. It is known that the ability of the EM algorithm to find a global maximum depends on the initialization $\mathcal{B}^0$. Also, the convergence rate of the EM algorithm is inversely related to the conditional Fisher information matrix of $\mathcal{X}$ given $\mathcal{Y}$ [61]. This rate is notoriously slow when the dimension of the complete data is large.

Recently, EM-based JDE techniques have attracted more attention for its ability to achieve the ML solution iteratively without wasting the system resources [31], [32]. Considering SISO systems, Georghiades and Han [34] proposed a JDE receiver based on the EM algorithm in time-variant Rayleigh flat fading channels. Naisiri and Khan applied the EM algorithm for synchronous CDMA systems in additive white Gaussian noise (AWGN) channels [35]. Motivated by the EM algorithm related to the problem of parameter estimation of superimposed signals [36], the authors in [37] investigated the application of the EM algorithm in CDMA systems over flat-fading channels. An iterative JDE receiver for DS-CDMA in frequency-selective fading channels has also been proposed in [62].

2.4 Channel Estimation For MIMO CDMA systems

In MIMO CDMA systems, perfect channel knowledge is essential for efficient detection [25]. Compared with SISO CDMA systems, channel estimation in MIMO systems becomes even more challenging as the number of simultaneous transmissions and interference levels increase. While the majority of the works in MIMO systems assume perfect channel estimation, relatively few researchers have investigated the effect of channel estimation errors and possible estimation techniques [23]. In particular, current research works are focused on superimposed pilot channel estimation for MIMO systems (e.g., [63]-[66] and references therein). For example, the authors in [22] examined the performance of superimposed training for MIMO channel estimation in single-user systems where a linear MMSE equalizer is introduced. Along the same lines, the authors in [29] have proposed an iterative channel estimation and detection scheme based on the superimposed training technique for single-input multiple-output (SIMO) systems. In [19], Chong and Milstein employed the training-based technique on a STS system with dual-transmit and dual-receive diversity. In their work, the channel estimation was based on employing distinct pilot spreading codes on STS signals transmitted from different antennas. With the help of these pilot signals, the channel coefficients are estimated using a conventional Rake receiver. These channel estimates are then used to combine the received signals in a Rake-like space-time combiner for final data estimates. It is noted that, both data and channel estimates suffer from intersymbol interference (ISI) and MAI.

In the literature, the proposed estimation techniques either suffer from low spectral efficiency (i.e., conventional training approach), from high computational complexity and slow convergence rate (i.e., blind channel estimation techniques), or from high power consumption (i.e., superimposed training-based approach). Recently, there has been a growing interest in EM-based JDE techniques because of its ability to achieve accurate estimation without wasting the system resources [32]. Therefore, an extensive effort has been focused on employing the EM algorithm in JDE techniques for MIMO systems [67]-

[69]. For example, the authors in [70] proposed various EM-based channel estimation techniques for MIMO systems. Choi [71] has proposed a general framework of EM-based JDE schemes considering different types of MIMO channels (e.g., Rician or Rayleigh fading). As well, many research efforts have considered the JDE problem for MIMO systems considering flat [38] and frequency-selective channels [31].

2.5 Conclusions

In this chapter, we have presented a review of existing works in the literature that are relevant to our work. We have discussed the transmit diversity schemes for WCDMA systems based on STS. Moreover, we have described the channel estimation techniques and the research efforts for employing these techniques in MIMO systems. Throughout the rest of the thesis, we focus our work on studying the performance of the STS schemes in MIMO CDMA systems over frequency-selective fading channels considering both the perfect and imperfect channel estimation cases.

Chapter 3

Performance Analysis of Space-Time Diversity in CDMA Systems

3.1 Introduction

In this chapter, we investigate the performance of DS-CDMA using STS system over frequency-selective fading channels. The underlying transmit diversity scheme, previously introduced in the literature, is based on two transmit and one receive antenna [50]. It was shown that when employed in flat fast fading channels, the received signal quality can be improved by utilizing the spatial and temporal diversities at the receiver side. In our work, we study the problem of multiuser interference in asynchronous CDMA systems that employ transmit/receive diversity using STS. At this stage, we assume that the channel state information is available at the receiver. In [72], an optimum receiver based on the ML algorithm is proposed for space-time coded asynchronous DS-CDMA systems. However, it suffers from high computational complexity. Alternatively, we employ a suboptimum detector at the base station, i.e., decorrelator detector, to overcome the effects of interference. Considering BPSK transmission, we analyze the system performance in terms of its probability of bit error. In particular, we derive the probability

of error over frequency-selective Rayleigh fading channels for both fast and slow fading channels. For the fast fading channel, both simulations and analytical results show that the full system diversity is achieved. On the other hand, when considering a slow fading channel, we show that the scheme reduces to conventional STS schemes [16], where the diversity order is half of that of fast fading.

3.2 Multiuser System Model

Throughout our analysis, we consider an uplink transmission for a DS-CDMA system with K users. The system employs two transmit antennas at the transmitter side and V receive antennas at the receiver side. We consider the STS system proposed in [50]. This scheme can be summarized as follows. Assuming b_1 and b_2 are data symbols assigned to each user in two consecutive symbol intervals, the space-time coded signals transmitted during the first transmission period from antenna 1 and 2 are $b_1^*\mathbf{c}_1 + b_2^*\mathbf{c}_2$ and $b_1\mathbf{c}_2 - b_2\mathbf{c}_1$ respectively, where $\mathbf{c}_1$ and $\mathbf{c}_2$ are the spreading codes. These space-time coded signals are switched with respect to the antenna order during the second transmission period. We assume that the channel is fixed for the duration of one symbol period and change independently from one symbol to another. Later, we consider the case of slow fading channel where the fading coefficients are fixed for the duration of at least two symbol periods.

For sake of simplicity, in what follows, we assume each user's signal travels through a multipath channel with L paths per transmit antenna. The low pass equivalent of the received signal at the v^{th} receive antenna can be expressed as (see Fig. 3.1)

$$r^v(t) = \sum_{k=1}^{K}\sum_{l=1}^{L} c_1^k(t-\tau_k-\tilde{\tau}_l)u_{1l,v}^{k,t} + c_2^k(t-\tau_k-\tilde{\tau}_l)u_{2l,v}^{k,t} + c_1^k(t-T_b-\tau_k-\tilde{\tau}_l) \times u_{1l,v}^{k,t+T_b} + c_2^k(t-T_b-\tau_k-\tilde{\tau}_l)u_{2l,v}^{k,t+T_b} + n^v(t), \quad (3.1)$$

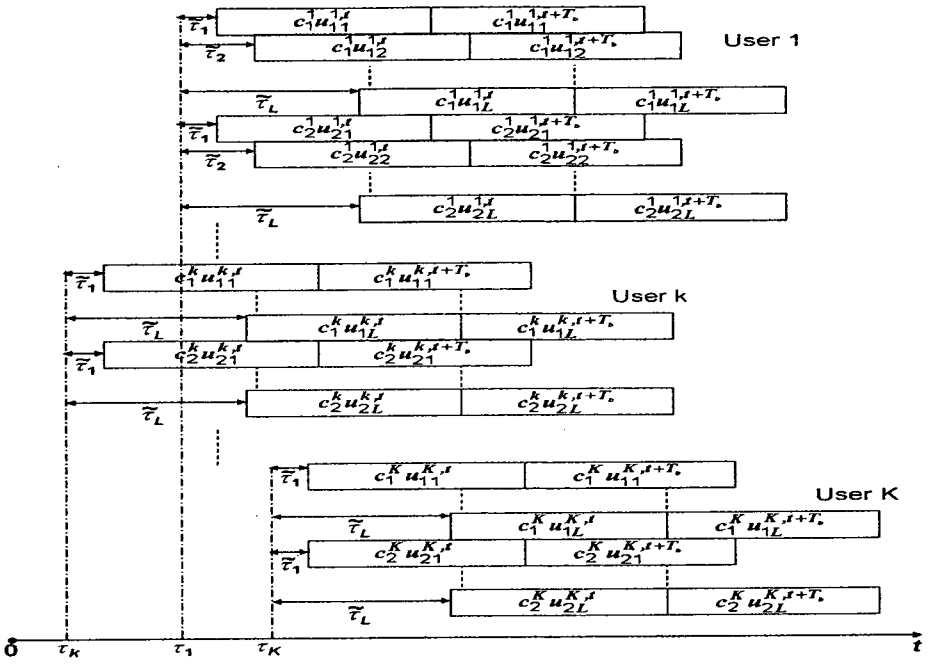

Figure 3.1: Received signal for K-user system considering single receive antenna.

where

$$
\begin{aligned}
u_{1l,v}^{k,t} &= \sqrt{E_s}(h_{1l,v}^{k,t} b_1^{k*} - h_{2l,v}^{k,t} b_2^{k}), \\
u_{2l,v}^{k,t} &= \sqrt{E_s}(h_{1l,v}^{k,t} b_2^{k*} + h_{2l,v}^{k,t} b_1^{k}), \\
u_{1l,v}^{k,t+T_b} &= \sqrt{E_s}(-h_{1l,v}^{k,t+T_b} b_2^{k} + h_{2l,v}^{k,t+T_b} b_1^{k*}), \\
u_{2l,v}^{k,t+T_b} &= \sqrt{E_s}(h_{1l,v}^{k,t+T_b} b_1^{k} + h_{2l,v}^{k,t+T_b} b_2^{k*}).
\end{aligned}
$$

In (3.1), E_s is the received signal energy for the single user, b_1^k and b_2^k are the even and odd k^{th} user data symbols, $c_1^k(t)$ and $c_2^k(t)$ are the two spreading codes assigned to the k^{th} user with processing gain T_b/T_c, where T_b is the bit period, T_c is the chip period, and τ_k represents the transmit delay of the k^{th} user signal, which is assumed to be multiple of chip periods. $\tilde{\tau}_l$ represents the delay of each path during each transmission period, which is modeled as an integer number of chips assumed to be much smaller than the symbol period, and hence we can neglect the effect of ISI. The channel coefficients $h_{ql,v}^{k,t}$

and $h_{ql,v}^{k,t+T_b}$, $(q = 1, 2)$ model the fading channel corresponding to the k^{th} user, l^{th} path from the q^{th} transmit antenna to the v^{th} receive antenna at time t and $t+T_b$ respectively. These fading coefficients are modeled as independent complex Gaussian random variables with zero mean and unity variance. The noise $n^v(t)$ is assumed to be complex Gaussian with zero mean and variance $\sigma_n^2 = N_o/2$ per dimension. As shown in Fig. 3.2, the v^{th} receiver structure consists of a bank of $2LK$ filters matched to the delayed versions of the signature waveforms of each user. Let P denote the space-time-block (ST-block) code interval ($P = 2$ symbols in our case). The output of the v^{th} filter bank, sampled at the chip rate during one ST-block interval is given, in a vector form, by

$$\boldsymbol{Y}_v = \boldsymbol{R}\boldsymbol{U}_v + \boldsymbol{N}_v. \tag{3.2}$$

The $2LPK \times 1$ vector $\boldsymbol{Y}_v$, in (3.2), includes the output of the matched filter bank at time t and $t + T_b$ and is given by

$$\boldsymbol{Y}_v = [y_{1,1,1}^{t,v}, y_{1,2,1}^{t,v}, \ldots, y_{1,2,L}^{t,v}, y_{1,1,1}^{t+T_b,v}, \ldots, y_{K,1,1}^{t,v}, \ldots, y_{K,2,L}^{t+T_b,v}]^T$$

where the superscript T denotes vector transpose and $y_{k,p,l}^{t,v}$, $y_{k,p,l}^{t+T_b,v}$, $p = 1, 2$, represent the outputs at the v^{th} receive antenna of the filter matched to the l^{th} path of the p^{th} sequence for user k at times t and $t + T_b$ respectively. The vector $\boldsymbol{U}_v$ represents the faded data transmitted to the v^{th} receive antenna and is given by

$$\boldsymbol{U}_v = [\boldsymbol{U}_{1,v}^T, \boldsymbol{U}_{2,v}^T, \ldots, \boldsymbol{U}_{k,v}^T, \ldots, \boldsymbol{U}_{K,v}^T]^T$$

where the $2LP \times 1$ vector $\boldsymbol{U}_{k,v}$, which represents the faded data transmitted by the k^{th} user to the v^{th} receive antenna over two successive symbols, is defined as

$$\boldsymbol{U}_{k,v} = [u_{11,v}^{k,t}, u_{21,v}^{k,t}, u_{12,v}^{k,t}, \ldots, u_{2L,v}^{k,t}, u_{11,v}^{k,t+T_b}, u_{21,v}^{k,t+T_b}, \ldots, u_{2L,v}^{k,t+T_b}]^T.$$

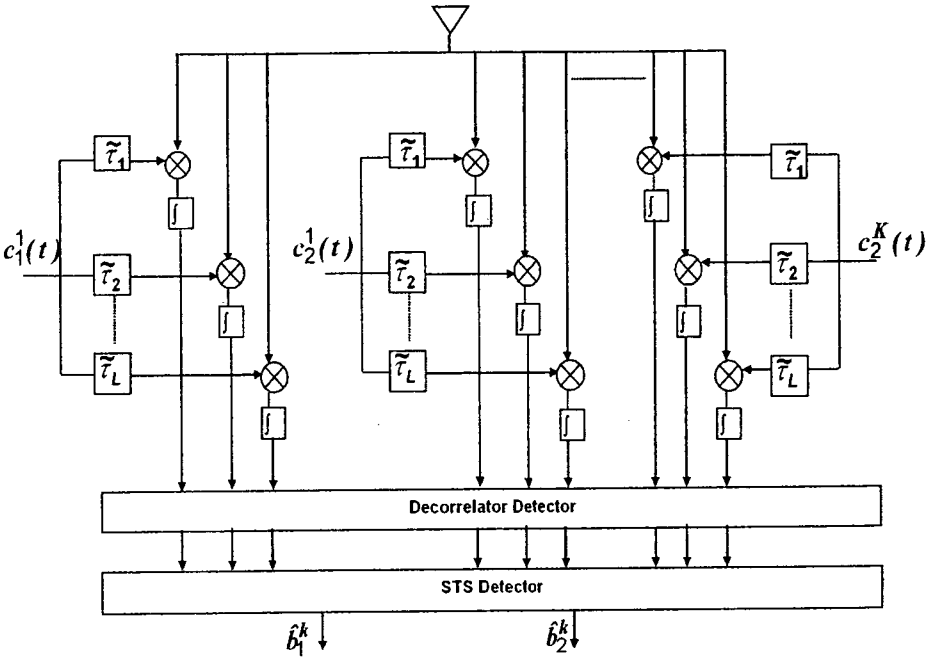

Figure 3.2: Multiuser receiver structure in case of single receive antenna.

The $2LPK \times 2LPK$ cross-correlation matrix $\boldsymbol{R}$ is given by [20]

$$\boldsymbol{R} = \begin{bmatrix} \boldsymbol{R_{11}} & \boldsymbol{R_{12}} & \cdots & \boldsymbol{R_{1K}} \\ \vdots & \cdots & \cdots & \vdots \\ \boldsymbol{R_{K1}} & \cdots & \cdots & \boldsymbol{R_{KK}} \end{bmatrix}$$

where $\boldsymbol{R}_{kw'}, w' = 1, \cdots, K$, is $2LP \times 2LP$ matrix with elements [20]

$$\boldsymbol{R}_{kw'} = \int_{\tau_k}^{\tau_k + PT} \boldsymbol{C}_k(t) \boldsymbol{C}_{w'}^H(t)\, dt,$$

and $\boldsymbol{C}_k(t)$ represents all the delayed versions of the two codes assigned to the k^{th} user

during the two symbol periods, described as

$$\boldsymbol{C}_k(t) = \begin{bmatrix} c_1^k(t-\tau_k-\tilde{\tau}_1) \\ c_2^k(t-\tau_k-\tilde{\tau}_1) \\ \vdots \\ c_1^k(t-\tau_k-\tilde{\tau}_L) \\ \vdots \\ c_1^k(t-T_b-\tau_k-\tilde{\tau}_1) \\ \vdots \\ c_2^k(t-T_b-\tau_k-\tilde{\tau}_L) \end{bmatrix}.$$

The $2LPK \times 1$ noise vector $\boldsymbol{N}_v$, in (3.2), is given by

$$\boldsymbol{N}_v = [\boldsymbol{N}_{1,v}^T, \boldsymbol{N}_{2,v}^T, \ldots, \boldsymbol{N}_{k,v}^T, \ldots, \boldsymbol{N}_{K,v}^T]^T$$

with

$$\boldsymbol{N}_{k,v} = [n_{11,v}^{k,t}, n_{21,v}^{k,t}, n_{12,v}^{k,t}, \ldots, n_{2L,v}^{k,t}, n_{11,v}^{k,t+T_b}, n_{21,v}^{k,t+T_b}, \ldots, n_{2L,v}^{k,t+T_b}]^T$$

and each of the elements $n_{pl,v}^{k,t}$, $n_{pl,v}^{k,t+T_b}$ ($p = 1, 2$ and $l = 1, \ldots, L$) are modeled as complex Gaussian random variables, each with variance $\sigma_n^2 = N_o/2$ per dimension. As will be shown later, this scheme yields to $D = 2PVL$ diversity order in fast fading channels. Note that the output of the matched filter bank suffers from MAI which can be eliminated using the decorrelator detector. In this case, the output of the v^{th} matched filter bank, $\boldsymbol{Y}_v$, is applied to a linear mapper $\boldsymbol{Z}_v = \boldsymbol{R}^{-1}\boldsymbol{Y}_v$ [73], where $\boldsymbol{R^{-1}}$ is the inverse of the cross-correlation matrix. The $2LPK \times 1$ vector $\boldsymbol{Z}_v$ represents the output of the v^{th} decorrelator during two successive symbol periods. It includes the L replicas of the signals from the two transmit antennas for each user during one ST-block interval, which can be expressed as follows

$$\boldsymbol{Z}_v = [\boldsymbol{Z}_{1,v}^T, \boldsymbol{Z}_{2,v}^T, \ldots, \boldsymbol{Z}_{k,v}^T, \ldots, \boldsymbol{Z}_{K,v}^T]^T$$

where the $2LP \times 1$ vector $\boldsymbol{Z}_{k,v}$ is defined by

$$\boldsymbol{Z}_{k,v} = [z_{11,v}^{k,t}, z_{21,v}^{k,t}, z_{12,v}^{k,t}, \ldots, z_{2L,v}^{k,t}, z_{11,v}^{k,t+T_b}, z_{21,v}^{k,t+T_b}, \ldots, z_{2L,v}^{k,t+T_b}]^T$$

and $z_{pl,v}^{k,t}$, $z_{pl,v}^{k,t+T_b}$ represent the output of the v^{th} decorrelator corresponding to the l^{th} path of the p^{th} sequence for user k at times t and $t+T_b$, respectively. The two transmitted symbols of the k^{th} user can be extracted by combining the V decorrelators outputs as follows

$$\hat{b}_1^k = \sum_{v=1}^{V}\sum_{l=1}^{L} h_{1l,v}^{k,t} z_{1l,v}^{k,t*} + h_{2l,v}^{k,t*} z_{2l,v}^{k,t} + h_{2l,v}^{k,t+T_b} z_{1l,v}^{k,t+T_b*} + h_{1l,v}^{k,t+T_b*} z_{2l,v}^{k,t+T_b} \tag{3.3}$$

$$\hat{b}_2^k = \sum_{v=1}^{V}\sum_{l=1}^{L} h_{1l,v}^{k,t} z_{2l,v}^{k,t*} - h_{2l,v}^{k,t*} z_{1l,v}^{k,t} - h_{1l,v}^{k,t+T_b*} z_{1l,v}^{k,t+T_b} + h_{2l,v}^{k,t+T_b} z_{2l,v}^{k,t+T_b*}. \tag{3.4}$$

Considering the first symbol of the k^{th} user and defining the variable $v_k = 2PL(k-1)$, we have

$$\begin{aligned}
\hat{b}_1^k = & \sum_{v=1}^{V}\sum_{l=1}^{L} \sqrt{E_s}(|h_{1l,v}^{k,t}|^2 + |h_{2l,v}^{k,t}|^2 + |h_{1l,v}^{k,t+T_b}|^2 + |h_{2l,v}^{k,t+T_b}|^2) b_1^k \\
& + \sum_{v=1}^{V}\sum_{l=1}^{L} h_{1l,v}^{k,t} (\boldsymbol{R}^{-1}\boldsymbol{N}_v)_{2l+v_k-1,1}^* + h_{2l,v}^{k,t*} (\boldsymbol{R}^{-1}\boldsymbol{N}_v)_{2l+v_k,1} \\
& + h_{2l,v}^{k,t+T_b} (\boldsymbol{R}^{-1}\boldsymbol{N}_v)_{2(L+l)+v_k-1,1}^* + h_{1l,v}^{k,t+T_b*} (\boldsymbol{R}^{-1}\boldsymbol{N}_v)_{2(L+l)+v_k,1}.
\end{aligned} \tag{3.5}$$

From (3.5), one can easily see that a diversity order of $2LPV$ is achieved for the single-user system with no MAI. In the following sections, we derive the probability of bit errors for the multiuser system when employing the decorrelator detector after signal combining.

3.3 Performance Analysis

In what follows, and for the sack of simplicity, we consider BPSK transmission. To evaluate the average BER at the decorrelator output, we first obtain the pdf of the output

SNR of the decorrelator detector. Using this pdf, the probability of error for both the fast and slow fading channels can be evaluated. Without loss of generality, consider the case of finding the probability of error for the first symbol of user 1. To avoid complex notation, we drop its corresponding superscript from the fading coefficients.

3.3.1 Fast Fading

In this case, we consider the first $2LP$ elements from each of the V-decorrelator output vectors ($\boldsymbol{Z}_v$, $v = 1, \ldots, V$). Assuming fixed fading gains and perfect estimation of the cross-correlation matrix, the Gaussian approximation [74] can be used to find the conditional probability of bit error as

$$\tilde{P}_b(\hat{b}_1 = 1 | h^t_{11,1}, h^t_{21,1}, ..., h^{t+T_b}_{1L,V}, h^{t+T_b}_{2L,V}) = Q\left(\frac{\sum_{v=1}^{V}\sum_{l=1}^{L}\sqrt{E_s}(a^t_{1l,v} + a^t_{2l,v} + a^{t+T_b}_{1l,v} + a^{t+T_b}_{2l,v})}{\sqrt{\sigma^2_{\tilde{b}}}}\right) \quad (3.6)$$

where $Q(\cdot)$ is the Gaussian Q-function, $a^t_{1l,v} = |h^t_{1l,v}|^2$, $a^t_{2l,v} = |h^t_{2l,v}|^2$, $a^{t+T_b}_{1l,v} = |h^{t+T_b}_{1l,v}|^2$, $a^{t+T_b}_{2l,v} = |h^{t+T_b}_{2l,v}|^2$, and $\sigma^2_{\tilde{b}}$ is the variance of the noise term in (3.5) when $k = 1$. It is easy to show that

$$\sigma^2_{\tilde{b}} = \left(\frac{N_o}{2}\right)\sum_{v=1}^{V}\sum_{l=1}^{L} c_{2l-1}a^t_{1l,v} + c_{2l}a^t_{2l,v} + c_{2(L+l)-1}a^{t+T_b}_{2l,v} + c_{2(L+l)}a^{t+T_b}_{1l,v} \quad (3.7)$$

where c_{2l-1}, c_{2l}, $c_{2(L+l)-1}$ and $c_{2(L+l)}$ define the following terms $R^{-1}_{2l-1,2l-1}$, $R^{-1}_{2l,2l}$, $R^{-1}_{2(L+l)-1,2(L+l)-1}$ and $R^{-1}_{2(L+l),2(L+l)}$, respectively, and $R^{-1}_{i',i'}$ is the i'^{th} diagonal element of the inverse of the cross-correlation matrix. The variables $a^t_{ql,m}$ and $a^{t+T_b}_{ql,m}$ ($q = 1, 2$) are chi-square distributed with two degrees of freedom and characteristic function [75]

$$\phi(j\omega) = \frac{1}{1 - j2\omega}. \quad (3.8)$$

Define the variable α as

$$\alpha = \frac{A}{\sqrt{B}} \tag{3.9}$$

where

$$A = \sum_{v=1}^{V} \sum_{l=1}^{L} a_{1l,v}^{t} + a_{2l,v}^{t} + a_{1l,v}^{t+T_b} + a_{2l,v}^{t+T_b}$$

and

$$B = \sum_{v=1}^{V} \sum_{l=1}^{L} c_{2l-1} a_{1l,v}^{t} + c_{2l} a_{2l,v}^{t} + c_{2(L+l)-1} a_{2l,v}^{t+T_b} + c_{2(L+l)} a_{1l,v}^{t+T_b}.$$

Hence, the joint characteristic function of A and B is given by [75]

$$\begin{aligned}
\phi_{A,B}(\omega_1, \omega_2) &= E[\exp j(\omega_1 A + \omega_2 B)] \\
&= E\Big[\exp j \sum_{v=1}^{V} \sum_{l=1}^{L} a_{1l,v}^{t}(\omega_1 + c_{2l-1}\omega_2) + a_{2l,v}^{t}(\omega_1 + c_{2l}\omega_2) \\
&\qquad + a_{2l,v}^{t+T_b}(\omega_1 + c_{2(L+l)-1}\omega_2) + a_{1l,v}^{t+T_b}(\omega_1 + c_{2(L+l)}\omega_2) \Big]
\end{aligned} \tag{3.10}$$

where $E[\cdot]$ denotes the expected value of the enclosed argument. Defining $y = \frac{1}{2} - j\omega_1$ and assuming independent fading channels, one can show that

$$\phi_{A,B}(\omega_1, \omega_2) = \frac{1}{(2)^{4LV}} \prod_{u=1}^{4L} \frac{1}{(y - jc_u\omega_2)^V}. \tag{3.11}$$

In order to simplify our analysis, we use a partial fraction expansion method of a rational function with high order poles. For further details regarding this method, the reader is referred to [76]. Furthermore, we consider the special case where the rational function has no zeros. Thus, the characteristic function in (3.11) is reduced to

$$\phi_{A,B}(\omega_1, \omega_2) = \frac{\prod_{u=1}^{4L} \frac{1}{c_u^V}}{(2)^{4LV}} \left(\sum_{u=1}^{4L} \sum_{v'=0}^{V-1} \frac{C_{uv'}}{(\omega_2 - \frac{y}{jc_u})^{V-v'}} \right) \tag{3.12}$$

where

$$C_{uv'} = \frac{K_{uv'}}{y^{4VL-V+v'}}, \qquad u = 1, \ldots, 4L, \; v' = 0, \ldots, V-1$$

represents the residue terms obtained from the partial fraction expansion [76]. An exact expression for each of $K_{uv'}$, ($u = 1, \ldots, 4L$ and $v' = 0, \ldots, V-1$) can also be obtained in terms of the cross-correlation coefficients between the users' signature waveforms [76]. From (3.12), the joint pdf, $f_{A,B}$, can be obtained as [75]

$$\begin{aligned} f_{A,B} &= \frac{1}{4\pi^2} \int_{-\infty}^{\infty} \int_{-\infty}^{\infty} \phi_{A,B}(\omega_1, \omega_2) \exp\left(-j(\omega_1 A + \omega_2 B)\right) d\omega_1 d\omega_2 \\ &= \frac{\prod_{u=1}^{4L} \frac{1}{c_u^V}}{4\pi^2 (2)^{4LV}} \sum_{u=1}^{4L} \sum_{v'=0}^{V-1} \lambda_{uv'} B^{V-v'-1} \left(A - \frac{B}{c_u}\right)^{4VL-V+v'-1} \exp\left(-\frac{A}{2}\right) \end{aligned} \tag{3.13}$$

where $\Gamma(\cdot)$ is the Gamma function and $\lambda_{uv'} = \frac{4\pi^2 K_{uv'}}{j^{V-v'}\Gamma(V-v')\Gamma(4VL-V+v')}$. One way to obtain the pdf of the SNR in (3.9) is through variable transformation. From (3.9) and by assuming that $W = B$, the joint pdf of α and W can be determined through the following relation [75]

$$f_{\alpha,W} = f_{A,B} |\Omega(\alpha, W)| \tag{3.14}$$

where $|\Omega(\alpha, W)| = \sqrt{W}$ is the Jacobian of the transformation. Finally with the substitution of (3.9) in (3.14), and after some algebraic manipulations, we get

$$\begin{aligned} f_{\alpha,W} = \frac{\prod_{u=1}^{4L} \frac{1}{c_u^V}}{4\pi^2 (2)^{4LV}} \sum_{u=1}^{4L} \sum_{v'=0}^{V-1} \lambda_{uv'} W^{V-v'-\frac{1}{2}} \left(\alpha\sqrt{W} - \frac{W}{c_u}\right)^{4VL-V+v'-1} \\ \times \exp\left(-\frac{\alpha\sqrt{W}}{2}\right). \end{aligned} \tag{3.15}$$

From (3.15), the pdf of the SNR can be expressed as

$$f_\alpha = \frac{\prod_{u=1}^{4L} \frac{1}{c_u^V}}{4\pi^2 (2)^{4LV}} \sum_{u=1}^{4L} \sum_{v'=0}^{V-1} \lambda_{uv'} P_{uv'} \tag{3.16}$$

where

$$P_{uv'} = \int_0^{c_u^2\alpha^2} W^{V-v'-\frac{1}{2}} \left(\alpha\sqrt{W} - \frac{W}{c_u}\right)^{4VL-V+v'-1} \exp\left(-\frac{\alpha\sqrt{W}}{2}\right) dW. \tag{3.17}$$

Using the binomial series expansion, the integration in (3.17) can be reduced to

$$P_{uv'} = \sum_{d=0}^{4VL-V+v'-1} \binom{4VL-V+v'-1}{d} \frac{(-1)^{4VL-V+v'-1-d}\alpha^d}{c_u^{4VL-V+v'-1-d}} \times \int_0^{c_u^2\alpha^2} (\sqrt{W})^{8VL-3-d} \exp\left(-\frac{\alpha\sqrt{W}}{2}\right) dW. \tag{3.18}$$

In what follows, we denote the integration in (3.18) by $\mathcal{I}_{ud}$ and use

$$\int_{c_1}^{c_2} x^n e^{-ax} dx = \frac{1}{a(n+1)} \Big[c_2^n (ac_2)^{-\frac{n}{2}} e^{-\frac{ac_2}{2}} M(\frac{n}{2}, \frac{n+1}{2}, ac_2) - c_1^n (ac_1)^{-\frac{n}{2}} \times e^{-\frac{ac_1}{2}} M(\frac{n}{2}, \frac{n+1}{2}, ac_1)\Big] \tag{3.19}$$

where $M(k, m, z)$ represents the WhittakerM function [77]. Using the substitution $t = \sqrt{W}$, we get

$$\begin{aligned} \mathcal{I}_{ud} &= 2\int_0^{c_u\alpha} t^{8VL-2-d} \exp\left(-\frac{\alpha t}{2}\right) dt \\ &= \frac{2^{\frac{8VL-d+2}{2}} \sigma^{8VL-d} c_u^{\frac{8VL-2-d}{2}}}{(8VL-1-d)\alpha} \exp\left(-\frac{c_u\alpha^2}{4}\right) \\ &\times M(\frac{8VL-2-d}{2}, \frac{8VL-1-d}{2}, \frac{c_u\alpha^2}{2}). \end{aligned} \tag{3.20}$$

In terms of the confluent hypergeometric function ([77], Eq.(13.1.32)),

$$\mathcal{I}_{ud} = \frac{2(\alpha c_u)^{8VL-1-d}}{8VL-1-d} \exp\left(-\frac{c_u\alpha^2}{2}\right) {}_1F_1(1; 8VL-d; \frac{c_u\alpha^2}{2}). \tag{3.21}$$

Substituting (3.21) in (3.18), we obtain

$$P_{uv'} = 2\alpha^{8VL-1} c_u^{4VL+V-v'} \exp\left(-\frac{c_u\alpha^2}{2}\right) \sum_{d=0}^{4VL-V+v'-1} \binom{4VL-V+v'-1}{d} \times \frac{(-1)^{4VL-V+v'-1-d}}{8VL-d-1} {}_1F_1(1; 8VL-d; \frac{c_u\alpha^2}{2}). \quad (3.22)$$

Finally, the probability function of the SNR in (3.16) can be obtained using (3.22).

3.3.2 Slow Fading

For the slow fading channel, the fading coefficients are assumed to be fixed for the duration of at least two consecutive symbol intervals. Hence (3.6) reduces to

$$\tilde{P}_b(\hat{b}_1 = 1 | h_{11,1}, h_{21,1}, ..., h_{1L,V}, h_{2L,V}) = Q\left(\frac{2\sqrt{E_s}\sum_{v=1}^{V}\sum_{l=1}^{L}(a_{1l,v} + a_{2l,v})}{\sqrt{\sigma_{\tilde{b}}^2}}\right) \quad (3.23)$$

where $a_{1l,v} = |h_{1l,v}^t|^2 = |h_{1l,v}^{t+T_b}|^2$, $a_{2l,v}^t = |h_{2l,v}^t|^2 = |h_{2l,v}^{t+T_b}|^2$, and

$$\sigma_{\tilde{b}}^2 = \sigma_n^2 \sum_{v=1}^{V}\sum_{l=1}^{L} |h_{1l,v}|^2 \left(R_{2l-1,2l-1}^{-1} + R_{2(L+l),2(L+l)}^{-1}\right) + |h_{2l,v}|^2 \left(R_{2l,2l}^{-1} + R_{2(L+l)-1,2(L+l)-1}^{-1}\right).$$

Following the same procedure as in the fast fading case, one can show that the joint characteristic function in (3.12) reduces to

$$\phi_{A,B}(\omega_1, \omega_2) = \frac{\prod_{u=1}^{2L} \frac{1}{c_u^V}}{(2)^{2LV}} \left(\sum_{u=1}^{2L}\sum_{v'=0}^{V-1} \frac{C_{uv'}}{(\omega_2 - \frac{y}{jc_u})^{V-v'}}\right). \quad (3.24)$$

where

$$C_{uv'} = \frac{K_{uv'}}{y^{2VL-V+v'}}.$$

Similar to the fast fading channel, it is straightforward to show that

$$f_{A,B} = \frac{\prod_{u=1}^{2L} \frac{1}{c_u^V}}{4\pi^2(2\sigma^2)^{2LV}} \sum_{u=1}^{2L} \sum_{v'=0}^{V-1} \lambda_{uv'} B^{V-v'-1} \left(A - \frac{B}{c_u}\right)^{2VL-V+v'-1} \exp\left(-\frac{A}{2\sigma^2}\right), \quad (3.25)$$

where $\lambda_{uv'} = \frac{4\pi^2 K_{uv'}}{j^{V-v'}\Gamma(V-v')\Gamma(2VL-V+v')}$. Using the transformation in (3.9),

$$f_\alpha = \frac{\prod_{u=1}^{2L} \frac{1}{c_u^V}}{4\pi^2(2)^{2LV}} \sum_{u=1}^{2L} \sum_{v'=0}^{V-1} \lambda_{uv'} P_{uv'} \quad (3.26)$$

with

$$P_{uv'} = 2\alpha^{4VL-1} c_u^{2VL+V-v'} \exp\left(-\frac{c_u\alpha^2}{2}\right) \sum_{d=0}^{2VL-V+v'-1} \binom{2VL-V+v'-1}{d} \times \frac{(-1)^{2VL-V+v'-1-d}}{4VL-d-1} {}_1F_1(1; 4VL-d; \frac{c_u\alpha^2}{2}).$$

3.4 Probability of Bit Error

For the fast fading channel, the probability of error can be obtained by averaging the conditional bit error in (3.6) over the pdf in (3.16)

$$P_b = \int_0^\infty Q\left(\sqrt{\gamma\alpha^2}\right) f_\alpha d\alpha, \quad (3.27)$$

where $\gamma = \frac{E_s}{\sigma_n^2}$. To simplify the analysis, we use the *preferred* form of the Gaussian Q-function [78]

$$Q(x) = \frac{1}{\pi} \int_0^{\frac{\pi}{2}} \exp^{-\frac{x^2}{2sin^2\theta}} d\theta. \quad (3.28)$$

Substituting (3.16) and (3.28) in (3.27), we get

$$P_b = \frac{1}{\pi}\int_0^{\frac{\pi}{2}}\int_0^{\infty} \exp^{-\frac{\gamma\alpha^2}{2sin^2\theta}} f_\alpha d\alpha d\theta$$
$$= \frac{\prod_{u=1}^{4L} \frac{1}{c_u^V}}{4\pi^3} \sum_{u=1}^{4L}\sum_{v'=0}^{V-1} \lambda_{uv'} F_{uv'}, \tag{3.29}$$

where

$$F_{uv'} = \frac{1}{(2)^{4VL}}\int_0^{\frac{\pi}{2}}\int_0^{\infty} \exp^{-\frac{\gamma\alpha^2}{2sin^2\theta}} P_{uv'} d\alpha d\theta.$$

Substituting $P_{uv'}$ from (3.22), we get

$$F_{uv'} = 2c_u^{4VL+V-v'} \sum_{d=0}^{4VL-V+v'-1} \binom{4VL-V+v'-1}{d} \frac{(-1)^{4VL-V+v'-1-d}}{8VL-1-d} G_d \tag{3.30}$$

where by using ([79], Eq. (7.621.4)),

$$G_d = \frac{\Gamma(4VL)}{2\overline{\gamma}^{4VL}}\int_0^{\frac{\pi}{2}} (sin^2\theta)^{4VL}\ {}_2F_1(8VL-d-1, 4VL; 8VL-d; -\frac{c_u sin^2\theta}{\overline{\gamma}}) d\theta \tag{3.31}$$

where $\overline{\gamma} = \frac{E\left[|h_{ql,v}|^2\right]E_s}{\sigma_n^2}$ is the average SNR per channel, and ${}_2F_1(.,.;.;.)$ is a special case of the generalized hypergeometric function ([79], Eq. (9.14.1)). Substituting $V' = sin^2\theta$ in (3.31) and by using the integral in ([79], Eq. (7.512.12)), one can show that

$$G_d = \frac{\Gamma(1/2)\Gamma(\frac{8VL+1}{2})}{16VL\overline{\gamma}^{4VL}}$$
$$\times\ {}_3F_2(\frac{8VL+1}{2}, 8VL-d-1, 4VL; 4VL+1, 8VL-d; -\frac{c_u}{\overline{\gamma}}). \tag{3.32}$$

Finally, by substituting (3.32) in (3.30), we can evaluate the average probability of error in (29). From (3.32) we can examine the asymptotic BER performance as $\bar{\gamma}$ gets large. In this case, in the limit, the hypergeometric function ${}_3F_2(\cdot,\cdot,\cdot) \to 1$ and hence

$$P_b(\bar{\gamma} \to \infty) \equiv \mathcal{W}\left(\frac{1}{\bar{\gamma}}\right)^{4VL}, \quad \mathcal{W} \in \mathbb{R}.$$

That is, our system achieves the full system diversity of $4VL$. The same argument applies for the slow fading channel discussed below, where the full system diversity of $2VL$ is also achieved. The BER for the slow fading channel can be found in a similar way by averaging the conditional BER in (3.23) over the SNR pdf in (3.26). That is,

$$P_b = \frac{\prod_{u=1}^{2L} \frac{1}{c_u^V}}{4\pi^3} \sum_{u=1}^{2L} \sum_{v'=0}^{V-1} \lambda_{uv'} F_{uv'}, \tag{3.33}$$

where

$$F_{uv'} = 2c_u^{2VL+V-v'} \sum_{d=0}^{2VL-V+v'-1} \binom{2VL-V+v'-1}{d} \frac{(-1)^{2VL-V+v'-1-d}}{4VL-1-d} G_d$$

and

$$G_d = \frac{\Gamma(1/2)\Gamma(\frac{4VL+1}{2})}{8VL\bar{\gamma}^{2VL}} \, {}_3F_2(\frac{4VL+1}{2}, 4VL-d-1, 2VL; 2VL+1, 4VL-d; -\frac{c_u}{\bar{\gamma}}).$$

3.5 Numerical and Simulation Results

In this section we examine the BER performance of the space-time system discussed in the previous sections using both Monte-Carlo simulations and the analytical results in (3.29) and (3.33). In all cases, we consider a DS-CDMA system with BPSK transmission where the user data is spread using Gold codes of length 31 chips. The delay between users, τ_k, is assumed to be multiple of chip periods within the symbol interval. To neglect the effect of ISI, the delay of each path, $\tilde{\tau}_l$, is taken as a multiple of chip periods of length less than 10% of the symbol period. In cases where ISI is dominant, one can resort to pulse shaping/equalization techniques to overcome the degradation in the system performance. Furthermore, we assume perfect knowledge of the channel coefficients at the receiver. Also, in all the results, we assume that all the channels are independent. Our results and analysis are based on two transmit antennas at the user side and V receive antennas at the

base station. However, one can generalize these results to $U > 2$ transmit antennas. In this case to ensure full diversity using simple decoding, one has to search for a spreading code matrix that satisfies the full rank criterion using orthogonal designs as discussed in [10].

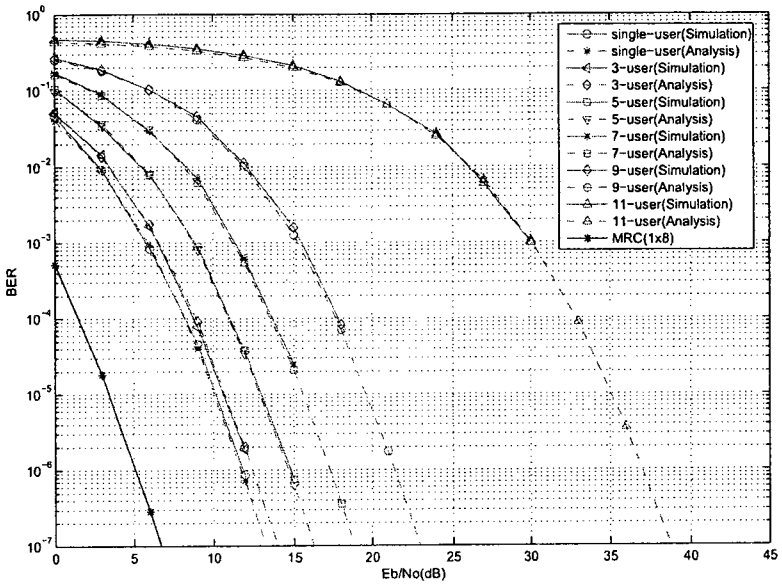

Figure 3.3: BER performance for asynchronous DS-CDMA systems with two transmit and one receive antenna over frequency-selective fast fading channels with L=2 paths.

Fig. 3.3 presents the error performance for different number of users in the frequency-selective fast fading channel. For reference, we include the BER performance of the maximal-ratio-combiner (MRC) with eight receive diversity branches. Note that the performance of the MRC is merely used for diversity order comparisons, and the SNR gap is due to the fixed transmit power constraint and noise enhancement of the decorrelator. The results in Fig. 3.3 demonstrate the accuracy of the derived BER expression in (3.29) when compared with simulation results. Furthermore, it is evident that a diversity order of eight is achieved for different number of users. This diversity is delivered by the U=2 transmit antennas, L=2 paths, V=1 receive antenna, and $P = 2$ length of the ST-block

interval.

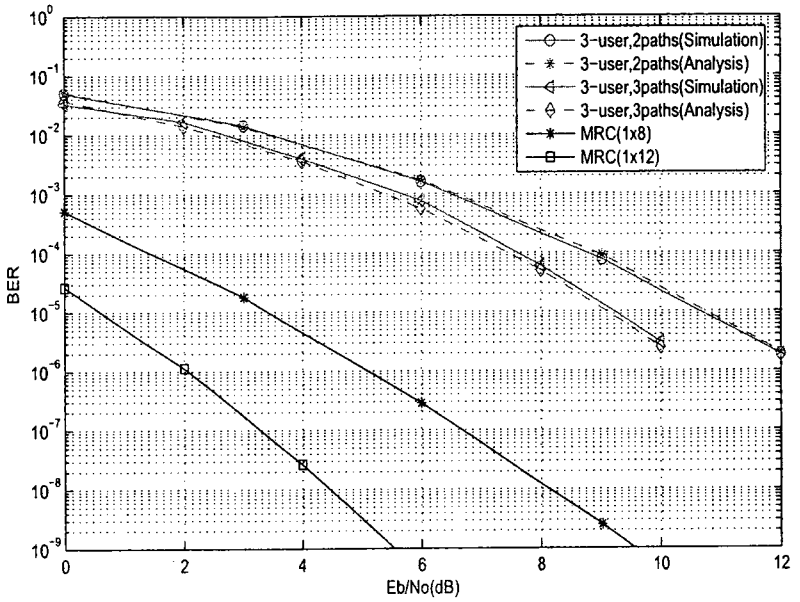

Figure 3.4: BER performance for a 3-user system as a function of the number of paths, L=2,3, over frequency-selective fast fading channels.

Fig. 3.4 shows the BER performance of the STS scheme for a 3-user system considering two and three paths per transmit antenna. The results clearly show the multipath diversity gain delivered by the RAKE receiver when the number of resolvable paths increases for 2×1 antenna configuration. In this case, the transmit diversity scheme with $L = 3$ paths achieves diversity order ULP =12 when compared with the MRC with the same number of diversity branches.

Fig. 3.5 examines the BER performance for 2×2 antenna configuration, where we consider transmission over frequency-selective fast fading channel with two resolvable paths. The accuracy of the derived BER as function of the number of users (K), the number of resolvable paths (L) and the number of receive antennas (V) is evident for different number of users. It should also be noticed that the diversity gain is improved when doubling the number of receive antennas

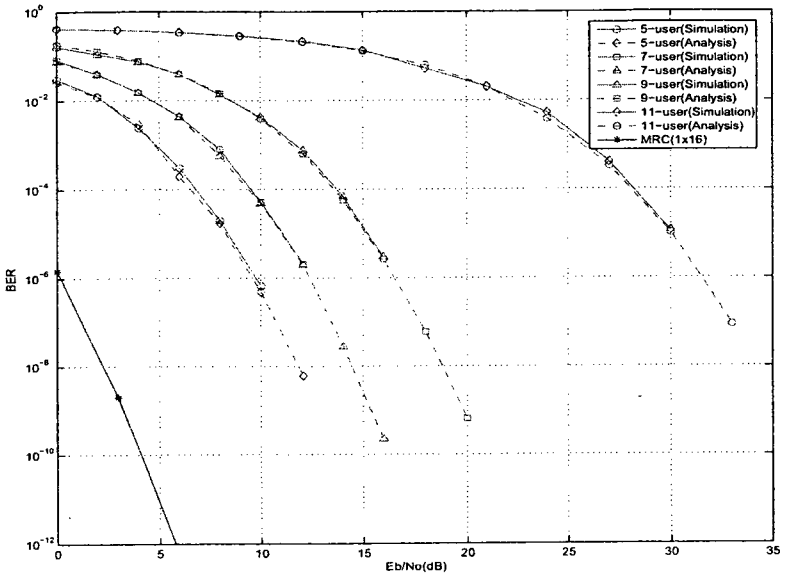

Figure 3.5: BER performance for a multiuser system with two transmit and two receive antennas over frequency-selective fast fading channels with L=2 paths.

Finally, Fig. 3.6 shows both the simulations and analytical results as a function of the number of users for the slow fading channel. The results show that the proposed system is able to deliver the same diversity order as the MRC with four diversity branches. Note that the diversity order of four is due to the U=2 transmit antennas and $L = 2$ paths.

3.6 Conclusions

The performance of transmit diversity using STS in DS-CDMA systems has been examined through simulations and mathematical analysis. Our results show that the full system diversity can be maintained when a decorrelator detector is employed at the base station. With perfect CSI at the receiver side, these results are valid for both fast and slow fading channels, where the resulting SNR loss from the optimal single-user system is only a function of the number of active users. Throughout our work, we assumed a perfect channel state information at the receiver side. In the subsequent chapters, we

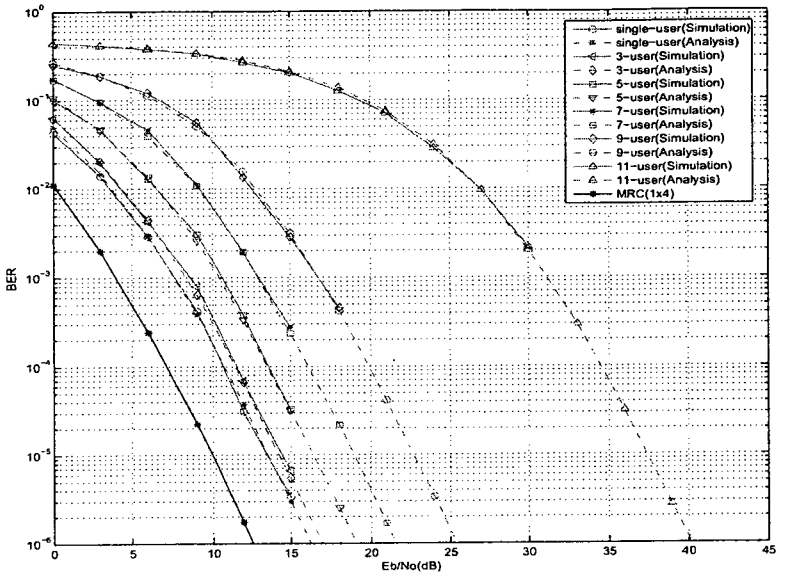

Figure 3.6: BER performance for asynchronous DS-CDMA systems with two transmit and one receive antenna over frequency-selective slow fading channels with $L = 2$ paths.

investigate the effect of imperfect channel estimation and possible estimation techniques for STS systems.

Chapter 4

A Channel Estimation and Data Detection Scheme for Multiuser MIMO-CDMA Systems in Fading Channels

4.1 Introduction

In this chapter, we examine the effect of channel estimation errors on the performance of MIMO CDMA systems. Channel estimation based on training techniques has been widely considered throughout the literature. However, employing these training techniques in MIMO-CDMA systems degrades the system performance due to multiuser interference. This degradation is clear as the diversity advantage of the MIMO system diminishes with the increased level of interference. As a remedy to this problem, we propose a channel estimation and data detection scheme based on the superimposed training technique for STS systems. The proposed scheme enhances the performance of the space-time system by eliminating the interference effect from both the channel and data estimates

using two decorrelators; channel and data decorrelators. We investigate the performance of the proposed estimation technique considering an asynchronous CDMA uplink transmission over frequency-selective slow fading channels. In particular, we analyze the BER performance of the multiuser system with two transmit and V receive antenna configuration over Rayleigh fading channels. Compared with other conventional estimation techniques, our results show that the proposed estimation technique is more robust to channel estimation errors. Furthermore, both simulations and analytical results indicate that full system diversity is achieved.

4.2 System Model

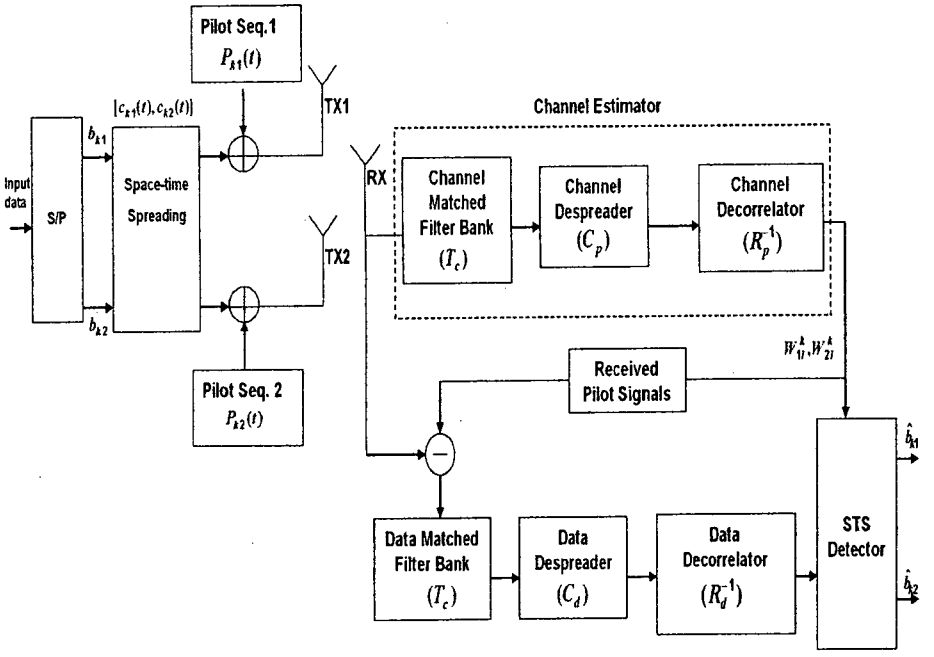

Figure 4.1: Block diagram of pilot-sequence-assisted STS transmission system corresponding to a single receive antenna.

The transmit diversity scheme considered in our work consists of two transmit antennas at the mobile station and V receive antennas at the base station. The system block diagram for the k^{th} transmitting user is shown in Fig. 4.1, where real valued data

symbols using BPSK baseband modulation and real valued spreading are assumed [48]. We consider the original STS scheme proposed in [16] with two spreading codes per user. As seen in Fig. 4.1, following the STS, two pilot spreading codes are assigned to each user for the purpose of channel estimation. Each pilot sequence is added (superimposed) on the STS signal before transmission from the corresponding antenna. We also consider an uplink asynchronous transmission from K users over frequency-selective slow-fading channel (see Fig. 4.2), where the fading coefficients are fixed for the duration of M-symbol data block but change independently from one block to another. Given the space-time scheme in [16], the duration of the space-time codeword is $T_s = 2T_b$, where T_b is the bit duration. The received complex low-pass equivalent signal at the v^{th} receive antenna is given by

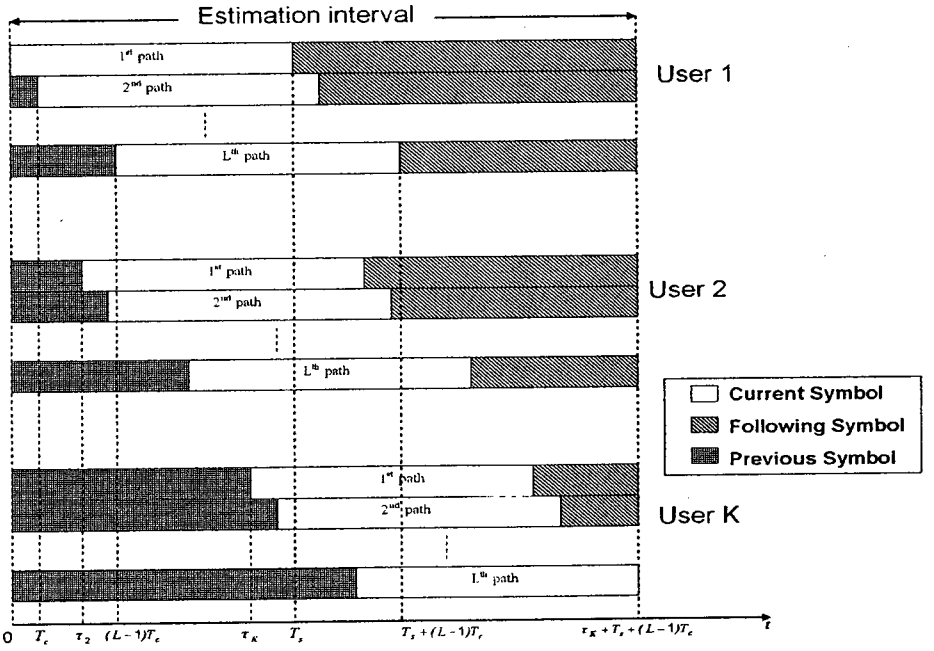

Figure 4.2: Asynchronous transmission of K code sequences, each has a period $T_s = 2N$ chips, over frequency selective fading channel with L resolvable paths. The estimation interval is $T_s + \tau_K + (L-1)T_c$.

$$r^{v}(t) = \sum_{k=1}^{K}\sum_{l=1}^{L}\sum_{m=0}^{M-1} h_{1l}^{k,v}\left[\sqrt{\frac{\rho_p}{2}}P_{k1}(t - mT_s - \tau_k - \tilde{\tau}_l) + \sqrt{\frac{\rho_d}{2}}(b_{k1}[m]c_{k1}(t - mT_s - \tau_k - \tilde{\tau}_l) + b_{k2}[m]c_{k2}(t - mT_s - \tau_k - \tilde{\tau}_l))\right] + h_{2l}^{k,v}\left[\sqrt{\frac{\rho_p}{2}}P_{k2}(t - mT_s - \tau_k - \tilde{\tau}_l) + \sqrt{\frac{\rho_d}{2}}(b_{k2}[m]c_{k1}(t - mT_s - \tau_k - \tilde{\tau}_l) - b_{k1}[m]c_{k2}(t - mT_s - \tau_k - \tilde{\tau}_l))\right] + n^{v}(t), \quad (4.1)$$

where ρ_p and ρ_d represent the pilot and data signal-to-noise ratios (SNRs), respectively. The data bits, $b_{k1}[m]$ and $b_{k2}[m]$, represent the odd and even data streams of the k^{th} user within the m^{th} codeword interval. In (4.1), $c_{k1}(t)$ and $c_{k2}(t)$ are the k^{th} user data spreading sequences with processing gain $2N$, where $N = T_b/T_c$ represents the number of chips per bit, and T_c is the chip duration. The two pilot spreading sequences, $P_{k1}(t)$ and $P_{k2}(t)$, assigned to the k^{th} user have a period of $2T_b$. In our analysis, we assume that the pilot and data spreading sequences assigned to the K users are mutually orthogonal at the transmitter side. However due to asynchronous transmission, this orthogonality condition between codes is no longer valid at the receiver side. τ_k represents the transmit delay of the k^{th} user signal which is assumed to be multiple of chip periods within T_s. $\tilde{\tau}_l$ is the l^{th} path delay ($\tilde{\tau}_l = lT_c$), $h_{ql}^{k,v}$, $q = 1, 2$, is the channel coefficient corresponding to the k^{th} user, l^{th} path from the q^{th} transmit antenna to v^{th} receive antenna, and L is the total number of resolvable paths. These fading coefficients are modelled as independent complex Gaussian random variables with zero mean and variance $\sigma_h^2 = \frac{1}{L}$. We also consider a time-invariant channel over the duration of an M-symbol data block. The noise $n^{v}(t)$ is Gaussian with zero mean and unit variance. At the receiver, the received signal is first sent to a channel estimator, where the path gain estimates $\{W_{ql}^{k,v}, W_{ql}^{k,v}\}$ of the l^{th} path between transmit antenna q=1,2, and receive antenna v are obtained. Then, the STS signals are detected using the estimated path gains. The receiver structure is further illustrated in the following sections.

4.3 Channel Estimation

At the receiver side, the received signal at each receive antenna is chip-matched filtered, sampled at a rate $1/T_c$, and accumulated over an observation interval of $(2N + \tau_{max} + L - 1)$ chips corresponding to the first symbol of the received data block for the K-user system. The $(\tau_{max} + L - 1)$ samples are due to the maximum multipath delay (i.e., delay of the L^{th} path) corresponding to the user with the maximum transmit delay, τ_{max}. We have chosen to employ the first symbol observation interval in channel estimation since it is the symbol with the least MAI and ISI contributions.

Fig. 4.2 shows a block diagram of the asynchronous transmission of K users code sequences, each with a period of $T_s = 2N$ chips over frequency-selective fading channel with L resolvable paths. As shown, the estimation interval corresponding to the m^{th} STS symbol interval ($m = 0, 1, \ldots, M - 1$) starts from the first path of the first user corresponding to the m^{th} transmission period (i.e., τ_1 represents the minimum user delay (τ_1=0)) to the end of the L^{th} path of the K^{th} user's m^{th} symbol (τ_K is the maximum user delay (τ_K=τ_{max})). Assuming perfect knowledge of the users' delays, one can construct the code matrices corresponding to the current, following or previous symbol transmissions within the observation interval.

Let $\mathbf{y}^v[0]$ denote the observation vector at the v^{th} receive antenna containing all samples related to the STS symbols transmitted by the K users within the observation interval. Then

$$\mathbf{y}^v[0] = \mathbf{C}[0]\mathbf{H}^v\mathbf{b}[0] + \mathbf{C}[1]\mathbf{H}^v\mathbf{b}[1] + \mathbf{n}^v[0] \tag{4.2}$$

where $\mathbf{C}[0] = [\mathbf{C}_1[0], \mathbf{C}_2[0], ..., \mathbf{C}_K[0]]$ represents the code matrix corresponding to the current received symbols, $\mathbf{b}[0]$, within the observation interval. The sub-matrix $\mathbf{C}_k[0]$, $(k = 1, 2, ..., K)$ is a $[(2N + L - 1 + \tau_{max}) \times 4L]$ matrix containing the pilot and data sequences of user k associated with the L resolvable paths. In the same way, $\mathbf{C}[1] = [\mathbf{C}_1[1], \mathbf{C}_2[1], ..., \mathbf{C}_K[1]]$ represents the code matrix of the following received symbols, $\mathbf{b}[1]$,

within the observation interval. $\mathbf{C}_k[1]$, $(k = 1, 2, ..., K)$ is a $[(2N+L-1+\tau_{max})\times 4L]$ matrix consisting of the pilot and data code sequences of user k associated with the following STS symbol within the current observation window. The definition of theses matrices is given in Appendix A.1. The second term in the right-hand side of (4.2) represents the interference due to the following symbols, $\mathbf{b}[1]$, of the K-user system. In (4.2), $\mathbf{H}^v$ is the channel impulse response of the K-user system at the v^{th} receive antenna, and is defined by

$$\mathbf{H}^v = diag\{\mathbf{H}_1^v, \mathbf{H}_2^v, ..., \mathbf{H}_K^v\}$$

where

$$\mathbf{H}_k^v = [\mathbf{H}_k^{vT}(1), \mathbf{H}_k^{vT}(2), ..., \mathbf{H}_k^{vT}(L)]^T, \qquad k = 1, 2, ...K,$$

and $\mathbf{H}_k^v(l)$, $(l = 1, 2, ..., L)$ is determined according to the STS scheme in [16]. Here, $\mathbf{H}_k^v(l)$ is modified to include the effect of pilot transmission as follows

$$\mathbf{H}_k^v(l) = \begin{bmatrix} h_{1l}^{k,v} & 0 & 0 & 0 \\ 0 & h_{2l}^{k,v} & 0 & 0 \\ 0 & 0 & h_{1l}^{k,v} & h_{2l}^{k,v} \\ 0 & 0 & -h_{2l}^{k,v} & h_{1l}^{k,v} \end{bmatrix}.$$

The transmitted data vector from the K users during the m^{th} symbol duration, $\mathbf{b}[m]$, is given by

$$\mathbf{b}[m] = [\mathbf{b}_1^T[m], \mathbf{b}_2^T[m], ..., \mathbf{b}_K^T[m]]^T, \qquad m = 0, 1, \ldots, M-1$$

where

$$\mathbf{b}_k[m] = \left[\sqrt{\frac{\rho_p}{2}}, \sqrt{\frac{\rho_p}{2}}, \sqrt{\frac{\rho_d}{2}} b_{k1}[m], \sqrt{\frac{\rho_d}{2}} b_{k2}[m]\right]^T, \qquad k = 1, 2, ..., K.$$

Finally, in (4.2), $\mathbf{n}^v[0]$ is a $[(2N + L - 1 + \tau_{max}) \times 1]$ vector representing the AWGN samples at the v^{th} receive antenna, each with zero mean and unit variance. From (4.2),

the received signal can be represented in a more compact form as

$$\mathbf{y}^v[0] = \mathbf{C}_p\mathbf{H}_p^v\mathbf{b} + \mathbf{n}^v[0] \tag{4.3}$$

where

$$\mathbf{C}_p = [\mathbf{C}[0], \mathbf{C}[1]], \quad \mathbf{H}_p^v = \mathbf{I}_2 \otimes \mathbf{H}^v, \quad \mathbf{b} = [\mathbf{b}[0]^T, \mathbf{b}[1]^T]^T,$$

and $\otimes$ denotes *Kronecker product* operation [57]. After sampling and despearding of the received signal, $\mathbf{y}^v[0]$, with the pilot and data code matrix $\mathbf{C}_p$, the output is given by

$$\mathbf{y}_c^v[0] = \mathbf{R}_p\mathbf{H}_p^v\mathbf{b} + \mathbf{N}_{cc}^v[0] \tag{4.4}$$

where $\mathbf{R}_p = \mathbf{C}_p^H\mathbf{C}_p$, is the pilot and data cross-correlation matrix, $\mathbf{N}_{cc}^v[0]$ is modelled as $N_c(\mathbf{0},\mathbf{R}_p)$ (zero mean complex Gaussian vector with covariance $\mathbf{R}_p$). In order to estimate the covariance matrix $\mathbf{R}_p$, we assume that the channel delays are known at the receiver and the channel coefficients are constant within a data block of M symbols, i.e., quasi-static fading channel. Note that, the authors in [19] have based their channel estimation on the channel despreader output, $\mathbf{y}_c^v[0]$. That is the channel estimation in [19] treats the multiuser interference and ISI as background noise. Hence, the error signal in the channel estimates are affected by the presence of ISI, MAI and thermal noise. The self interference between the two pilot signals of each user was also neglected in [19]. Here, we consider an asynchronous uplink channel where multiuser interference can limit the system performance. However to overcome the effects of multiuser interference resulting from the asynchronous transmission, we employ, after the despreader, a decorrelator detector at each receive antenna for channel estimation. This will show to improve the reliability of the estimation process. In this case, the output of the v^{th} channel decorrelator is given by

$$\mathbf{y}_d^v[0] = \mathbf{H}_p^v\mathbf{b} + \mathbf{N}_{cd}^v[0] \tag{4.5}$$

where $\mathbf{N}_{cd}^{v}[0]$ is $N_c(\mathbf{0}, \mathbf{R}_p^{-H})$. Note that the cross-correlation matrix inversion is based on the pseudo-inverse or the *Moore-Penrose* generalized inverse [80] which can be calculated using the singular value decomposition in $O(L^3K^3)$ operations [81]. Since this is implemented at each receive antenna, the total number of arithmetic operations needed by the overall removal operation is $O(VL^3K^3)$. For more details on the generalization of the decorrelator detector when $\mathbf{R}_p$ is rank deficient, the reader is referred to [[20] p. 241-242]. From (4.5), the first $4LK$ elements are then chosen from the v^{th} decorrelator output vector, $\mathbf{y}_d^v[0]$, for estimating the channel coefficients at the v^{th} receive antenna, yielding to

$$\begin{aligned} W_{1l}^{k,v} &= B' h_{1l}^{k,v} + w_{1l}^{k,v}, \\ W_{2l}^{k,v} &= B' h_{2l}^{k,v} + w_{2l}^{k,v}, \qquad k = 1, 2, ..., K; l = 1, 2, ..., L \end{aligned} \tag{4.6}$$

where $B' = \sqrt{\frac{\rho_p}{2}}$, $w_{1l}^{k,v}$ and $w_{2l}^{k,v}$ represent the errors in the channel estimates corresponding to the l^{th} path between the q^{th} transmit antenna (q=1,2) and the v^{th} receive antenna. From (4.6), we obtain the corresponding channel estimates as

$$\begin{aligned} \hat{h}_{1l}^{k,v} &= h_{1l}^{k,v} + e_{1l}^{k,v}, \\ \hat{h}_{2l}^{k,v} &= h_{2l}^{k,v} + e_{2l}^{k,v}, \qquad k = 1, 2, ..., K; l = 1, 2, ..., L \end{aligned} \tag{4.7}$$

where $e_{ql}^{k,v} = \frac{w_{ql}^{k,v}}{B'}$, $(q = 1, 2)$.

4.4 Data Detection

Having obtained the channel estimates as discussed in the previous section, and prior to data detection, the effect of the pilot sequences at each receive antenna is elimi-

nated from the received signal defined in (4.1) as

$$r^{v'}(t) = \sum_{k=1}^{K}\sum_{l=1}^{L}\sum_{m=0}^{M-1} h_{1l}^{k,v}\Big[A'(b_{k1}[m]c_{k1}(t-mT_s-\tau_k-\tilde{\tau}_l)+b_{k2}[m]c_{k2}(t-mT_s - \tau_k-\tilde{\tau}_l))\Big] + h_{2l}^{k,v}\Big[A'(b_{k2}[m]c_{k1}(t-mT_s-\tau_k-\tilde{\tau}_l)-b_{k1}[m]c_{k2}(t-mT_s-\tau_k - \tilde{\tau}_l))\Big] - B'e_{1l}^{k,v}P_{k1}(t-mT_s-\tau_k-\tilde{\tau}_l) - B'e_{2l}^{k,v}P_{k2}(t-mT_s-\tau_k-\tilde{\tau}_l)+n^v(t) \quad (4.8)$$

where $A' = \sqrt{\frac{\rho_d}{2}}$. In (4.8), the terms corresponding to the received pilot sequences are due to the errors in the channel estimates. Then, similar to the channel estimation procedure, $r^{v'}(t)$ is filtered, sampled at a rate $1/T_c$, and accumulated over an observation interval of $(2N+\tau_{max}+L-1)$ chips for the m^{th} data symbol of the received data block.

Using vector notation and with the help of Fig. 4.2, the data chip-matched filter output at the v^{th} receive antenna, $\mathbf{g}^v[m]$, can be expressed as

$$\mathbf{g}^v[0] = \mathbf{C}'[0]\mathbf{H}^{v'}\mathbf{b}'[0] + \mathbf{C}'[1]\mathbf{H}^{v'}\mathbf{b}'[1] - \mathbf{P}[0]\mathbf{E}^{v'} - \mathbf{P}[1]\mathbf{E}^{v'} + \mathbf{n}^v[0], \quad (4.9)$$

$$\mathbf{g}^v[m] = \mathbf{C}'[0]\mathbf{H}^{v'}\mathbf{b}'[m] + \mathbf{C}'[-1]\mathbf{H}^{v'}\mathbf{b}'[m-1] + \mathbf{C}'[1]\mathbf{H}^{v'}\mathbf{b}'[m+1] - \mathbf{P}[0]\mathbf{E}^{v'} - \mathbf{P}[-1]\mathbf{E}^{v'} - \mathbf{P}[1]\mathbf{E}^{v'} + \mathbf{n}^v[m], m = 1, ..., M-2 \quad (4.10)$$

$$\mathbf{g}^v[M-1] = \mathbf{C}'[0]\mathbf{H}^{v'}\mathbf{b}'[M-1] + \mathbf{C}'[-1]\mathbf{H}^{v'}\mathbf{b}'[M-2] - \mathbf{P}[0]\mathbf{E}^{v'} - \mathbf{P}[-1]\mathbf{E}^{v'} + \mathbf{n}^v[M-1], \quad (4.11)$$

where $\mathbf{C}'[0]$, $\mathbf{C}'[1]$, and $\mathbf{C}'[-1]$ include the data sequences corresponding to the current, following and previous STS symbols of the K-user system within the observation interval respectively, each has a dimension of $(2N+L-1+\tau_{max}) \times 2LK$ (see Appendix A.1). Similarly, $\mathbf{P}[0]$, $\mathbf{P}[1]$ and $\mathbf{P}[-1]$ have the same definitions of $\mathbf{C}'[0]$, $\mathbf{C}'[1]$, and $\mathbf{C}'[-1]$ except that the data sequences are replaced by the pilot sequences. In (4.9)-(4.11), the

channel impulse response of the K users, $\mathbf{H}^{v'}$, is defined by

$$\mathbf{H}^{v'} = diag\{\mathbf{H}_1^{v'}, \mathbf{H}_2^{v'}, ..., \mathbf{H}_K^{v'}\}$$

where

$$\mathbf{H}_k^{v'} = [\mathbf{H}_k^{v'^T}(1), \mathbf{H}_k^{v'^T}(2), ..., \mathbf{H}_k^{v'^T}(L)]^T, \qquad k = 1, 2, ...K,$$

$\mathbf{H}_k^{v'}(l), (l = 1, \ldots, L)$ is defined according to the employed STS scheme in [16] as

$$\mathbf{H}_k^{v'}(l) = \begin{bmatrix} h_{1l}^{k,v} & h_{2l}^{k,v} \\ -h_{2l}^{k,v} & h_{1l}^{k,v} \end{bmatrix}.$$

In (4.9), $\mathbf{E}^{v'}$ represents the channel estimation error vector of the K users which is given by

$$\mathbf{E}^{v'} = [\mathbf{E}_1^{v'^T}, \mathbf{E}_2^{v'^T}, ..., \mathbf{E}_K^{v'^T}]^T$$

where

$$\mathbf{E}_k^{v'} = \left[e_{11}^{k,v}, e_{21}^{k,v}, e_{12}^{k,v}, \ldots, e_{1L}^{k,v}, e_{2L}^{k,v}\right]^T, k = 1, 2, ..., K.$$

Finally, in (4.10), $\mathbf{b}'[m], (m = 0, \ldots, M-1)$ is given by

$$\mathbf{b}'[m] = [\mathbf{b}_1'^T[m], \mathbf{b}_2'^T[m], ..., \mathbf{b}_K'^T[m]]^T,$$

where

$$\mathbf{b}_k'[m] = [A'b_{k1}[m], A'b_{k2}[m]]^T, k = 1, 2, \ldots, K, m = 0, \ldots, M-1.$$

From (4.9)-(4.11), the received signal can be represented in a more compact form as

$$\mathbf{g}^v[m] = \mathbf{C}_d\mathbf{H}_d^v\mathbf{b}_d - B'\mathbf{P}_p\mathbf{E}^v + \mathbf{n}^v[m], \qquad m = 1, ..., M-2 \tag{4.12}$$

where

$$\mathbf{C}_d = [\mathbf{C}'[0], \mathbf{C}'[-1], \mathbf{C}'[1]], \tag{4.13}$$

$$\mathbf{P}_p = [\mathbf{P}[0], \mathbf{P}[-1], \mathbf{P}[1]], \tag{4.14}$$

$$\mathbf{H}_d^v = \mathbf{I}_3 \otimes \mathbf{H}^{v'}, \tag{4.15}$$

$$\mathbf{E}^v = [\mathbf{E}^{v'^T}, \mathbf{E}^{v'^T}, \mathbf{E}^{v'^T}]^T, \tag{4.16}$$

$$\mathbf{b}_d = [\mathbf{b}'[m]^T, \mathbf{b}'[m-1]^T, \mathbf{b}'[m+1]^T]^T. \tag{4.17}$$

Note that in the case of $m = 0$, one can exclude from (4.13)-(4.17), the effect of previous STS symbols on the data chip-matched filter output, $\mathbf{g}^v[m]$. Also, when $m = M - 1$, the effect of following symbols are excluded. After sampling the received signal, the data matched filter output, $\mathbf{g}^v[m]$ $(v = 1, \ldots, V)$, is correlated with the data code matrix, $\mathbf{C}_d$, as follows

$$\mathbf{g}_c^v[m] = \mathbf{R}_d \mathbf{H}_d^v \mathbf{b}_d - B' \mathbf{C}_d^H \mathbf{P}_p \mathbf{E}^v + \mathbf{N}_{dc}^v[m] \tag{4.18}$$

where $\mathbf{R}_d = \mathbf{C}_d^H \mathbf{C}_d$ represents the data cross-correlation matrix, and $\mathbf{N}_{dc}^v[m]$ is modelled as $N_c(\mathbf{0}, \mathbf{R}_d)$. It is clear from (4.18) that the data correlator output, $\mathbf{g}_c^v[m]$, suffers from MAI and ISI. Afterwards, the output of the data correlator (despreader) at each receive antenna is applied to a linear mapper defined by the inverse of the cross-correlation matrix, $\mathbf{R}_d^{-1}$, corresponding to the data code sequences to give

$$\mathbf{g}_d^v[m] = \mathbf{H}_d^v \mathbf{b}_d - B' \mathbf{Q}_d \mathbf{E}^v + \mathbf{N}_{dd}^v[m] \tag{4.19}$$

where $\mathbf{Q}_d = \mathbf{R}_d^{-1} \mathbf{C}_d^H \mathbf{P}_p$, and $\mathbf{N}_{dd}^v[m]$ is modeled as $N_c(\mathbf{0}, \mathbf{R}_d^{-H})$. Finally, the first $2LK$ elements of each decorrelator output vector, $\mathbf{g}_d^v[m]$ $(v = 1, \ldots, V)$, are combined with the corresponding channel estimates defined in (4.7) for final data estimates. Without loss of generality, we consider the first user as the desired user. Thus the decision variables for

the odd and even data bits are given by

$$\hat{b}_{11}[m] = \sum_{v=1}^{V} \sum_{l=1}^{L} Re\left\{ \hat{h}_{1l}^{1,v*} (\mathbf{g}_d^v[m])_{2l-1,1} - \hat{h}_{2l}^{1,v*} (\mathbf{g}_d^v[m])_{2l,1} \right\}, \tag{4.20}$$

$$\hat{b}_{12}[m] = \sum_{v=1}^{V} \sum_{l=1}^{L} Re\left\{ \hat{h}_{2l}^{1,v*} (\mathbf{g}_d^v[m])_{2l-1,1} + \hat{h}_{1l}^{1,v*} (\mathbf{g}_d^v[m])_{2l,1} \right\} \tag{4.21}$$

where $(\mathbf{g}_d^v[m])_{\zeta,1}$ $(\zeta = 1, 2, ..., 2L)$, is the ζ^{th} element of the v^{th} decorrelator output vector.

In the above analysis, we have considered the case of two transmit antennas. However, the estimation technique can be generalized to the case of $U \geq 2$ transmit antennas as follows. The transmitted data is first serial-to-parallel converted to U parallel substreams. As in the two transmit antenna case, the U parallel bits are spread using the STS scheme in [8]. Following the STS, the U parallel data bits are superimposed by U distinct pilot spreading codes, where each pilot sequence is assigned to a different antenna. Upon reception, the received signal is sampled at the chip rate and accumulated over an estimation interval of $UN + L - 1 + \tau_{max}$. Following the same procedure as in the two-antenna case, the received signal after sampling, is de-spread using $\mathbf{C}_p$ for channel estimation or $\mathbf{C}_d$ for data detection. Subsequently, decorrelation is implemented to remove the effect of MAI and ISI from both channel and data estimates.

4.5 Performance Analysis

In this section, we evaluate the performance of the proposed estimation technique in terms of its probability of bit error. We start by finding the decision variables corresponding to the data estimates at the decorrelator output and after signal combining. Then, we obtain the pdf of these decision variables which will facilitate the evaluation of the average probability of error.

4.5.1 BER Analysis

From (4.19), $(\mathbf{g}_d^v[m])_{2l-1,1}$ and $(\mathbf{g}_d^v[m])_{2l,1}$ in (4.20) and (4.21) are given by,

$$(\mathbf{g}_d^v[m])_{2l-1,1} = A'h_{1l}^{1,v}b_{11}[m] + A'h_{2l}^{1,v}b_{12}[m] - B'(\mathbf{Q}_d\mathbf{E}^v)_{2l-1,1} + (\mathbf{N}_{dd}^v)_{2l-1,1}, \tag{4.22}$$

$$(\mathbf{g}_d^v[m])_{2l,1} = -A'h_{2l}^{1,v}b_{11}[m] + A'h_{1l}^{1,v}b_{12}[m] - B'(\mathbf{Q}_d\mathbf{E}^v)_{2l,1} + (\mathbf{N}_{dd}^v)_{2l,1} \tag{4.23}$$

where $(\mathbf{Q}_d\mathbf{E}^v)_{2l-1,1}$ and $(\mathbf{Q}_d\mathbf{E}^v)_{2l,1}$ are defined in terms of the channel estimation errors corresponding to the K users at the v^{th} receive antenna. By partitioning $\mathbf{Q}_d$ into three groups: $\mathbf{Q}_{d1}$, $\mathbf{Q}_{d2}$ and $\mathbf{Q}_{d3}$ where each group has the same dimensions of $6LK \times 2LK$, $\mathbf{Q}_d\mathbf{E}^v$ is defined as $\mathbf{Q}_{ds}\mathbf{E}^{v'}$ where $\mathbf{Q}_{ds} = \mathbf{Q}_{d1} + \mathbf{Q}_{d2} + \mathbf{Q}_{d3}$. Consequently, $(\mathbf{Q}_d\mathbf{E}^v)_{2l-1,1}$ and $(\mathbf{Q}_d\mathbf{E}^v)_{2l,1}$ are derived as

$$(\mathbf{Q}_d\mathbf{E}^v)_{2l-1,1} = \mathbf{X}_{2l-1}\mathbf{E}^{v'}, \tag{4.24}$$

$$(\mathbf{Q}_d\mathbf{E}^v)_{2l,1} = \mathbf{X}_{2l}\mathbf{E}^{v'} \tag{4.25}$$

where $\mathbf{X}_\xi$ $(\xi = 2l-1, 2l)$, is a $[1 \times 2LK]$ vector consisting of the elements of the ξ^{th} raw of $\mathbf{Q}_{ds}$. Using (4.7) and (4.22)-(4.25), (4.20) can be written as

$$\begin{aligned}\hat{b}_{11}[m] = \sum_{v=1}^{V}\sum_{l=1}^{L} Re\{&(A'|h_{1l}^{1,v}|^2 + A'|h_{2l}^{1,v}|^2 + A'e_{1l}^{1v*}h_{1l}^{1,v} + A'e_{2l}^{1,v*}h_{2l}^{1,v})b_{11}[m] + (A' \\ &\times e_{1l}^{1,v*}h_{2l}^{1,v} - A'e_{2l}^{1,v*}h_{1l}^{1,v})b_{12}[m] - B'h_{1l}^{1,v*}\mathbf{X}_{2l-1}\mathbf{E}^{v'} - B'e_{1l}^{1,v*}\mathbf{X}_{2l-1}\mathbf{E}^{v'} + B'h_{2l}^{1,v*} \\ &\times \mathbf{X}_{2l}\mathbf{E}^{v'} + B'e_{2l}^{1,v*}\mathbf{X}_{2l}\mathbf{E}^{v'} + h_{1l}^{1,v*}(\mathbf{N}_{dd}^v)_{2l-1,1} + e_{1l}^{1,v*}(\mathbf{N}_{dd}^v)_{2l-1,1} - h_{2l}^{1,v*}(\mathbf{N}_{dd}^v)_{2l,1} \\ &- e_{2l}^{1,v*}(\mathbf{N}_{dd}^v)_{2l,1}\}.\end{aligned} \tag{4.26}$$

Now consider the case of $b_{11}[m] = +1$, then the probability of error is given by

$$P_b = \frac{1}{2}\tilde{P}_b(\hat{b}_{11}[m] < 0 | b_{12}[m] = +1) + \frac{1}{2}\tilde{P}_b(\hat{b}_{11}[m] < 0 | b_{12}[m] = -1). \tag{4.27}$$

Let the estimate $\hat{b}_{11}[m]$ equivalent to, $\mathcal{Z}_1$ when $b_{12}[m] = +1$, and $\mathcal{Z}_2$ when $b_{12}[m] = -1$. Then (4.27) can be written as

$$P_b = \frac{1}{2}\tilde{P}_b(\mathcal{Z}_1 < 0) + \frac{1}{2}\tilde{P}_b(\mathcal{Z}_2 < 0). \tag{4.28}$$

Given the complex variables x and y, we have

$$Re\{xy^*\} = \frac{1}{2}(xy^* + yx^*). \tag{4.29}$$

Then $\mathcal{Z}_1$ and $\mathcal{Z}_2$ can be expressed as a sum of independent symmetric quadratic forms as follows:

$$\mathcal{Z}_1 = \sum_{v=1}^{V} \mathbf{X}^{vH}\mathbf{S}_1\mathbf{X}^v = \sum_{v=1}^{V} Z_{1v}, \tag{4.30}$$

$$\mathcal{Z}_2 = \sum_{v=1}^{V} \mathbf{X}^{vH}\mathbf{S}_2\mathbf{X}^v = \sum_{v=1}^{V} Z_{2v}, \tag{4.31}$$

where

$$\mathbf{X}^v = [h_{11}^{1,v}, h_{21}^{1,v}, h_{12}^{1,v}, \ldots, h_{2L}^{1,v}, e_{11}^{1,v}, e_{21}^{1,v}, \ldots, e_{2L}^{1,v}, \ldots, e_{2L}^{K,v}, (\mathbf{N}_{dd}^v)_{1,1}, (\mathbf{N}_{dd}^v)_{2,1}, \ldots$$
$$, (\mathbf{N}_{dd}^v)_{2L-1,1}, (\mathbf{N}_{dd}^v)_{2L,1}]^T, \tag{4.32}$$

It should be noted that $\mathbf{X}^v$ is a $[4L + 2LK]$ complex normal vector with zero mean and covariance matrix $\mathbf{R}_x$ (the derivation of $\mathbf{R}_x$ is done in Appendix A.2). In (4.30)-(4.31), $\mathbf{S}_1$ and $\mathbf{S}_2$ are coefficient matrices of the quadratic forms Z_{1v} and Z_{2v} respectively , which are defined in Appendix A.3. The vectors $\mathbf{X}^v$ $(v = 1, \ldots, V)$, are statistically independent with the same covariance matrix $\mathbf{R}_x$. Also, the coefficient matrices, $\mathbf{S}_1$ and $\mathbf{S}_2$ are identical for each receive antenna.

From (4.30), we can find the characteristic function of the decision statistic $\mathcal{Z}_1$ as [82],[83]

$$\Phi_{Z_1}(\omega) = E\left[\exp\left[j\omega Z_1\right]\right] = E\left[\exp\left(j\omega \sum_{v=1}^{V} Z_{1v}\right)\right]$$
$$= \prod_{v=1}^{V} \phi_{Z_{1v}}(\omega) \tag{4.33}$$

where

$$\phi_{Z_{1v}}(\omega) = E\left[\exp\left(j\omega Z_{1v}\right)\right] \tag{4.34}$$

Note that the characteristic function of the quadratic form in (4.34) can be derived in terms of the eigenvalues of the matrix $\mathbf{S}_1\mathbf{R}_x$ as [83]

$$\phi_{Z_{1v}}(\omega) = \prod_{n=1}^{N'} \frac{1}{(1 - j\omega\lambda_n)} \tag{4.35}$$

where λ_n, $n = 1, \ldots, N'$, are the N' eigenvalues of the $\mathbf{S}_1\mathbf{R}_x$ matrix. Based on the matrix structure of $\mathbf{R}_x$ and $\mathbf{S}_1$ (see Appendix A.2 and A.3), both $\mathbf{S}_1$ and $\mathbf{R}_x$ are symmetric matrices. Also, we can notice that $\mathbf{R}_x$ is positive definite while $\mathbf{S}_1$ is generally singular matrix. Accordingly, the eigenvalues, λ_n, $n = 1, \ldots, N'$, are real valued but may be positive or negative. Substituting (4.35) in (4.33), the characteristic function $\Phi_{Z_1}(\omega)$ is given by

$$\Phi_{Z_1}(\omega) = \prod_{n=1}^{N'} \frac{1}{(1 - j\omega\lambda_n)^V}. \tag{4.36}$$

From (4.36), we can find the pdf of Z_1, f_{Z_1}, [75]. Using this pdf, one can evaluate the probability $\tilde{P}_b(Z_1 < 0)$ as follows [84]:

$$\tilde{P}_b(Z_1 < 0) = \int_{-\infty}^{0} f_{Z_1} dZ_1$$
$$= \frac{1}{2\pi} \int_{-\infty}^{0} \int_{-\infty}^{\infty} \Phi_{Z_1}(\omega) \exp[-j\omega Z_1] d\omega dZ_1$$
$$= \frac{1}{2} - \frac{1}{2\pi} \int_{-\infty}^{\infty} \left[\prod_{n=1}^{N'} \frac{1}{(1 - j\omega\lambda_n)^V}\right] (j\omega)^{-1} d\omega. \tag{4.37}$$

The remaining integral in (4.37) can be evaluated using contour integration, where we consider the integral along an indented contour C oriented in the positive direction as shown in Fig. 4.3. The contour integral is then given by

$$\oint_C f(z)dz = \oint_C \left[\prod_{n=1}^{N'} \frac{1}{(1-jz\lambda_n)^V}\right] (jz)^{-1}dz. \tag{4.38}$$

Note that the integrand in (4.38) has singularities at $z = 0$ and $z = -j/\lambda_1, \ldots, -j/\lambda_{N'}$.

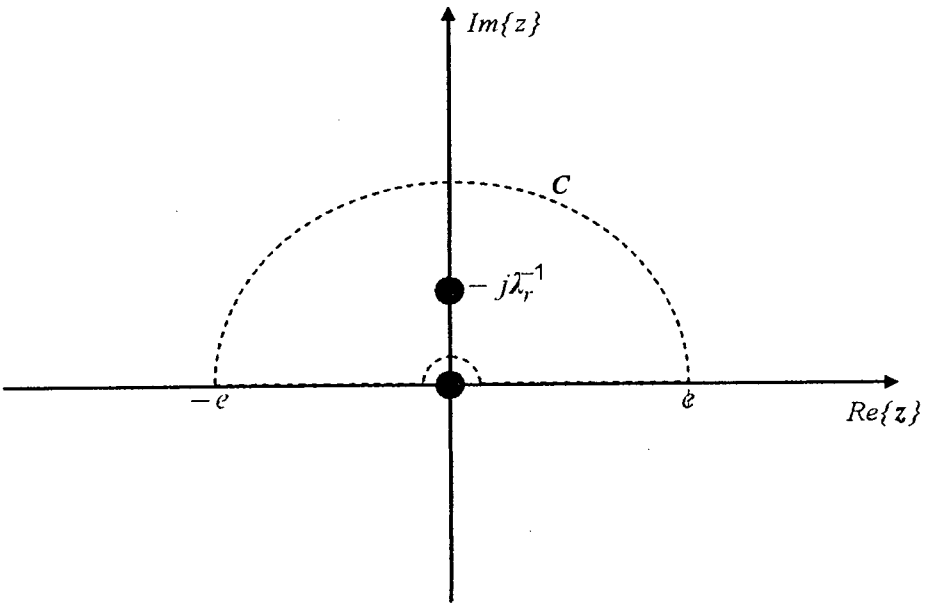

Figure 4.3: The indented contour C.

Since the contour C is located in the upper half-plane, the poles bounded by this contour are based on the negative eigenvalues (i.e., $\{\lambda_n\} < 0$). Using the residue theorem [85], the contour integral defined in (4.38) is given by,

$$\oint_C f(z)dz = j\pi Res(f(z), z = 0) + j2\pi \sum_{r=1}^{n_1} Res\left(f(z), z = -\frac{j}{\lambda_r}\right) \tag{4.39}$$

where $Res(f(z), z_o)$ denotes the residue of $f(z)$ at the pole $z = z_o$ and n_1 represents the

number of negative eigenvalues of the matrix $\mathbf{S}_1\mathbf{R}_x$. In order to evaluate the residues, we use the partial fraction expansion method of a rational function with high order poles. For further details regarding this method, the reader is referred to [76]. In (4.39), for all values of V, we have

$$Res(f(z), z = 0) = -j. \tag{4.40}$$

For the remaining distinct poles, the residues are found for different values of V according to [76]. For instance, for $V = 1, 2, 3$ receive antennas, we have respectively

$$\text{Case 1 } (V{=}1)\text{: } Res\left(f(z), z = -\frac{j}{\lambda_r}\right) = \prod_{r'=1,\lambda_{r'}\neq\lambda_r}^{N'} \frac{j}{\left(1 - \frac{\lambda_{r'}}{\lambda_r}\right)}, \tag{4.41}$$

$$\begin{aligned}\text{Case 2 } (V{=}2)\text{: } Res\left(f(z), z = -\frac{j}{\lambda_r}\right) &= j\lambda_r \times \prod_{n=1,\lambda_n\neq 0}^{N'} \lambda_n^{-2} \\ &\times \prod_{r'=1,\lambda_{r'}\neq\lambda_r}^{N'} \left(\frac{1}{(\lambda_{r'}^{-1} - \lambda_r^{-1})^2} \times \left[\lambda_r - \sum_{r'=1,\lambda_{r'}\neq\lambda_r}^{N'} \frac{2}{\lambda_{r'}^{-1} - \lambda_r^{-1}}\right]\right),\end{aligned} \tag{4.42}$$

$$\begin{aligned}\text{Case 3 } (V{=}3)\text{: } Res\left(f(z), z = -\frac{j}{\lambda_r}\right) &= \frac{j\lambda_r}{2} \times \prod_{n=1,\lambda_n\neq 0}^{N'} \lambda_n^{-3} \\ &\times \prod_{r'=1,\lambda_{r'}\neq\lambda_r}^{N'} \left(\frac{1}{(\lambda_{r'}^{-1} - \lambda_r^{-1})^3} \left[\lambda_r^2 + \sum_{r'=1,\lambda_{r'}\neq\lambda_r}^{N'} \frac{3}{(\lambda_{r'}^{-1} - \lambda_r^{-1})^2}\right.\right. \\ &\left.\left. + \left(\lambda_r - \sum_{r'=1,\lambda_{r'}\neq\lambda_r}^{N'} \frac{3}{\lambda_{r'}^{-1} - \lambda_r^{-1}}\right)^2\right]\right).\end{aligned} \tag{4.43}$$

Now using the obtained residues, we can evaluate the contour integral in (4.39). Note that the contour C can be split into a straight part (real part) and curved part. Let $f'(z) = P'(z)/Q'(z)$ where the degree of $P'(z)$ and $Q'(z)$ are u and s, respectively, then

the integration over the curved path tends to zero for large $|z|$ ($|z| \rightarrow \infty$) when $s \geq u+2$ [[85], theorem (19.5)]. Given this fact, and considering the limit as e goes to infinity, the integration defined in (4.39) can be evaluated as

$$\int_{-\infty}^{\infty} f(z_e)dz_e = j\pi Res(f(z), z=0) + j2\pi \sum_{r=1}^{n_1} Res\left(f(z), z=-\frac{j}{\lambda_r}\right) \tag{4.44}$$

where e represents the radius of the contour C, and z_e denotes the real part of the complex variable z. Substituting (4.44) in (4.37), we get $\tilde{P}_b(\mathcal{Z}_1 < 0)$ for the cases V=1,2, and 3 antennas respectively as follows,

$$\text{Case 1 } (V{=}1)\text{: } \tilde{P}_b(\mathcal{Z}_1 < 0) = \left(\prod_{n=1,\lambda_n\neq 0}^{N'} \lambda_n^{-1}\right) \times \sum_{r=1}^{n_1} (\lambda_r \times \prod_{r'=1,\lambda_{r'}\neq\lambda_r}^{N'} \frac{1}{\left(\lambda_{r'}^{-1} - \lambda_r^{-1}\right)}\Bigg), \tag{4.45}$$

$$\text{Case 2 } (V{=}2)\text{: } \tilde{P}_b(\mathcal{Z}_1 < 0) = \left(\prod_{n=1,\lambda_n\neq 0}^{N'} \lambda_n^{-2}\right) \times \sum_{r=1}^{n_1} \left(\lambda_r \prod_{r'=1,\lambda_{r'}\neq\lambda_r}^{N'} \frac{1}{(\lambda_{r'}^{-1} - \lambda_r^{-1})^2} \times \left[\lambda_r - \sum_{r'=1,\lambda_{r'}\neq\lambda_r}^{N'} \frac{2}{\lambda_{r'}^{-1} - \lambda_r^{-1}}\right]\right), \tag{4.46}$$

$$\text{Case 3 } (V{=}3)\text{: } \tilde{P}_b(\mathcal{Z}_1 < 0) = \left(\prod_{n=1,\lambda_n \neq 0}^{N'} \lambda_n^{-3} \right) \times \sum_{r=1}^{n_1} \left(\frac{\lambda_r}{2} \prod_{r'=1,\lambda_{r'} \neq \lambda_r}^{N'} \frac{1}{(\lambda_{r'}^{-1} - \lambda_r^{-1})^3} \right.$$
$$\times \left[\lambda_r^2 + \sum_{r'=1,\lambda_{r'} \neq \lambda_r}^{N'} \frac{3}{(\lambda_{r'}^{-1} - \lambda_r^{-1})^2} + \left(\lambda_r \right. \right.$$
$$\left. \left. - \sum_{r'=1,\lambda_{r'} \neq \lambda_r}^{N'} \frac{3}{\lambda_{r'}^{-1} - \lambda_r^{-1}} \right)^2 \right] \Bigg) . \tag{4.47}$$

Following the same procedure, we can evaluate the probability, $\tilde{P}_b(\mathcal{Z}_2 < 0)$, by replacing λ_n by β_n and n_1 by n_2, where β_n, $n = 1, \ldots, N$, are the eigenvalues of $\mathbf{S_2 R}_x$ and n_2 is the number of the corresponding negative eigenvalues. Finally, the average BER in (4.28) is obtained.

In the above analysis, we considered a uniform multipath intensity profile (MIP). However, this analysis can be generalized to the exponential MIP in the same manner where the subscript l is added to the corresponding variance of each multipath component, i.e., σ_h^2 is replaced by $\sigma_{hl}^2, l = 1, \ldots, L$ where σ_{hl}^2 is defined by [86]

$$\sigma_{hl}^2 = \sigma_o^2 \exp\left(-\frac{\kappa(l-1)}{L} \right), \quad l = 1, \ldots, L, \tag{4.48}$$

σ_o^2 is the average power of the initial path, and κ is the normalized decay factor. To keep the total fading power equal unity at each transmit antenna, we have

$$\sigma_o^2 = \frac{\exp\left(-\frac{\kappa}{L}\right) - 1}{\exp\left(-\kappa\right) - 1}. \tag{4.49}$$

Thus, the covariance of the channel vector $\mathbf{h}^v$, $\mathbf{R}_{H-H}$, is defined by a diagonal matrix with elements $\sigma_{h1}^2, \sigma_{h2}^2, \ldots, \sigma_{hL}^2$ (see Appendix A.2). Based on these assumptions, and following the same procedure as above, the closed forms of the average BER will have the same expressions as in (4.45)-(4.47), regardless the channel power delay profile.

4.5.2 Asymptotic Performance and Diversity

One way to prove that our system can deliver the full system diversity is through a comparison with the corresponding MRC with the same number of diversity branches. In that, we show that the slope of the BER performance for the two systems at high SNR is identical, indicating equal diversity orders. This approach is investigated in more details in the following section. On the other hand, if the eigenvalues of the matrix $\mathbf{S}_1\mathbf{R}_x$ of each receive antenna can be evaluated in terms of the received signal parameters, then expressions ((4.45)-(4.47)) can also be used to provide further insight into the proposed system performance. Unfortunately, a straightforward application of this approach proved to be difficult as the dimension of the corresponding matrix is $(4L+2LK) \times (4L+2LK)$.

In [87], Russ and Varanasi have encountered a similar problem when dealing with noncoherent multiuser detection over Rayleigh fading channels. Similarly Brehler and Varanasi [88] have noticed the same problem in analyzing the performance of quadratic receivers in fading channels. In these works, the authors have presented the BER performance of their receivers as a function of the eigenvalues of some parametric matrices. A remedy to this problem was proposed in [87] and [88], where the authors examined the asymptotic behavior of the corresponding eigenvalues as the SNR increases ($\rho_d \rightarrow \infty$). Using empirical results, the authors in [88] observed that half of the nonzero eigenvalues asymptotically approach -1 while the other half are positive and linearly proportional to ρ_d. As a result, they concluded that such a structure of eigenvalues is sufficient to prove the full system diversity is equal to the number of asymptotic positive (negative) eigenvalues.

In the previous section, we have shown that $\mathbf{S}_1\mathbf{R}_x$ is defined for any v^{th} receive antenna, $v = 1, \cdots, V$ (see Appendix A.2 and A.3). Therefore, the estimated eigenvalues of this matrix are equivalent to the eigenvalues of a STS system with two transmit and one receive antenna assuming L resolvable paths per transmit antenna (equivalent to a system with $2L$ diversity order).

Following the same approach as in [87] and [88], we have noticed that half of the nonzero eigenvalues are asymptotically equal to ϵ, ($\epsilon \rightarrow 0^-$ as the SNR $\rho_d \rightarrow \infty$), where 0^- denotes a very small negative value. The remaining half of the nonzero asymptotic eigenvalues is positive and linearly proportional to ρ_d. It should be noted, however, that this result did not turn out to be identical to the result obtained in [88] since we consider a different system configuration. Similarly, the structure of these eigenvalues show that the number of asymptotic positive (negative) eigenvalues is equivalent to the full diversity of a STS system with $2L$ diversity order.

Fig. 4.4 shows a sample of our results where we consider the proposed system with five users, two transmit and one receive antenna, for $L = 2, 3$ resolvable paths. This system produces a group of 8 nonzero eigenvalues for the first case ($L = 2$), and a group of 12 nonzero eigenvalues for the second case ($L = 3$). For each group, half of the nonzero eigenvalues is positive and the other is negative. This confirms that the number of positive eigenvalues represents the full system diversity, where the number of positive eigenvalues of each group (four and six respectively) is equal to the full system diversity of each case.

By utilizing this asymptotic behavior of eigenvalues, we are able to study the behavior of the BER as $\rho_d \rightarrow \infty$. Note that the first term in the right-hand side of (4.45)-(4.47) takes the form $\prod_{n=1,\lambda_n \neq 0}^{N'} \lambda_n^{-V}$ where V=1,2 and 3 receive antennas. In the asymptotic case, this term is proportional to ρ_d^{-2LV}. The remaining terms which belong to the right-hand side of these equations include a common factor in the form

$$\left(\prod_{r'=1,\lambda_{r'} \neq \lambda_r}^{N'} \frac{1}{(\lambda_{r'}^{-1} - \lambda_r^{-1})^V} = \prod_{r'=1,\lambda_{r'} \neq \lambda_r}^{N'} \frac{\lambda_r^V}{(\frac{\lambda_r}{\lambda_{r'}} - 1)^V} \right), V = 1, 2, 3.$$

Taking the limit of this term as $\rho_d \rightarrow \infty$, and substituting with the positive and negative asymptotic eigenvalues, one can easily show that the limit of this term has a constant value independent of SNR, ρ_d. Consequently, the BER expressions in (4.45)-(4.47) show

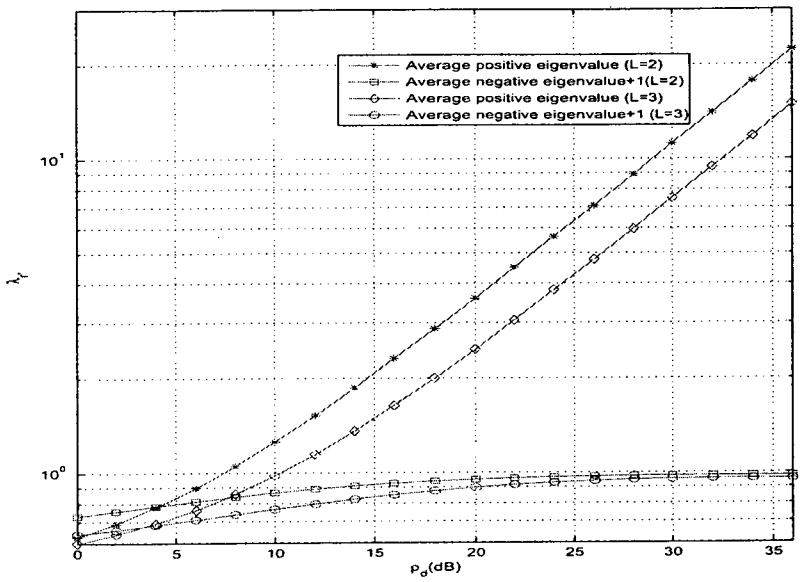

Figure 4.4: Asymptotic nonzero eigenvalues of 5-user STS system with L=2,3 paths, two antennas at the transmitter and one antenna at the receiver side.

that the proposed system achieves a diversity order of $2LV$.

4.6 Simulation Results

In this section, we examine the BER performance of the STS system employing the proposed channel and data estimation technique. Both Monte-Carlo simulations and the analytical results are presented for different system configurations. In all cases, we consider a DS-CDMA system with two transmit and $V = 1, 2, 3$ receive antennas. We also consider an uplink asynchronous transmission of a data block of thousand symbols (M=1000) over a frequency-selective slow-fading channel. Throughout the simulations, we consider a multiuser system where all users are assigned Walsh code sequences of length 64 chips for the pilot and data sequences. The delay among user signals, (τ_k, $k \in \{1, 2, ..., K\}$), are assumed to be multiple of chip periods within T_s. Without loss of generality, we assume that the users' delays satisfy the condition $\tau_1 = 0 \leq \ldots \leq \tau_k \leq \ldots \leq \tau_K \leq T_s$ [73]. The

path delay is also assumed to be multiple of chip intervals, $\tilde{\tau}_l = lT_c$, $l = 1, 2, \ldots, L$. Since we assume that the channel coefficients are constant during the transmission of the data block, we consider in all our simulations that the pilot sequence is superimposed to the STS signal during the first symbol period of each data block. This estimation interval includes sufficient information about the channel in order to implement the estimation process; the multipath channel coefficients and the delayed versions of the pilot sequences assigned to the K users. This enables us to implement the despreading and the decorrelation successively in order to get the channel estimates. In this case, the average pilot signal to noise ratio among the frame, $PNR = 10\log\rho_d - 10\log M$. Along our simulations, we compare the BER performance of the STS system versus different data signal to noise ratios, ρ_d.

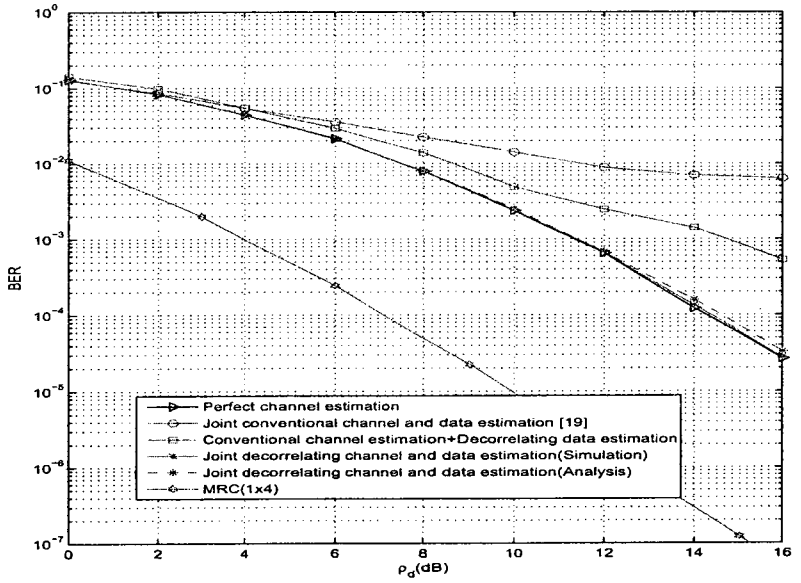

Figure 4.5: Comparison between different channel estimation and data detection techniques for the 5-user STS system with L=2 paths, PNR=5dB, two antennas at the transmitter and one antenna at the receiver side.

Fig. 4.5 shows the BER performance for different channel estimation and data detection techniques: (i) perfect knowledge of the channel at the receiver (reference case);

(ii) conventional channel estimation and data detection [19] (no MAI removal from both the channel and data estimates); (iii) conventional channel estimation followed by decorrelating data detection (only interference removal from the data estimates); and (iv) the proposed decorrelating channel and data estimation technique. Confirmed by simulations, our analytical results prove that the proposed scheme achieves a performance very close to the perfect channel estimation case for PNR=5dB. Examining the results in Fig. 4.5, one can see the effect of interference removal from both channel and data estimates on the system performance. Note that the third system renders a slight improvement over the conventional technique [19], due to the MAI removal from the data estimates but still affected by the imperfect channel estimation. With MAI removal from both the channel and data estimates, the proposed receiver outperforms the other estimation techniques. For reference, we included the BER performance of the MRC with four diversity branches. We can notice that the proposed scheme is able to deliver the full system diversity ($2VL$) at the prescribed PNR.

Fig. 4.6 shows the performance of the proposed system with the same antenna configuration as a function of PNR. Compared with the perfect channel estimation case, the proposed receiver achieves accurate estimates for PNR greater than 0 dB. Fig. 4.7 also shows the performance of the proposed scheme when the number of resolvable paths is increased to $L = 3$ per transmit antenna. The proposed receiver is shown to offer accurate channel estimates even when the number of resolvable paths increases. Also note that the system in this case offers a diversity order of six ($2VL = 6$), as evident from the comparison with the equivalent MRC with same number of diversity branches. In Fig. 4.8, the BER performance of our system is examined for 2×3 MIMO systems with two resolvable paths per transmit antenna and different number of users. The results conclude that the effect of increased interference only appears as a SNR loss and no diversity loss is incurred.

In Fig. 4.9 we investigate the performance of our proposed system considering

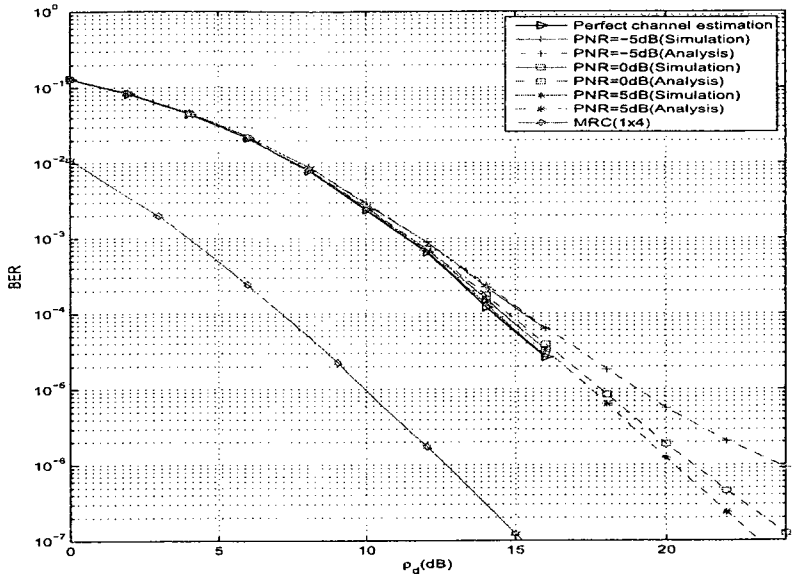

Figure 4.6: Effect of different PNR values on the BER performance of the proposed estimation technique for a 5-user STS system with L=2 paths, two antennas at the transmitter and one antenna at the receiver side.

different channel power delay profiles, namely uniform MIP with unity total fade power ($\sigma_h^2 = 1/L$) and exponential MIP with unity total fade power (see equation (4.48)). The results show that the realistic channel assumptions are interpreted as SNR loss without affecting the full system diversity.

In all the results, our analytical results are shown to be in excellent agreement with the simulated ones, and the full system diversity is maintained.

4.7 Conclusions

We have proposed a channel estimation and data detection technique based on the superimposed training approach for STS systems. In particular, we have shown that the proposed scheme is robust to channel interference caused by the multiple-access transmission in asynchronous CDMA uplinks. Furthermore, this scheme achieves accurate channel

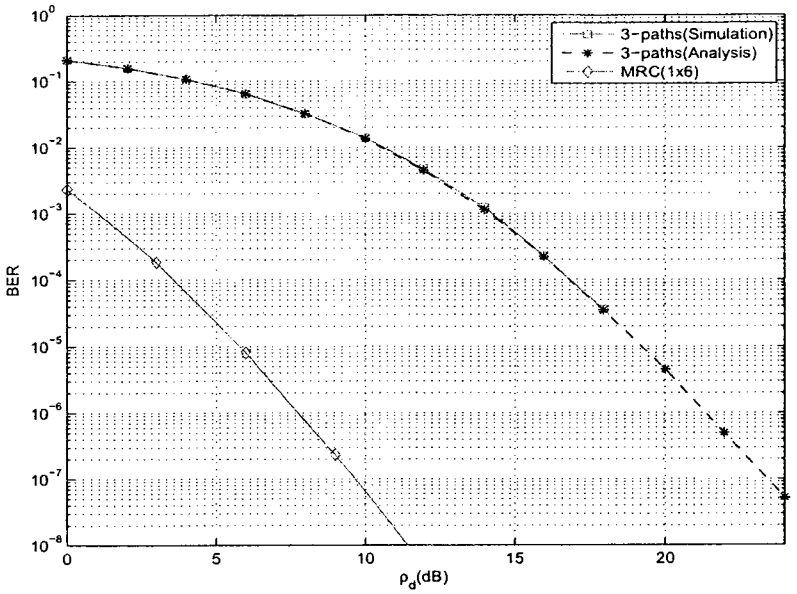

Figure 4.7: BER performance of the proposed estimation technique for a 5-user STS system with L=3 paths and PNR=5dB, two antennas at the transmitter and one antenna at the receiver side.

estimates and offers high spectral efficiency. However, there is a power penalty since a portion of the transmitted power is assigned to the training sequences. In addition, each user is assigned four spreading codes. This wastes the system resources. Therefore, in the following chapter, we provide another JDE technique based on the EM algorithm. This technique has the advantage of achieving the ML solution iteratively without wasting the system resources at the expense of some additional computational resources.

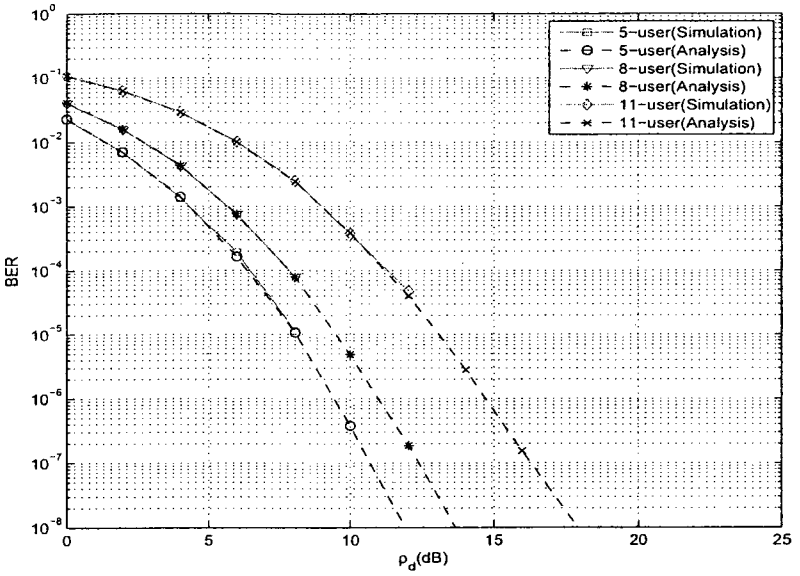

Figure 4.8: BER performance of the proposed estimation technique for the multiuser STS system with L=2 paths and PNR=5dB. The STS system employs two transmit antennas and V=3 antennas at the receiver side.

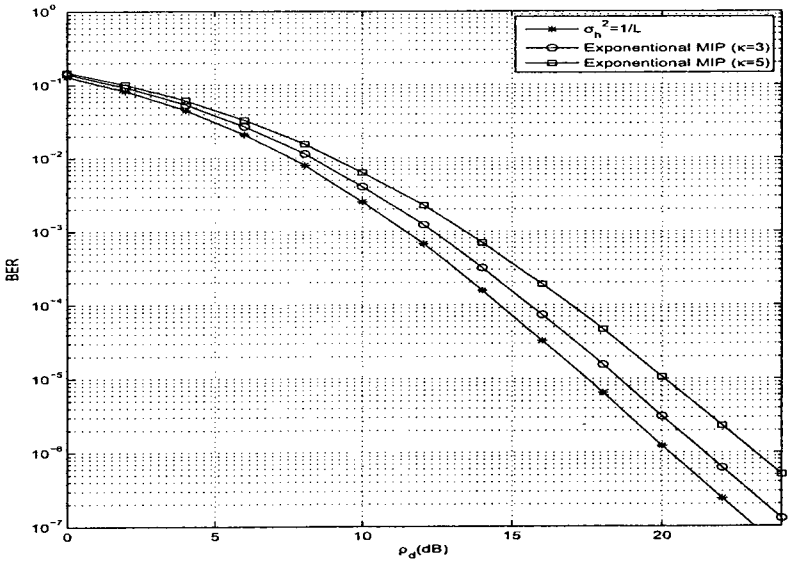

Figure 4.9: BER performance of the proposed system considering different channel delay profiles. The STS system employs two transmit and one receive antenna with L= 2 paths and PNR=5dB.

Chapter 5

EM-Based Joint Channel Estimation and Data Detection for MIMO-CDMA Systems

5.1 Introduction

In this chapter, we present an iterative joint channel estimation and data detection technique for MIMO CDMA systems over frequency-selective fading channels. The proposed receiver performs the channel estimation and data detection using the expectation-maximization (EM) algorithm. We derive a closed-form expression for the optimized weight coefficients of the EM algorithm, which is shown to provide large performance improvement relative to the conventional equal-weight EM-based signal decomposition. Our results show that the receiver can achieve near-optimum performance with modest complexity using very few training symbols.

5.2 System Model

Throughout our work, we consider a transmit diversity scheme with U=2 transmit antennas at the mobile user and V multiple receive antennas at the base station. We also consider the original STS scheme proposed in [16] for an asynchronous K-user system over a slow frequency-selective fading channel with L resolvable paths. The channel coefficients are, therefore, considered fixed within a block of M codewords, where each codeword has a period of $T_s = 2T_b$ and T_b denotes the bit period. The received complex low-pass equivalent signal at the v^{th} receive antenna is given by

$$r^v(t) = \sum_{k=1}^{K}\sum_{l=1}^{L}\sum_{m=0}^{M-1} h_{1l}^{k,v}\Big[b_{k1}[m]c_{k1}(t - mT_s - \tau_k - \tilde{\tau}_l) + b_{k2}[m]c_{k2}(t - mT_s - \tau_k - \\ - \tilde{\tau}_l)\Big] + h_{2l}^{k,v}\Big[b_{k2}[m]c_{k1}(t - mT_s - \tau_k - \tilde{\tau}_l) - b_{k1}[m]c_{k2}(t - mT_s - \tau_k - \tilde{\tau}_l)\Big] + n^v(t), \tag{5.1}$$

where $b_{k1}[m]$ and $b_{k2}[m]$ are the odd and even data streams of the k^{th} user within the m^{th} codeword interval. The codes $c_{k1}(t)$ and $c_{k2}(t)$ represent the k^{th} user's spreading sequences with processing gain $2N$, where $N = T_b/T_c$ is the number of chips per bit, and T_c is the chip duration. In (5.1), $h_{ql}^{k,v}$, $q = 1, 2$, is the attenuation coefficient corresponding to the k^{th} user, l^{th}path from the q^{th} transmit antenna to the v^{th} receive antenna, where $h_{ql}^{k,v} = \sqrt{\frac{E_k}{2}}\alpha_{ql}^{k,v}$, $\alpha_{ql}^{k,v}$ is the corresponding fading channel coefficient and E_k is the k^{th} user transmit energy. These attenuation coefficients are modeled as independent complex Gaussian random variables with zero mean and variance σ_k^2, where $\sigma_k^2 = \frac{E_k}{2}\sigma_h^2$, and $\sigma_h^2 = \frac{1}{L}$. The noise $n^v(t)$ is Gaussian with zero mean and variance N_o. At the receiver side, the received signal at each receive antenna is chip-matched filtered, sampled at a rate $1/T_c$, and accumulated over an observation interval of $(2N + \tau_{max} + L - 1)$ chips corresponding to the m^{th} symbol of the received data block for the K-user system. The $(\tau_{max} + L - 1)$ samples are due to the maximum multipath delay (i.e., delay of the l^{th} path) corresponding to the

user with the maximum transmit delay, τ_{max}. Let $\mathbf{y}^v[m]$ denote the observation vector at the v^{th} receive antenna containing all samples related to the STS symbols transmitted by the K users within the observation interval. Then, we have

$$\mathbf{y}^v[m] = (\mathbf{C}[0]\mathbf{B}(m) + \mathbf{C}[-1]\mathbf{B}(m-1) + \mathbf{C}[1]\mathbf{B}(m+1))\,\mathbf{h}^v + \mathbf{n}^v[m], \quad m = 1, \ldots, M-2, \quad (5.2)$$

where $\mathbf{C}[0]$, $\mathbf{C}[-1]$, and $\mathbf{C}[1]$ include the code sequences corresponding to the current, previous and following STS symbols of the K-user system within the observation interval respectively, each has a dimension of $(2N + L - 1 + \tau_{max}) \times 2LK$ (see Appendix A.1). In (5.2), $\mathbf{B}(m)$, $m = 0, \ldots, M-1$, represents the users data matrix within the m^{th} period, defined as

$$\mathbf{B}(m) = diag\{\mathbf{B}_1(m), \mathbf{B}_2(m), \ldots, \mathbf{B}_K(m)\},$$

where

$$\mathbf{B}_k(m) = \mathbf{I}_L \otimes \tilde{\mathbf{b}}_k(m), \quad \tilde{\mathbf{b}}_k(m) = \begin{bmatrix} b_{k1}[m] & b_{k2}[m] \\ b_{k2}[m] & -b_{k1}[m] \end{bmatrix}, k = 1, \ldots, K; m = 0, \ldots, M-1,$$

and $\mathbf{I}_L$ is an identity matrix of L-dimension. Also, $\mathbf{h}^v$ is $(2LK \times 1)$ channel coefficients vector defined as

$$\mathbf{h}^v = [\mathbf{h}_1^{vT}, \mathbf{h}_2^{vT}, \ldots, \mathbf{h}_K^{vT}]^T,$$

where $\mathbf{h}_k^v = [h_{11}^{k,v}, h_{21}^{k,v}, \ldots, h_{2L}^{k,v}]^T$. Finally, in (5.2), $\mathbf{n}^v[m]$ is a $[(2N + L - 1 + \tau_{max}) \times 1]$ vector representing the AWGN samples at the v^{th} receive antenna, each with zero mean and variance N_o. Note that in the case of $m = 0$, one can exclude from (5.2) the effect of previous STS symbols on the data chip-matched filter output, $\mathbf{y}^v[m]$. Also, when $m = M - 1$, the effect of following symbols are excluded. After sampling the received signal, the matched filter output at the v^{th} receive antenna , $\mathbf{y}^v[m]$, is correlated with the

code matrix, $\mathbf{C}[0]$, as follows

$$\mathbf{y}_c^v[m] = \left(\mathbf{R}[0]\mathbf{B}(m) + \mathbf{R}[-1]\mathbf{B}(m-1) + \mathbf{R}[1]\mathbf{B}(m+1)\right)\mathbf{h}^v + \mathbf{n}_c^v[m], \quad m = 1, \ldots, M-2, \quad (5.3)$$

where $\mathbf{R}[0] = \mathbf{C}^H[0]\mathbf{C}[0]$, $\mathbf{R}[-1] = \mathbf{C}^H[0]\mathbf{C}[-1]$, and $\mathbf{R}[1] = \mathbf{C}^H[0]\mathbf{C}[1]$. Also, we can notice that $\mathbf{R}[1] = \mathbf{R}[-1]^T$ (see Appendix A.1). In (5.3), $\mathbf{n}_c^v[m]$ is modelled as $N_c(\mathbf{0}, \mathbf{R}[0])$. Similar to [20], let

$$\mathbf{R}[0] = \mathbf{F}[0]^T\mathbf{F}[0] + \mathbf{F}[1]^T\mathbf{F}[1], \quad (5.4)$$

and

$$\mathbf{R}[-1] = \mathbf{F}[0]^T\mathbf{F}[1], \quad (5.5)$$

where $\mathbf{F}[0]$ is a lower triangular matrix, and $\mathbf{F}[1]$ is an upper right triangular matrix with zero diagonal. If $\mathbf{y}_c^v[m]$ is passed through a filter with impulse response $(\mathbf{F}[0] + \mathbf{F}[1]z)^{-T}$ [20], then

$$\mathbf{y}_w^v[m] = \sum_{\Delta m=0}^{1} \mathbf{F}[\Delta m]\mathbf{B}\left(m - \Delta m\right)\mathbf{h}^v + \mathbf{n}_w^v[m], \quad (5.6)$$

where $\mathbf{n}_w^v[m]$ is a complex Gaussian vector with zero mean and covariance matrix $N_o\mathbf{I}_{2LK}$, and $\mathbf{I}_{2LK}$ is an identity matrix of dimension $2LK$. Note that both $\mathbf{y}_c^v[m]$ and $\mathbf{y}_w^v[m]$ have the same information about the transmitted data. Due to the whitening noise property of (5.6), our subsequent analysis will be based on $\mathbf{y}_w^v[m]$.

5.3 EM-Based ST Receiver

In [37], the EM algorithm is proposed as a JDE technique for SISO CDMA systems. Here, we extend this work to MIMO CDMA systems. Our subsequent analysis is based on the approach proposed in [36] for the estimation problem of superimposed signals. Using this approach, the observed data is decomposed into their signal components. Then, the

parameters of each signal component are estimated separately and iteratively using the EM algorithm. Accordingly, we decompose the whitening filter output, $\mathbf{y}_w^v[m]$, into a sum of K statistically independent components, i.e.,

$$\mathbf{y}_w^v[m] = \sum_{k=1}^{K} \mathbf{g}_k^v(m), \tag{5.7}$$

where $\mathbf{g}_k^v(m) = \sum_{\Delta m=0}^{1} \mathbf{F}_k[\Delta m]\mathbf{B}_k(m-\Delta m)\mathbf{h}_k^v + \mathbf{n}_{wk}^v[m]$, $\mathbf{F}_k[\Delta m]$ is $2LK \times 2L$ matrix including the $2L$ columns corresponding to the k^{th} user in the matrix $\mathbf{F}[\Delta m]$, $\mathbf{n}_{wk}^v[m]$ is a complex Gaussian vector with zero mean and covariance matrix $\beta_k^v N_o \mathbf{I}_{2LK}$ and β_k^v is a non-negative value satisfying the constraint $\sum_{k=1}^{K} \beta_k^v = 1$. Our goal is to obtain the users' data estimates using the EM algorithm. First, we define the EM algorithm parameters:

1. *Observed data*, $\mathbf{y}_w$, which includes the outputs of the V whitening matched filters within a frame of M codes is given by

$$\mathbf{y}_w = [\mathbf{y}_w^{1\,T}, \mathbf{y}_w^{2\,T}, \ldots, \mathbf{y}_w^{V\,T}]^T$$

where

$$\mathbf{y}_w^v = [\mathbf{y}_w^v[0]^T, \mathbf{y}_w^v[1]^T, \ldots, \mathbf{y}_w^v[M-1]^T]^T, v = 1, \ldots, V.$$

2. *Parameters to be estimated*, $\mathbf{b}$, includes the transmitted data bits from the K users within the frame period

$$\mathbf{b} = [\mathbf{b}_1^T, \mathbf{b}_2^T, \ldots, \mathbf{b}_K^T]^T,$$

where

$$\mathbf{b}_k = [\mathbf{b}_k[0]^T, \mathbf{b}_k[1]^T, \ldots, \mathbf{b}_k[M-1]^T]^T, k = 1, \ldots, K,$$

and $\mathbf{b}_k[m] = [b_{k1}[m], b_{k2}[m]]^T, m = 0, \ldots, M-1$.

3. *Complete data*, $\mathbf{G}$: we employ the complete data definition in [37], where the unknown channel coefficient vectors are included as a part of the complete data as

follows:

$$\mathbf{G} = [\mathbf{G}^{1^T}, \mathbf{G}^{2^T}, \ldots, \mathbf{G}^{V^T}]^T,$$

where

$$\mathbf{G}^v = [(\mathbf{g}_1^v, \mathbf{h}_1^v), (\mathbf{g}_2^v, \mathbf{h}_2^v), \ldots, (\mathbf{g}_K^v, \mathbf{h}_K^v)], v = 1, \ldots, V,$$

and

$$\mathbf{g}_k^v = [\mathbf{g}_k^v(0), \mathbf{g}_k^v(1), \ldots, \mathbf{g}_k^v(M-1)], k = 1, \ldots, K.$$

Since the components of $\mathbf{G}$ given $\mathbf{b}$ are statistically independent, the complete log-likelihood function is given by

$$\Phi(\mathbf{G}|\mathbf{b}) = \sum_{v=1}^{V} \sum_{k=1}^{K} \Phi(\mathbf{g}_k^v, \mathbf{h}_k^v|\mathbf{b}_k), \tag{5.8}$$

where

$$\Phi(\mathbf{g}_k^v, \mathbf{h}_k^v|\mathbf{b}_k) = \Phi(\mathbf{g}_k^v|\mathbf{h}_k^v, \mathbf{b}_k) + \Phi(\mathbf{h}_k^v|\mathbf{b}_k). \tag{5.9}$$

The second summand in (5.9) is neglected as it is independent of $\mathbf{b}$. Therefore, (5.9) is reduced to

$$\begin{aligned}\Phi(\mathbf{g}_k^v, \mathbf{h}_k^v|\mathbf{b}_k) \propto -\sum_{m=0}^{M-1} \left(\mathbf{g}_k^v(m) - \sum_{\Delta m=0}^{1} \mathbf{F}_k[\Delta m]\mathbf{B}_k(m-\Delta m)\mathbf{h}_k^v \right)^H \\ \times \left(\mathbf{g}_k^v(m) - \sum_{\Delta m=0}^{1} \mathbf{F}_k[\Delta m]\mathbf{B}_k(m-\Delta m)\mathbf{h}_k^v \right).\end{aligned} \tag{5.10}$$

By neglecting the terms in (5.10) which are independent of $\mathbf{b}$, the conditional likelihood in (5.10) can be simplified to

$$\begin{aligned}\Phi(\mathbf{g}_k^v, \mathbf{h}_k^v|\mathbf{b}_k) \propto \sum_{m=0}^{M-1} 2Re\{&\mathbf{h}_k^{vH}\mathbf{B}_k(m)\mathbf{F}_k[0]^T\mathbf{g}_k^v(m) + \mathbf{h}_k^{vH}\mathbf{B}_k(m)\mathbf{F}_k[1]^T\mathbf{g}_k^v(m+1) \\ &- \mathbf{h}_k^{vH}\mathbf{B}_k(m)\mathbf{R}_{kk}[-1]\mathbf{B}_k(m-1)\mathbf{h}_k^v - \mathbf{h}_k^{vH}\mathbf{B}_k(m+1)\mathbf{R}_{kk}[-1] \\ &\times \mathbf{B}_k(m)\mathbf{h}_k^v\} - \mathbf{h}_k^{vH}\mathbf{B}_k(m)\mathbf{R}_{kk}[0]\mathbf{B}_k(m)\mathbf{h}_k^v, \end{aligned} \tag{5.11}$$

where $\mathbf{R}_{kk}[-1] = \mathbf{F}_k[0]^T\mathbf{F}_k[1]$, and $\mathbf{R}_{kk}[0] = \mathbf{F}_k[0]^T\mathbf{F}_k[0]+\mathbf{F}_k[1]^T\mathbf{F}_k[1]$. At the i^{th} iteration, the E-step of the EM algorithm is implemented by taking the expectation of the complete log-likelihood function defined in (5.8) with respect to the observed data vector, $\mathbf{y}_w$, and the current EM data estimates, $\mathbf{b}^i$, i.e.,

$$\mathcal{Q}(\mathbf{b}|\mathbf{b}^i) = \sum_{k=1}^{K} \mathcal{Q}_k(\mathbf{b}_k|\mathbf{b}^i), \tag{5.12}$$

where

$$\mathcal{Q}_k(\mathbf{b}_k|\mathbf{b}^i) = \sum_{v=1}^{V} E\left[\Phi(\mathbf{g}_k^v, \mathbf{h}_k^v|\mathbf{b}_k)|\mathbf{y}_w, \mathbf{b}^i\right] \tag{5.13}$$

From (5.11), the expectation of the individual log-likelihood function is reduced to

$$\begin{aligned}\mathcal{Q}_k(\mathbf{b}_k|\mathbf{b}^i) = \sum_{v=1}^{V}\sum_{m=0}^{M-1} 2Re\{&E\left[\mathbf{h}_k^{vH}\mathbf{B}_k(m)\mathbf{F}_k[0]^T\mathbf{g}_k^v(m) + \mathbf{h}_k^{vH}\mathbf{B}_k(m)\mathbf{F}_k[1]^T\right. \\ &\times\mathbf{g}_k^v(m+1) - \mathbf{h}_k^{vH}\mathbf{B}_k(m)\mathbf{R}_{kk}[-1]\mathbf{B}_k(m-1)\mathbf{h}_k^v - \mathbf{h}_k^{vH}\mathbf{B}_k(m+1)\mathbf{R}_{kk}[-1] \\ &\left.\times\mathbf{B}_k(m)\mathbf{h}_k^v|\mathbf{y}_w, \mathbf{b}^i\right]\} - E\left[\mathbf{h}_k^{vH}\mathbf{B}_k(m)\mathbf{R}_{kk}[0]\mathbf{B}_k(m)\mathbf{h}_k^v|\mathbf{y}_w, \mathbf{b}^i\right]. \end{aligned} \tag{5.14}$$

To find the joint conditional expectation in (5.14), we evaluate $E\left[\mathbf{g}_k^v(m_s)|\mathbf{y}_w, \mathbf{b}^i, \mathbf{h}\right]$, $m_s \in \{m, m+1\}$, where $\mathbf{h} = [\mathbf{h}^1, \mathbf{h}^2, \ldots, \mathbf{h}^V]$. Then the subsequent expression is used to find $E\left[f(\mathbf{h}_k^v)|\mathbf{y}_w, \mathbf{b}^i\right]$, where $f(\mathbf{h}_k^v)$ denotes the resultant function in $\mathbf{h}_k^v$. By noting that the

conditional probability density function, $P_c\left(\mathbf{g}_k^v(m_s)|\mathbf{y}_w, \mathbf{b}^i, \mathbf{h}\right)$ is Gaussian with mean [36]

$$E\left[\mathbf{g}_k^v(m_s)|\mathbf{y}_w, \mathbf{b}^i, \mathbf{h}\right] = \sum_{\Delta m=0}^{1} \mathbf{F}_k[\Delta m]\mathbf{B}_k(m_s - \Delta m)^i \mathbf{h}_k^v + \beta_k^v \Bigg(\mathbf{y}^v(m_s) - \sum_{j=1}^{K} \sum_{\Delta m=0}^{1} \mathbf{F}_j[\Delta m]\mathbf{B}_j(m_s - \Delta m)^i \mathbf{h}_j^v \Bigg), m_s \in \{m, m+1\}, \quad (5.15)$$

The conditional expectation of the likelihood function in (5.14), after some algebraic manipulations, can be expressed as (see Appendix B.1)

$$\begin{aligned}
\mathcal{Q}_k(\mathbf{b}_k|\mathbf{b}^i) = \sum_{v=1}^{V}\sum_{m=1}^{M} Re\Bigg\{ \sum_{l=1}^{L}\sum_{l'=1}^{L} \Bigg(& (1-\beta_k^v)\Big(\rho_{1,ll',m}^{kk^i}(-1) + \rho_{1,ll',m}^{kk^i}(1) + \\
& \rho_{1,ll',m}^{kk^i}(0)\Big) - \rho_{1,ll',m}^{kk}(-1) - \rho_{1,ll',m}^{kk}(1)\Big)\Big(h_{1l}^{k,v}\Big)^{i^*}\Big(h_{1l'}^{k,v}\Big)^{i} + \Bigg((1-\beta_k^v) \\
& \Big(\rho_{2,ll',m}^{kk^i}(-1) + \rho_{2,ll',m}^{kk^i}(1) + \rho_{2,ll',m}^{kk^i}(0)\Big) - \rho_{2,ll',m}^{kk}(-1) - \rho_{2,ll',m}^{kk}(1)\Big)\Big(h_{1l}^{k,v}\Big)^{i^*} \\
& \times \Big(h_{2l'}^{k,v}\Big)^{i} + \Bigg((1-\beta_k^v)\Big(\rho_{3,ll',m}^{kk^i}(-1) + \rho_{3,ll',m}^{kk^i}(1) + \rho_{3,ll',m}^{kk^i}(0)\Big) - \rho_{3,ll',m}^{kk}(-1) \\
& -\rho_{3,ll',m}^{kk}(1)\Big)\Big(h_{2l}^{k,v}\Big)^{i^*}\Big(h_{1l'}^{k,v}\Big)^{i} + \Bigg((1-\beta_k^v)\Big(\rho_{4,ll',m}^{kk^i}(-1) + \rho_{4,ll',m}^{kk^i}(1) + \rho_{4,ll',m}^{kk^i}(0)\Big) \\
& -\rho_{4,ll',m}^{kk}(-1) - \rho_{4,ll',m}^{kk}(1)\Big)\Big(h_{2l}^{k,v}\Big)^{i^*}\Big(h_{2l'}^{k,v}\Big)^{i} - \sum_{l=1}^{L}\sum_{l'=1,l'>l}^{L} \rho_{1,ll',m}^{kk}(0)\Big(h_{1l}^{k,v}\Big)^{i^*}\Big(h_{1l'}^{k,v}\Big)^{i} \\
& +\rho_{2,ll',m}^{kk}(0)\Big(h_{1l}^{k,v}\Big)^{i^*}\Big(h_{2l'}^{k,v}\Big)^{i} + \rho_{3,ll',m}^{kk}(0)\Big(h_{2l}^{k,v}\Big)^{i^*}\Big(h_{1l'}^{k,v}\Big)^{i} + \rho_{4,ll',m}^{kk}(0)\Big(h_{2l}^{k,v}\Big)^{i^*}\Big(h_{2l'}^{k,v}\Big)^{i} \\
& +\beta_k^v(\mathbf{h}_k^v)^{iH}\mathbf{B}_k(m)\Bigg(\mathbf{y}_{c,k}^v[m] - \sum_{j=1,j\neq k}^{K}\Bigg(\mathbf{R}_{kj}[-1]\mathbf{B}_j(m-1)^i + \mathbf{R}_{kj}[-1]^T\mathbf{B}_j(m+1)^i \\
& +\mathbf{R}_{kj}[0]\mathbf{B}_j(m)^i\Big)\Big(\mathbf{h}_j^v\Big)^i\Bigg)\Bigg)\Bigg\}, \quad (5.16)
\end{aligned}$$

where $\rho_{1,ll',m}^{kk^i}(m_p), \rho_{2,ll',m}^{kk^i}(m_p), \rho_{3,ll',m}^{kk^i}(m_p)$, and $\rho_{4,ll',m}^{kk^i}(m_p)$, $m_p \in \{-1, 0, 1\}$, are defined in terms of the cross-correlation coefficients between the l^{th} path of the k^{th} user's code sequences during the transmission of the m^{th} STS symbol and the l'^{th} path of the same user's code sequences during the transmission of the $(m+m_p)^{th}$ STS symbol, and the k^{th} user's current and next data estimates. The index i when excluded from the previous

defined parameters means that the effect of current data estimates are not considered (see Appendix B.1). Also, $\mathbf{y}_{c,k}^{v}[m]$ is a $(2L \times 1)$ vector including the outputs corresponding to the k^{th} user at the despreader output, defined as $\mathbf{y}_{c,k}^{v}[m] = \mathbf{F}_k[0]^T\mathbf{y}_w^v[m] + \mathbf{F}_k[1]^T\mathbf{y}_w^v[m+1]$ [89]. In (5.16), the conditional expectation of the attenuation coefficients given $\mathbf{y}_w$ and $\mathbf{b}^i$ is given by

$$(h_{ql}^{k,v})^i = E\left[\mathbf{h}^v|\mathbf{y}_w, \mathbf{b}^i\right]_{2L(k-1)+q+2(l-1)} = \left[(\mathbf{h}^v)^i\right]_{2L(k-1)+q+2(l-1)}, \tag{5.17}$$

$$(h_{ql}^{k,v*}h_{q'l'}^{j,v})^i = (h_{ql}^{k,v})^{i^*}(h_{q'l'}^{j,v})^i + (\mathbf{\Omega}_{hh}^i)_{2L(k-1)+q+2(l-1),2L(j-1)+q'+2(l'-1)}, \tag{5.18}$$

where $q, q' \in \{1, 2\}$, $l, l' \in \{1, \ldots, L\}$, $k, j \in \{1, \ldots, K\}$ and

$$\mathbf{\Omega}_{hh}^i = E\left[(\mathbf{h}^v - (\mathbf{h}^v)^i)(\mathbf{h}^v - (\mathbf{h}^v)^i)^H|\mathbf{y}_w, \mathbf{b}^i\right]. \tag{5.19}$$

In Appendix B.3, we prove that the conditional distribution of the channel vector, $\mathbf{h}^v$, given $\mathbf{y}_w$ and $\mathbf{b}^i$ is Gaussian with mean

$$(\mathbf{h}^v)^i = \Bigg(\sum_{m=0}^{M-1}\mathbf{B}(m)^i\left(\mathbf{R}[0]\mathbf{B}(m)^i + \mathbf{R}[-1]\mathbf{B}(m-1)^i + \mathbf{R}[1]\mathbf{B}(m+1)^i\right) + N_o\mathbf{\Sigma}_{hh}^{-1}\Bigg)^{-1} \times \sum_{m=0}^{M-1}\mathbf{B}(m)^i\mathbf{y}_c^v(m), \tag{5.20}$$

and covariance

$$\mathbf{\Omega}_{hh}^i = N_o\Bigg(\sum_{m=0}^{M-1}\mathbf{B}(m)^i\left(\mathbf{R}[0]\mathbf{B}(m)^i + \mathbf{R}[-1]\mathbf{B}(m-1)^i + \mathbf{R}[1]\mathbf{B}(m+1)^i\right) + N_o\mathbf{\Sigma}_{hh}^{-1}\Bigg)^{-1}, \tag{5.21}$$

where $\Sigma_{hh} = diag\{\Sigma_{h1}, \Sigma_{h2}, \ldots, \Sigma_{hK}\}$, $\Sigma_{hk} = \sigma_k^2\mathbf{I}_{2L}$. From (5.12), the M-step of the EM algorithm is performed by maximizing the individual likelihood functions $\mathcal{Q}_k(\mathbf{b}_k|\mathbf{b}^i)$,

$k = 1, \ldots, K$, as

$$\mathbf{b}_k^{i+1} = \arg \max_{\mathbf{b}_k} \mathcal{Q}_k(\mathbf{b}_k|\mathbf{b}^i). \tag{5.22}$$

In order to give further insight into the system performance, we consider a synchronous transmission over single path channel (L=1). In this case, (5.16) is reduced to

$$\mathcal{Q}_k(\mathbf{b}_k|\mathbf{b}^i) = \sum_{m=0}^{M-1} \mathcal{Q}_k(\mathbf{b}_k[m]|\mathbf{b}^i), \tag{5.23}$$

where

$$\begin{aligned}\mathcal{Q}_k(\mathbf{b}_k[m]|\mathbf{b}^i) = \sum_{v=1}^{V} Re\Big\{(1-\beta_k^v)\Big(\rho_{1,11,m}^{kk^i}(0)\Big|\Big(h_{1l}^{k,v}\Big)^i\Big|^2 + \rho_{2,11,m}^{kk^i}(0)\Big(h_{1l}^{k,v}\Big)^{i^*} \\ \times\Big(h_{2l}^{k,v}\Big)^i + \rho_{3,11,m}^{kk^i}(0)\Big(h_{2l}^{k,v}\Big)^{i^*}\Big(h_{1l}^{k,v}\Big)^i + \rho_{4,11,m}^{kk^i}(0)\Big|\Big(h_{2l}^{k,v}\Big)^i\Big|^2\Big) + \beta_k^v\,(\mathbf{h}_k^v)^{i^H} \\ \times\mathbf{B}_k(m)\Big(\mathbf{y}_{c,k}^v[m] - \sum_{j=1,j\neq k}^{K}\mathbf{R}_{kj}[0]\mathbf{B}_j(m)^i\,(\mathbf{h}_j^v)^i\Big)\Big\}\end{aligned} \tag{5.24}$$

From the likelihood function in (5.24), we notice that the EM-based ST receiver can be interpreted as follows: the channel coefficients of the K users are estimated based on the observed data, $\mathbf{y}_w$, and the previous data estimates $\mathbf{b}^i$. The data bits of each user are then detected from (5.24) based on the balancing weight, β_k^v, between the ST parallel interference cancelation receiver and the ST single-user coherent detector. We can also notice that by using the EM-algorithm, the K-user optimization problem is converted into K parallel single-user optimization problems leading to low computational complexity. A block diagram of the proposed ST EM-JDE receiver is shown in Fig. 5.1.

5.4 EM Optimized Weights and Initialization

In this section, we derive the optimized weights of the EM algorithm to ensure optimum performance. Also the conditions on the EM initialization are derived and

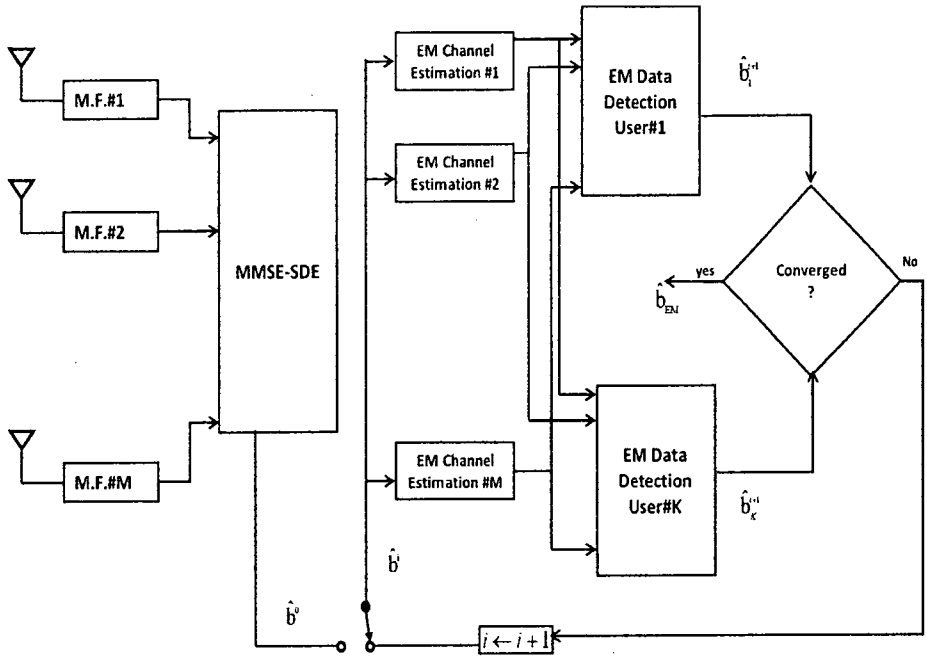

Figure 5.1: ST JDE receiver based on the EM algorithm.

discussed in detail.

5.4.1 Optimized Weights (β_k^v)

As discussed before, the decoupling of the received superimposed signal involved in the EM algorithm depends heavily on the choice of the balancing weight at each iteration, β_k^v. Here we obtain an optimized weight that, as will be shown later, brings the performance of the EM receiver close to the single-user bound. In [37], the authors derived a closed-form expression of the optimized weights for SISO CDMA systems for flat fading channels, using the so-called optimization via complete data technique. In this technique, the optimum weights are derived based on the MMSE criterion. A shortcoming of this method is that it does not take into account the effect of cross-correlations between the signature waveforms. Therefore, the authors in [90] proposed another technique, called optimization via projected complete data, where the effect of cross-correlation is taken into consideration. This optimization technique shows performance enhancement com-

pared to the first technique especially for frequency-selective channels [91]. Throughout our work, we consider the first technique for the flat fading channels, while we employ the second technique for the frequency-selective fading channels.

In (5.16), we notice that $Q_k(\mathbf{b}_k|\mathbf{b}^i)$ is a sum of V statistically independent terms given $\mathbf{b}$ and its EM estimate $\mathbf{b}^i$, which are related to the V receive antennas. Since the spatial channels corresponding to the links between transmit and receive antennas are considered independent, β_k^v can be separately optimized.

In this case, we choose the weight coefficients to minimize the linear mean-square error between the true signal vector, $\mathbf{g}_k^v(m_s)$, and its estimate $(\mathbf{g}_k^v(m_s))^i$
$= E\left[\mathbf{g}_k^v(m_s)|\mathbf{y}_w, \mathbf{b}^i\right]$, $m_s \in \{m, m+1\}$, after being projected on $\mathbf{F}_k[0]$ and $\mathbf{F}_k[1]$ respectively as

$$\beta_k^v = \arg\min_{\beta_k^v} E\left[\| E_g \|^2\right], \tag{5.25}$$

where

$$E_g = \mathbf{F}_k[0]^T \left(\mathbf{g}_k^v(m) - \mathbf{g}_k^v(m)^i\right) + \mathbf{F}_k[1]^T \left(\mathbf{g}_k^v(m+1) - \mathbf{g}_k^v(m+1)^i\right), \tag{5.26}$$

and $\| \cdot \|$ denotes the vector norm. Taking the expectation of (5.15) with respect to $\mathbf{h}^v$, we have

$$E\left[\mathbf{g}_k^v(m_s)|\mathbf{y}_w, \mathbf{b}^i\right] = \sum_{\Delta m=0}^{1} \mathbf{F}_k[\Delta m]\mathbf{B}_k(m_s - \Delta m)^i \left(\mathbf{h}_k^v\right)^i + \beta_k^v \Bigg(\mathbf{y}_w^v(m_s) - \sum_{j=1}^{K} \sum_{\Delta m=0}^{1} \mathbf{F}_j[\Delta m]\mathbf{B}_j(m_s - \Delta m)^i \left(\mathbf{h}_j^v\right)^i \Bigg), m_s \in \{m, m+1\} \tag{5.27}$$

In order to simplify our analysis, we assume that $M \to \infty$, i.e. the random channel

coefficients are assumed to be known to the receiver (see Appendix B.4). It follows that

$$E\left[\mathbf{g}_k^v(m_s)|\mathbf{y}_w,\mathbf{b}^i\right] = \sum_{\Delta m=0}^{1}\mathbf{F}_k[\Delta m]\mathbf{B}_k(m_s-\Delta m)^i\mathbf{h}_k^v + \beta_k^v\Bigg(\mathbf{y}_w^v(m_s) - \sum_{j=1}^{K}\sum_{\Delta m=0}^{1}\mathbf{F}_j[\Delta m]\mathbf{B}_j(m_s-\Delta m)^i\mathbf{h}_j^v\Bigg), m_s\in\{m,m+1\} \quad (5.28)$$

Substituting $\mathbf{g}_k^v(m_s)$ and $(\mathbf{g}_k^v(m_s))^i$, $m_s\in\{m,m+1\}$, in (5.26), we have

$$\begin{aligned}E_g = {}& \mathbf{R}_{kk}[0]\left(\mathbf{B}_k(m)-\mathbf{B}_k(m)^i\right)\mathbf{h}_k^v + \mathbf{R}_{kk}[-1]\left(\mathbf{B}_k(m-1)-\mathbf{B}_k(m-1)^i\right)\mathbf{h}_k^v\\ &+\mathbf{R}_{kk}[-1]^T\left(\mathbf{B}_k(m+1)-\mathbf{B}_k(m+1)^i\right)\mathbf{h}_k^v + \mathbf{F}_k[0]^T\mathbf{n}_{wk}^v[m]+\mathbf{F}_k[1]^T\mathbf{n}_{wk}^v[m+1]\\ &-\beta_k^v\mathbf{y}_{c,k}^v[m]+\beta_k^v\Bigg(\sum_{j=1}^{K}\mathbf{R}_{kj}[0]\mathbf{B}_j(m)^i\mathbf{h}_j^v+\mathbf{R}_{kj}[-1]\mathbf{B}_j(m-1)^i\mathbf{h}_j^v+\mathbf{R}_{kj}[-1]^T\\ &\times\mathbf{B}_j(m+1)^i\mathbf{h}_j^v\Bigg) \quad (5.29)\end{aligned}$$

where $\mathbf{R}_{kj}[-1] = \mathbf{F}_k[0]^T\mathbf{F}_j[1]$, and $\mathbf{R}_{kj}[0] = \mathbf{F}_k[0]^T\mathbf{F}_j[0]+\mathbf{F}_k[1]^T\mathbf{F}_j[1]$. Substituting $\mathbf{y}_{c,k}^v[m] = \sum_{j=1}^{K}\mathbf{R}_{kj}[0]\mathbf{B}_j(m)\mathbf{h}_j^v+\mathbf{R}_{kj}[-1]\mathbf{B}_j(m-1)\mathbf{h}_j^v+\mathbf{R}_{kj}[-1]^T\mathbf{B}_j(m+1)\mathbf{h}_j^v+\mathbf{n}_{c,k}^v[m]$, where $\mathbf{n}_{c,k}^v[m]$ is $(2L\times 1)$ vector including the noise samples corresponding to the k^{th} user at the v^{th} despreader output, and $\sqrt{\beta_k^v}\mathbf{n}_{c,k}^v[m] = \mathbf{F}_k[0]^T\mathbf{n}_{wk}^v[m]+\mathbf{F}_k[1]^T\mathbf{n}_{wk}^v[m+1]$, in (5.29), we have

$$\begin{aligned}E_g = {}& \mathbf{R}_{kk}[0]\left(\mathbf{B}_k(m)-\mathbf{B}_k(m)^i\right)\mathbf{h}_k^v + \mathbf{R}_{kk}[-1]\left(\mathbf{B}_k(m-1)-\mathbf{B}_k(m-1)^i\right)\mathbf{h}_k^v\\ &+\mathbf{R}_{kk}[-1]^T\left(\mathbf{B}_k(m+1)-\mathbf{B}_k(m+1)^i\right)\mathbf{h}_k^v+\sqrt{\beta_k^v}\mathbf{n}_{c,k}^v[m]-\beta_k^v\Bigg(\sum_{j=1}^{K}\mathbf{R}_{kj}[0]\\ &\times\left(\mathbf{B}_j(m)-\mathbf{B}_j(m)^i\right)\mathbf{h}_j^v+\mathbf{R}_{kj}[-1]\left(\mathbf{B}_j(m-1)-\mathbf{B}_j(m-1)^i\right)\mathbf{h}_j^v+\mathbf{R}_{kj}[-1]^T\\ &\times\left(\mathbf{B}_j(m+1)-\mathbf{B}_j(m+1)^i\right)\mathbf{h}_j^v+\mathbf{n}_{c,k}^v[m]\Bigg) \quad (5.30)\end{aligned}$$

Now, we can find the value of $\| E_g \|^2$ as follows. By neglecting the terms independent of

β_k^v, we have

$$\begin{aligned}
\| E_g \|^2 = 2\sqrt{\beta_k^v} Re\Big\{ & \mathbf{h}_k^{vH} \Big(\left(\mathbf{B}_k(m) - \mathbf{B}_k(m)^i\right)^T \mathbf{R}_{kk}[0]^T + \left(\mathbf{B}_k(m-1)\right. \\
& \left. -\mathbf{B}_k(m-1)^i\right)^T \mathbf{R}_{kk}[-1]^T + \left(\mathbf{B}_k(m+1) - \mathbf{B}_k(m+1)^i\right)^T \mathbf{R}_{kk}[-1] \Big) \\
& \times \mathbf{n}_{c,k}^v[m] \Big\} - 2\beta_k^v Re\Big\{ \mathbf{h}_k^{vH} \Big(\left(\mathbf{B}_k(m) - \mathbf{B}_k(m)^i\right)^T \mathbf{R}_{kk}[0]^T + \left(\mathbf{B}_k(m-1)\right. \\
& \left. -\mathbf{B}_k(m-1)^i\right)^T \mathbf{R}_{kk}[-1]^T + \left(\mathbf{B}_k(m+1) - \mathbf{B}_k(m+1)^i\right)^T \mathbf{R}_{kk}[-1] \Big) \\
& \times \Big(\sum_{j=1}^{K} \left(\mathbf{R}_{kj}[0] \left(\mathbf{B}_j(m) - \mathbf{B}_j(m)^i\right) + \mathbf{R}_{kj}[-1] \left(\mathbf{B}_j(m-1) - \mathbf{B}_j(m-1)^i\right)\right. \\
& \left. + \mathbf{R}_{kj}[-1]^T \left(\mathbf{B}_j(m+1) - \mathbf{B}_j(m+1)^i\right)\right) \mathbf{h}_j^v + \mathbf{n}_{c,k}^v[m] \Big) \Big\} - 2\beta_k^v \sqrt{\beta_k^v} \\
& \times Re\Big\{ \mathbf{n}_{c,k}^v[m]^H \Big(\sum_{j=1}^{K} \left(\mathbf{R}_{kj}[0] \left(\mathbf{B}_j(m) - \mathbf{B}_j(m)^i\right) + \mathbf{R}_{kj}[-1] \left(\mathbf{B}_j(m-1)\right.\right. \\
& \left.\left. - \mathbf{B}_j(m-1)^i\right) + \mathbf{R}_{kj}[-1]^T \left(\mathbf{B}_j(m+1) - \mathbf{B}_j(m+1)^i\right)\right) \mathbf{h}_j^v + \mathbf{n}_{c,k}^v[m] \Big) \Big\} + \beta_k^{v2} \\
& \times \| \sum_{j=1}^{K} \left(\mathbf{R}_{kj}[0] \left(\mathbf{B}_j(m) - \mathbf{B}_j(m)^i\right) + \mathbf{R}_{kj}[-1] \left(\mathbf{B}_j(m-1) - \mathbf{B}_j(m-1)^i\right)\right. \\
& \left. + \mathbf{R}_{kj}[-1]^T \left(\mathbf{B}_j(m+1) - \mathbf{B}_j(m+1)^i\right)\right) \mathbf{h}_j^v + \mathbf{n}_{c,k}^v[m] \|^2 + \beta_k^v \mathbf{n}_{c,k}^v[m]^H \mathbf{n}_{c,k}^v[m]. \quad (5.31)
\end{aligned}$$

In our system model, we assume that the noise samples, $\mathbf{n}_{c,k}^v[m]$, and the channel coefficients, $\mathbf{h}_k^v$, are mutually independent, as well as

$$E\left[h_{ql}^{k,v^*} h_{q'l'}^{j,v}\right] = \begin{cases} \sigma_k^2, & j = k, q = q', l = l' \\ 0, & \text{otherwise} \end{cases}, \quad (5.32)$$

$$E\left[\mathbf{n}_{c,k}^v[m]^H \mathbf{n}_{c,k}^v[m]\right] = N_o \left(R_{kk,11}[0] + R_{kk,22}[0] + \ldots + R_{kk,2L2L}[0]\right), \quad (5.33)$$

where $R_{kk,\zeta\zeta}[0]$ $(\zeta = 1, 2, ..., 2L)$, represents the ζ^{th} diagonal element of $\mathbf{R}_{kk}[0]$. Therefore,

taking the expectation of (5.31) is reduced to (see Appendix B.2)

$$\begin{aligned}
\beta_k^v = \arg\min_{\beta_k^v} \Big\{ & N_o \left(\beta_k^v - 2\beta_k^{v\frac{3}{2}} + \beta_k^{v2}\right) \left(R_{kk,11}[0] + R_{kk,22}[0] + \ldots + R_{kk,2L2L}[0]\right) \\
& -4\sigma_k^2\beta_k^v \sum_{l=1}^{L} \left(r_{kk,0}(2l-1,2l-1) + r_{kk,0}(2l,2l)\right) \left(\left(1 - E\left[b_{k1}[m]b_{k1}[m]^i\right]\right)\right. \\
& \left. + \left(1 - E\left[b_{k2}[m]b_{k2}[m]^i\right]\right)\right) + \left(r_{kk,-1}(2l-1,2l-1) + r_{kk,-1}(2l,2l)\right) \\
& \times \left(\left(1 - E\left[b_{k1}[m-1]b_{k1}[m-1]^i\right]\right) + \left(1 - E\left[b_{k2}[m-1]b_{k2}[m-1]^i\right]\right)\right) \\
& + \left(r_{kk,1}(2l-1,2l-1) + r_{kk,1}(2l,2l)\right) \left(\left(1 - E\left[b_{k1}[m+1]b_{k1}[m+1]^i\right]\right)\right. \\
& \left. + \left(1 - E\left[b_{k2}[m+1]b_{k2}[m+1]^i\right]\right)\right) + 2\beta_k^{v2} \sum_{j=1}^{K} \sigma_j^2 \sum_{l=1}^{L} \left(r_{jj,0}(2l-1,2l-1)\right. \\
& \left. + r_{jj,0}(2l,2l)\right) \left(\left(1 - E\left[b_{j1}[m]b_{j1}[m]^i\right]\right) + \left(1 - E\left[b_{j2}[m]b_{j2}[m]^i\right]\right)\right) \\
& + \left(r_{jj,-1}(2l-1,2l-1) + r_{jj,-1}(2l,2l)\right) \left(\left(1 - E\left[b_{j1}[m-1]b_{j1}[m-1]^i\right]\right)\right. \\
& \left. + \left(1 - E\left[b_{j2}[m-1]b_{j2}[m-1]^i\right]\right)\right) + \left(r_{jj,1}(2l-1,2l-1) + r_{jj,1}(2l,2l)\right) \\
& \times \left(\left(1 - E\left[b_{j1}[m+1]b_{j1}[m+1]^i\right]\right) + \left(1 - E\left[b_{j2}[m+1]b_{j2}[m+1]^i\right]\right)\right)\Big\} \quad (5.34)
\end{aligned}$$

where $r_{jj,m_p}(\zeta,\zeta), j = 1,\ldots,K, \zeta = 1,\ldots,2L, m_p \in \{-1,0,1\}$, represents the ζ^{th} diagonal element of $\mathbf{R}_{jj}[m_p]^T\mathbf{R}_{jj}[m_p]$. We notice that

$$\begin{aligned}
\left(1 - E\left[b_{jq}[m+m_p]b_{jq}[m+m_p]^i\right]\right) = 2P_{e_{jq}}^{v,i}, j = 1,\ldots,k, q = 1,2, \\
m_p = -1,0,1, \quad (5.35)
\end{aligned}$$

where the probability of error, $P_{e_{jq}}^{v,i} = f\left(b_{jq}(m+m_p) \neq b_{jq}(m+m_p)^i\right), j = 1,\ldots,k,$

$q = 1, 2, m_p = -1, 0, 1$. Using (5.35), (5.34) can be expressed as

$$\begin{aligned}\beta_k^v = \arg\min_{\beta_k^v} \Big\{ & N_o \left(\beta_k^v - 2\beta_k^{v\frac{3}{2}} + \beta_k^{v2}\right) \left(R_{kk,11}[0] + R_{kk,22}[0] + \ldots + R_{kk,2L2L}[0]\right) \\ & - 8\sigma_k^2 \beta_k^v \left(P_{e_{k1}}^{v,i} + P_{e_{k2}}^{v,i}\right) \sum_{l=1}^{L} \left(r_{kk,0}(2l-1, 2l-1) + r_{kk,0}(2l, 2l)\right. \\ & \left. + r_{kk,-1}(2l-1, 2l-1) + r_{kk,-1}(2l, 2l) + r_{kk,1}(2l-1, 2l-1) + r_{kk,1}(2l, 2l)\right) \\ & + 4\beta_k^{v2} \sum_{j=1}^{K} \sigma_j^2 \left(P_{e_{j1}}^{v,i} + P_{e_{j2}}^{v,i}\right) \sum_{l=1}^{L} \left(r_{jj,0}(2l-1, 2l-1) + r_{jj,0}(2l, 2l)\right. \\ & \left. + r_{jj,-1}(2l-1, 2l-1) + r_{jj,-1}(2l, 2l) + r_{jj,1}(2l-1, 2l-1) + r_{jj,1}(2l, 2l)\right) \Big\}. \quad (5.36)\end{aligned}$$

Assume that $\alpha_k = R_{kk,11}[0] + R_{kk,22}[0] + \ldots + R_{kk,2L2L}[0]$, and $\theta_l^j = r_{jj,0}(2l-1, 2l-1) + r_{jj,0}(2l, 2l) + r_{jj,-1}(2l-1, 2l-1) + r_{jj,-1}(2l, 2l) + r_{jj,1}(2l-1, 2l-1) + r_{jj,1}(2l, 2l)$. By differentiating (5.36) with respect to β_k^v and substituting $x = \sqrt{\beta_k^v}$, we have

$$\begin{aligned}\left(2N_o\alpha_k + 8\sum_{j=1}^{K} \sigma_j^2 \left(P_{e_{j1}}^{v,i} + P_{e_{j2}}^{v,i}\right) \sum_{l=1}^{L} \theta_l^j\right) x^2 + \left(-3N_o\alpha_k\right) x & \\ + \left(N_o\alpha_k - 8\sigma_k^2 \left(P_{e_{k1}}^{v,i} + P_{e_{k2}}^{v,i}\right) \sum_{l=1}^{L} \theta_l^k\right) = 0. \quad (5.37)\end{aligned}$$

Solving(5.37) with respect to x results in two possible solutions for β_k^v. Assuming that the performance of the EM-based ST receiver with V=1 receive antenna will converge to the single-user (SU) bound with perfect CSI assuming transmission over frequency-selective fading channels. Then the probability of error of the odd and even data bits are defined as [16]

$$\begin{aligned}P_{e1} = \frac{1}{2} Q\left(Re\{\mathcal{G}(1,1) + \mathcal{G}(1,2)\} \sqrt{\frac{2}{\mathcal{G}(1,1)}}\right) & \\ + \frac{1}{2} Q\left(Re\{\mathcal{G}(1,1) - \mathcal{G}(1,2)\} \sqrt{\frac{2}{\mathcal{G}(1,1)}}\right), \quad (5.38)\end{aligned}$$

$$P_{e2} = \frac{1}{2}Q\left(Re\{\mathcal{G}(2,2)+\mathcal{G}(2,1)\}\sqrt{\frac{2}{\mathcal{G}(2,2)}}\right) + \frac{1}{2}Q\left(Re\{\mathcal{G}(2,2)-\mathcal{G}(2,1)\}\sqrt{\frac{2}{\mathcal{G}(2,2)}}\right), \quad (5.39)$$

where

$$\mathcal{G} = \left[(\mathbf{s}_1\mathbf{ch}_1 - \mathbf{s}_2\mathbf{ch}_2)(\mathbf{s}_2\mathbf{ch}_1 + \mathbf{s}_1\mathbf{ch}_2)\right]^H . \left[(\mathbf{s}_1\mathbf{ch}_1 - \mathbf{s}_2\mathbf{ch}_2)(\mathbf{s}_2\mathbf{ch}_1 + \mathbf{s}_1\mathbf{ch}_2)\right], \quad (5.40)$$

and $\mathbf{s}_1$ and $\mathbf{s}_2$ include the multipath versions of the two code assigned for every user, and $\mathbf{ch}_q$, $q = 1, 2$, include the multipath channel coefficients from the q^{th} transmit antenna to the receive antenna. Also, the Gaussian Q-function, $Q(x)$, is defined as, $Q(x) = 1/\sqrt{2\pi}\int_x^\infty e^{-x^2/2}dx$. Substituting with the EM channel estimates defined in (5.20) in the single-user bound, P_{e_1} and P_{e_2}, we obtain an approximation for $P_{e_{k1}}^{v,i}$, and $P_{e_{k2}}^{v,i}$. The importance of the optimized weight coefficients arises from the fact that it determines the best balance between the single-user matched filter detector and the ST PIC based detector. In the literature, the partial PIC has proven to be near-far resistant, where it achieves a performance close to the ML detector [92]. To explain how the weight coefficients control the performance of the EM receiver, consider the scenario of 2-user STS system with two transmit and one receive antenna assuming transmission over AWGN channel. In Fig. 5.2, we show the relation between the weight coefficients and the MAI level. As shown in the figure below, for extremely high MAI energy case, i.e., $\gamma_2 \rightarrow \infty$, where $\gamma_k, k = 1, 2$, represents the k^{th} user SNR, $\beta_1 \rightarrow 1$, and the detection of user one data is completely based on the output of ST PIC detector. On the other hand, $\beta_1 \rightarrow 1$ for very low MAI energy, i.e., $\gamma_2 \rightarrow 0$. Consequently, the performance of the EM-based ST receiver is close to that of single-user matched filter detector, which is the optimum detector in this case. For cases falling between these two extreme cases, the weights are

optimized in such a way to compensate for both the MAI interference and noise. In the case of equal power, the optimized weight coefficients of different users have equal values, i.e., $\beta_1 = \beta_2 = \frac{1}{2}$.

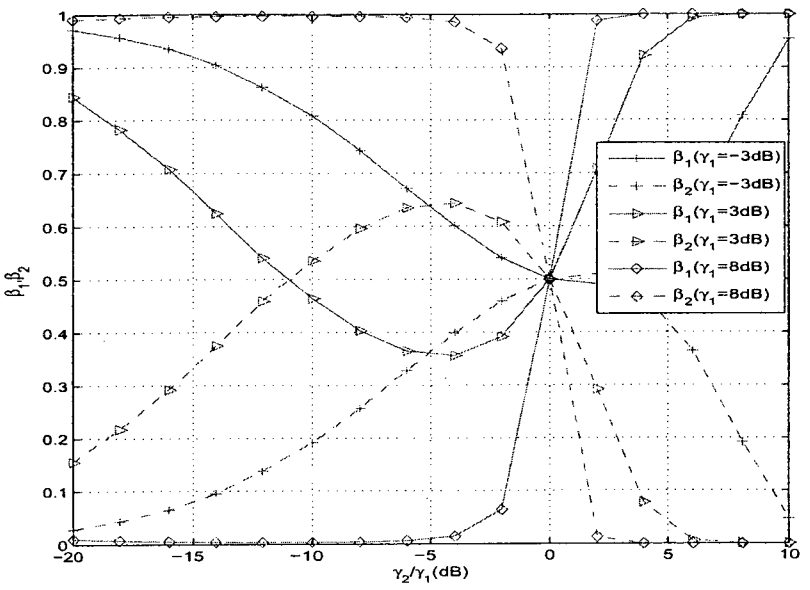

Figure 5.2: The behavior of the optimized weight coefficients for 2-user STS system assuming AWGN channel.

5.4.2 EM Initialization

Since the EM algorithm is sensitive to the initialization of the parameters to be estimated [67], as well as due to the high computational complexity of the joint estimation and detection in MIMO systems, our proposed EM-based ST receiver is initialized by reliable estimates, where we employ the ST MMSE separate detection and estimation (ST MMSE-SDE) technique. This will guarantee that the performance of our proposed receiver converges to the global maximum of the likelihood function with a fast rate. Furthermore, this will also ease the maximization of the individual likelihood functions $\mathcal{Q}_k(\mathbf{b}_k|\mathbf{b}^i)$ in (5.22). Since the estimation of the current codeword $(b_{k1}[m], b_{k2}[m])$ is

based on the knowledge of previous $(b_{k1}[m-1], b_{k2}[m-1])$ and following codewords $(b_{k1}[m+1], b_{k2}[m+1])$, the Viterbi algorithm can be used to evaluate (5.22) [20]. However, this will increase the complexity of the proposed receiver. Alternatively, for the first iteration, we assume that the ST MMSE-SDE estimates provide reliable estimation for the previous and following codewords, $b_{kq}[m-1] = b_{kq}[m-1]^0$, and $b_{kq}[m+1] = b_{kq}[m+1]^0$, $q \in \{1,2\}$, while for the subsequent iterations, we assume that $b_{kq}[m-1] = b_{kq}[m-1]^i$, and $b_{kq}[m+1] = b_{kq}[m+1]^{i-1}$. Consequently, the maximization of (5.22) is performed over 4 possibilities for the current k^{th} user data bits, $b_{k1}[m]$ and $b_{k2}[m]$, (i.e, {(1,1),(1,-1),(-1,1),(-1,-1)}) considering BPSK transmission. The MMSE-SDE receiver was first proposed in [37] for SISO systems. Here, we extend this work to MIMO CDMA systems as follows. In order to estimate the channel, we assume that each user transmits p' training codewords known at the receiver, i.e., each user transmits $2p'$ bits. Let $\mathbf{z}^v_{p'}$ includes the output of the v^{th} matched filter bank within a frame of p' codewords. Based on $\mathbf{z}^v_{p'}$, we can estimate the channel vector at each receive antenna, $\mathbf{h}^v_{mmse}$ [93]. Then, following the same procedure, the MMSE data estimate is obtained based on $\mathbf{z}^V$ while assuming $\mathbf{h} = \mathbf{h}_{mmse}$ [94], where $\mathbf{z}^V$ represents the output of the V matched filter banks within a frame of M codewords

5.5 Cramér-Rao Lower Bound (CRLB) on Channel Estimates

In search for minimum variance unbiased estimators (MVUE), the CRLB is commonly used in estimation theory to assess the accuracy of the estimator in terms of its error variance. Throughout our derivation, we consider synchronous transmission, i.e., $\tau_k = 0, k = 1, \ldots, K$, over flat fading channel, i.e., $L = 1$. In this case, (5.2) is reduced to

$$\mathbf{y}^v[m] = \mathbf{C}[0]\mathbf{B}(m)\mathbf{h}^v + \mathbf{n}^v[m], \quad m = 0, \ldots, M-1; v = 1, \ldots, V. \tag{5.41}$$

Let

$$\mathbf{y} = [\mathbf{y}(0), \mathbf{y}(1), \ldots, \mathbf{y}(M-1)], \tag{5.42}$$

where

$$\mathbf{y}(m) = [\mathbf{y}^1(m), \mathbf{y}^2(m), \ldots, \mathbf{y}^V(m)], \quad m = 0, \ldots, M-1. \tag{5.43}$$

Then, the log-likelihood function

$$\Phi(\mathbf{y}|\mathbf{h}, \mathbf{b}) \propto -\frac{1}{N_o}\left(\sum_{m=0}^{M-1}\sum_{v=1}^{V}\left(\mathbf{y}^v[m] - \mathbf{C}[0]\mathbf{B}(m)\mathbf{h}^v\right)^H\left(\mathbf{y}^v[m] - \mathbf{C}[0]\mathbf{B}(m)\mathbf{h}^v\right)\right). \tag{5.44}$$

Neglecting the terms independent of the channel vector $\mathbf{h}$, we have

$$\Phi(\mathbf{r}|\mathbf{h}, \mathbf{b}) = -\frac{1}{N_o}\left(\sum_{m=0}^{M-1}\sum_{v=1}^{V} -2Re\{\mathbf{h}^{vH}\mathbf{B}(m)\mathbf{y}_c^v[m]\} + \mathbf{h}^{vH}\mathbf{B}(m)^H\mathbf{R}[0]\mathbf{B}(m)\mathbf{h}^v\right). \tag{5.45}$$

Focusing on the channel estimates, we assume that the data vector, $\mathbf{b}$, is known a priori or has been correctly detected. The CRLB provides a lower bound on the mean-square error (MSE) of the channel estimates as follows

$$E\left\{\left|\left(h_{q1}^{k,v}\right)^i - h_{q1}^{k,v}\right|^2\right\} \geq -\frac{\left\{\frac{\partial}{\partial h_{q1}^{k,v}}E\left[\left(h_{q1}^{k,v}\right)^i\right]\right\}^2}{E\left\{\frac{\partial^2}{\partial h_{q1}^{k,v\,2}}\Phi(\mathbf{y}|\mathbf{h})\right\}}, q = 1, 2; k = 1, \ldots, K. \tag{5.46}$$

To evaluate $\frac{\partial}{\partial h_{q1}^{k,v}}E\left[\left(h_{q1}^{k,v}\right)^i\right]$, we replace $\mathbf{B}(m)^i$ by $\mathbf{B}(m)$ and substitute (5.2) in (5.20), yielding to

$$E\left[(\mathbf{h}^v)^i\right] = \boldsymbol{\mathcal{F}}\mathbf{h}^v, \tag{5.47}$$

where $\boldsymbol{\mathcal{F}} = E\left[\left(\sum_{m=0}^{M-1}\mathbf{B}(m)\mathbf{R}[0]\mathbf{B}(m) + N_o\boldsymbol{\Sigma}_{hh}^{-1}\right)^{-1}\sum_{m=0}^{M-1}\mathbf{B}(m)\mathbf{R}[0]\mathbf{B}(m)\right]$. Consider the asymptotic case when the average SNR of each user increases, $\frac{\sigma_k^2}{N_o} \rightarrow \infty$ for $k =$

$1, \ldots, K$. In this case, $\mathcal{F}$ becomes a unitary matrix, and

$$E\left[(\mathbf{h}^v)^i\right] = \mathbf{h}^v, \tag{5.48}$$

which proves that the EM estimates are asymptotically unbiased. Consequently, (5.46) is reduced to

$$E\left\{\left|\left(h_{q1}^{k,v}\right)^i - h_{q1}^{k,v}\right|^2\right\} \geq -\frac{1}{E\left\{\frac{\partial^2}{\partial h_{q1}^{k,v\,2}}\Phi(\mathbf{y}|\mathbf{h})\right\}}. \tag{5.49}$$

It is convenient to split the channel estimates into their real and imaginary components, $h_{q1}^{k,v} = h_{q1,r}^{k,v} + jh_{q1,i}^{k,v}$. Then, the CRLB can be computed as

$$E\left\{\left|\left(h_{q1}^{k,v}\right)^i - h_{q1}^{k,v}\right|^2\right\} \geq \frac{-1}{E\left\{\frac{\partial^2}{\partial h_{q1,r}^{k,v\,2}}\Phi(\mathbf{y}|\mathbf{h})\right\}} + \frac{-1}{E\left\{\frac{\partial^2}{\partial h_{q1,i}^{k,v\,2}}\Phi(\mathbf{y}|\mathbf{h})\right\}}. \tag{5.50}$$

By computing the second derivatives of (5.45) with respect to $h_{q1,r}^{k,v}$ and $h_{q1,i}^{k,v}$, and expressing the channel variables as $h_{q1}^{k,v} = \sqrt{\frac{E_k}{2}}\alpha_{q1}^{k,v}$, we obtain the following bound for the MSE of the EM channel estimates

$$E\left\{\left|\left(\alpha_{q1}^{k,v}\right)^i - \alpha_{q1}^{k,v}\right|^2\right\} \geq \frac{N_o}{E_k M}. \tag{5.51}$$

In (5.51), it is noted that the power of the estimation error is inversely proportional to both the SNR and the length of the observation window.

5.6 Simulation Results

In this section, we examine the BER performance of the proposed EM-JDE receiver in MIMO CDMA systems. In all cases, we consider a system with two transmit and $V = 1, 2$ receive antennas. We also consider an uplink asynchronous transmission of a data block of 40 codewords (M=40) over a frequency-selective fading channel. Without

loss of generality, we consider a 5-user system, where all users are assigned Gold codes of length 31 chips. We assume the first user as the desired one. A training codeword of eight training bits is used for the initialization of the EM receiver. Without loss of generality,

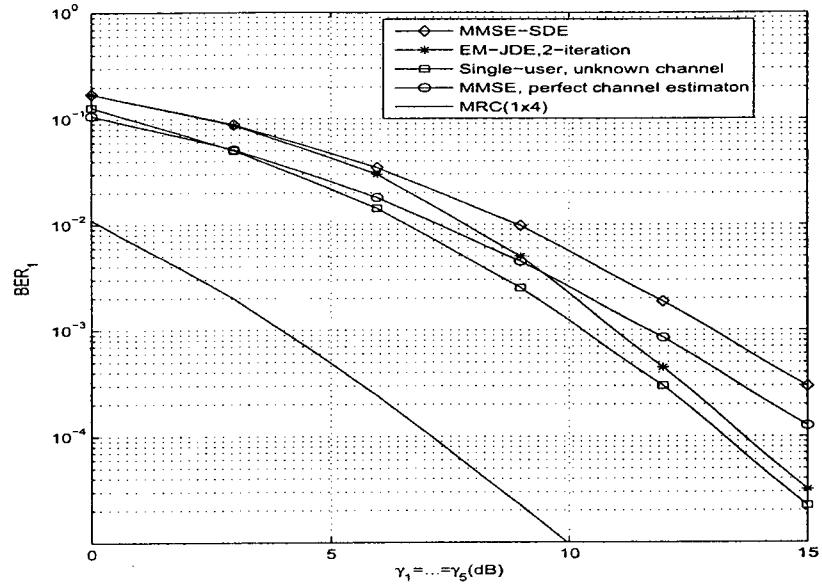

Figure 5.3: BER performance of the first user considering ST EM-JDE receiver with two transmit and one receive antenna over frequency-selective fading channels. The channel coefficients are assumed unknown at the receiver ($M = 40$, p'=8, $L = 2$, 2-iteration).

throughout all our simulation results, we only consider the average BER of the first user, BER_1, assuming different scenarios. As a reference, we include the BER performance of the ST MMSE-SDE receiver with perfect channel estimation. Fig. 5.3 presents the BER performance of the proposed ST EM-JDE and ST MMSE-SDE receivers using 2×1 antenna configuration. The results are also compared with the BER performance of the SU system assuming unknown channel. In order to show that our proposed receiver attains the full system diversity, we compare our results with a MRC with the same number of diversity branches assuming perfect channel estimation. The MRC represents an optimal combiner for a receive diversity scheme of one transmit and multiple receive antennas [53]. Considering the STS system with two transmit and one receive antenna, it is clear that

the EM based ST receiver attains the full system diversity, i.e., same as MRC with four diversity branches.

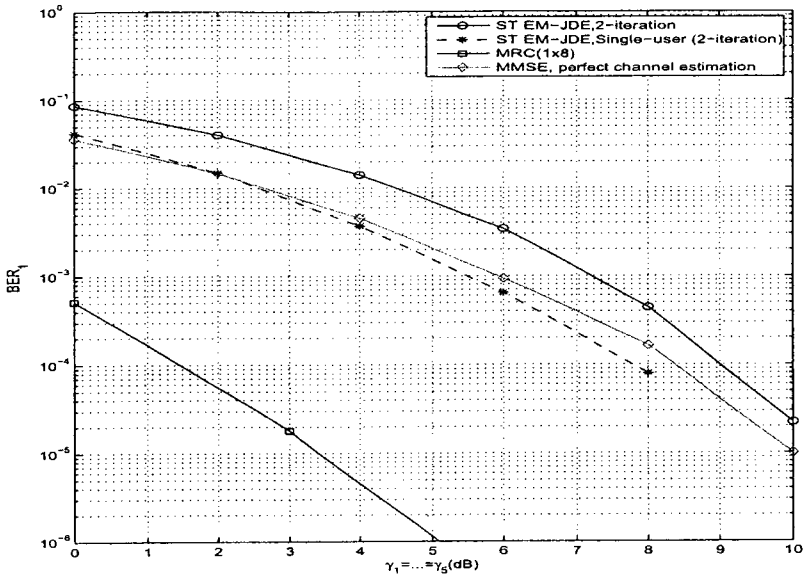

Figure 5.4: BER performance of the first user considering ST EM-JDE receiver with V=2 receive antennas, $M = 40, p' = 8, L = 2$, 2 iterations.

In Fig. 5.4, we examine the BER performance for 2×2 antenna configuration. The results show that the full system diversity is attained when comparing the results with MRC with eight diversity branches.

In Fig. 5.5 we examine the near-far effect property of the proposed receiver for $V = 1$ receive antenna. We fix the received SNR of the first user γ_1 at 15 dB, while the interfering users have equal SNR ratios relative to γ_1, varying from -10 to 60 dB. We also compare the performance of the ST EM-JDE receiver considering optimum β_k^v values (5.37) and equal β_k^v values ($\beta_k^v = 1/K$). The results show that the EM receiver with optimum β_k^v is near-far resistant. Also when the interference level is high, a reliable estimate of the MAI is obtained and consequently the MAI removal is performed efficiently. On the other hand, the performance of the MMSE-SDE receiver degrades due to the

noise enhancement. We can notice the effect of β_k^v on the performance of the ST EM-JDE receiver. That is, compared with the case of equal β_k^v, the optimum weights, β_k^v, achieve the best balance between the ST single-user coherent detector and the ST parallel interference cancelation receiver (5.16). The same conclusion also follows from Fig. 5.6.

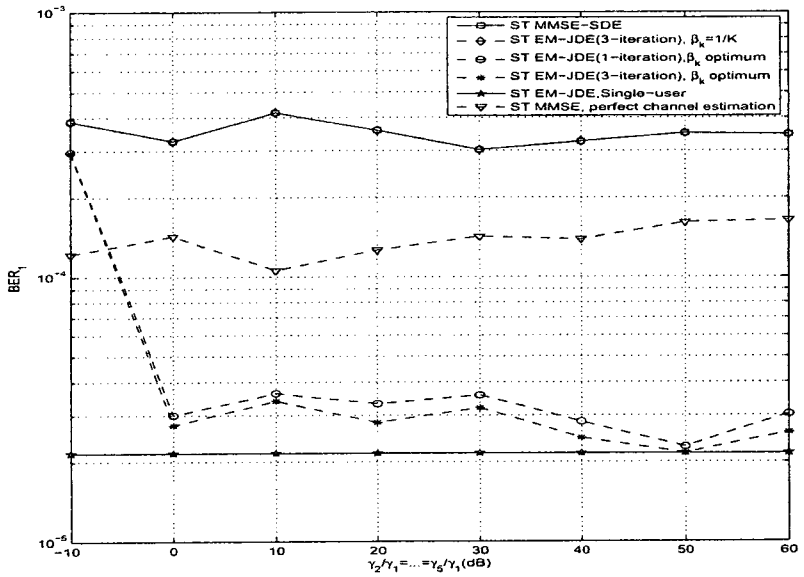

Figure 5.5: BER behavior of the first user as a function of the MAI level with V=1 receive antenna over frequency-selective fading channels, $M = 40, p' = 8, L = 2, \gamma_1$=15dB.

Finally, in Fig. 5.7 we assess the accuracy and the asymptotic performance of the channel estimates based on the EM algorithm for a system with V=2 receive antennas. We also assume synchronous transmission over flat fading channel, i.e., L=1. In this figure, we simulate the MSE of the channel estimate, $\widehat{h}_{11}^{1,1}$, averaged over 10^5 channel realizations at different SNRs. The results show that the channel estimates are asymptotically efficient where the average MSE of $h_{11}^{1,1}$ estimate converges to the CRLB at high SNR, confirming our analytical results presented in Sec. 5.5.

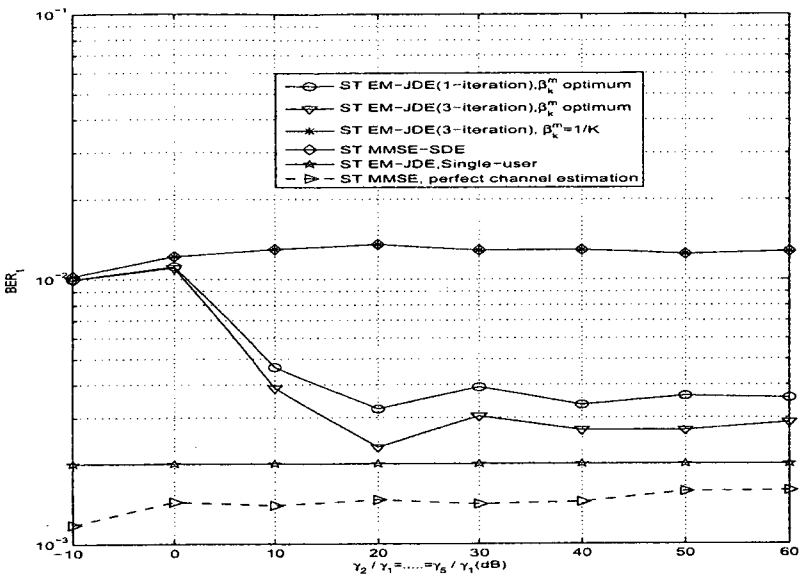

Figure 5.6: BER behavior of the first user as a function of the MAI level for V=2 receive antennas over flat fading channels, $M = 20, p' = 1, L = 1, \gamma_1$=8dB.

5.7 Conclusions

We have developed an iterative joint detection and estimation receiver based on the EM algorithm for STS systems. Using Monte-Carlo simulations, we examined the performance of our proposed receiver in frequency-selective fading channels. It was shown that with few training bits, the receiver can achieve performance close to the single-user bound in few iterations. We have also shown that the proposed receiver attains the full system diversity through accurate channel estimates.

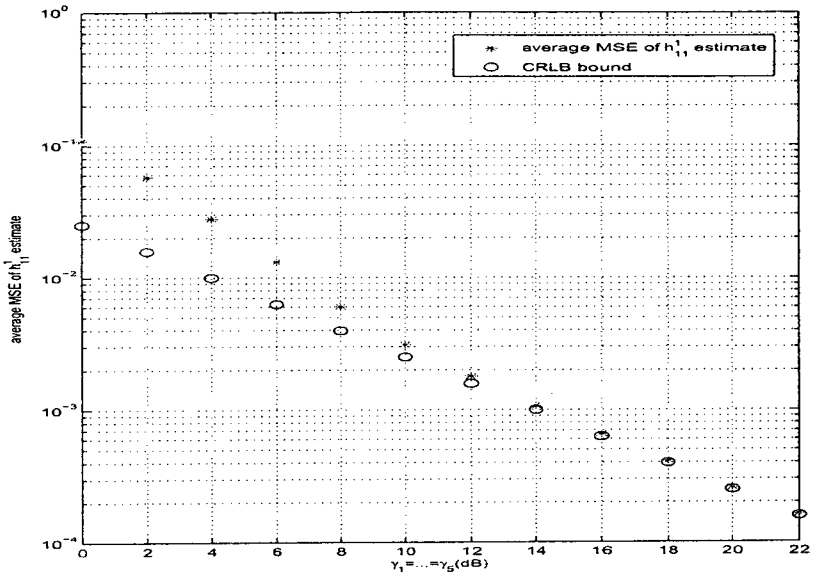

Figure 5.7: MSE of channel estimates in MIMO CDMA system with V=2 receive antennas considering flat fading channel, $M = 20, p' = 1,2$ iterations.

Chapter 6

Conclusions and Future Works

6.1 Summary and Conclusions

This section briefly summarizes the accomplished work and the major contributions in this thesis.

In Chapter 1,2, the essential background of the space-time processing techniques for the MIMO systems was provided. Given the importance of CDMA as a generic multiple-access scheme, we revised the standard transmit diversity scheme for WCDMA systems, known as STS. This scheme has the advantage of achieving the full system diversity without wasting the system resources. Since the detection process of MIMO CDMA systems is based on the perfect knowledge of the channel at the receiver side, a brief description of different channel models and possible channel estimation techniques were presented.

In Chapter 3, we investigated the performance of MIMO CDMA system over frequency-selective fast fading channels, where perfect CSI was assumed at the receiver side. We proposed a space-time receiver which utilizes the spatial and temporal diversity gains provided by the time-variant multipath fading channels. In our work, we also studied the effect of asynchronous transmissions on system performance. To mitigate the

effect of MAI, a decorrelator detector was employed at the receiver side. We derived the BER expression over frequency-selective fading channels considering both fast and slow fading cases. Finally, our proposed receiver was shown to achieve the full system diversity through simulation and analytical results.

In Chapter 4, the effect of channel estimation errors on the performance of MIMO CDMA systems was examined. It was shown that channel estimation based on training techniques degraded the performance of MIMO CDMA systems due to the increased level of interference. As a remedy to this problem, we proposed a channel estimation and data detection technique based on the superimposed training approach for MIMO CDMA systems. In our proposed technique, the interference effect was eliminated from both the channel and data estimates using two decorrlators; channel and data decorrelators. The performance of the proposed estimation technique was investigated over frequency-selective slow fading channels, where we derived a closed-form expression for the BER of the prescribed system. Finally, our proposed scheme was shown to be more robust to channel estimation errors. Furthermore, both analytical and simulation results indicated that the full system diversity was achieved.

Considering that training estimation techniques suffer either from low spectral efficiency (i.e., conventional training approach) or from high pilot power consumption (i.e., superimposed training-based approach), in Chapter 5, we presented an iterative JDE using the EM algorithm for MIMO CDMA systems over frequency-selective fading channels. We also derived a closed-form expression for the optimized weight coefficients of the EM algorithm, which was shown to provide significant performance enhancement relative to the conventional equal-weight EM-based signal decomposition. Finally, our simulation results illustrated that the proposed receiver achieved near-optimum performance with modest complexity using very few training symbols.

6.2 Future Works

In what follows we address some topics of interest for the future extension of this research.

- In this work, the users' delays and the channel impulse responses are assumed to occur at multiples of the chip period. Furthermore, the users' delays are assumed to be known at the receiver side. However, the effect of imperfect synchronization on the performance of STS systems as well as possible synchronization techniques are practical issues which have not been addressed in the proposed scheme throughout the thesis. Addressing these problems is an interesting research direction.

- Throughout this dissertation, the fading correlation in the MIMO CDMA channel was neglected. Recent research in [95] has shown the possible utilization of the channel correlation information to bring further advantages to the MIMO systems if the channel knowledge is available at the transmitter. Future works should focus on the effect of correlation on MIMO CDMA systems.

- Adaptive rate application in MIMO CDMA systems considering frequency-selective fading channels is a promising and practical problem that should be considered in the future research.

Appendix A

A.1 Definition of Pilot and Data Code Matrices

In this section, we drive the pilot and data code matrices corresponding to the current, following and previous STS symbols of the K-user system within the observation interval respectively, with the aid of Fig. 4.2. In (4.2), the nonzero elements in $\mathbf{C}[0]$ include the periods of the transmitted sequences with blank background in Fig. 4.2. Therefore $\mathbf{C}_k[0]$ is defined by

$$\mathbf{C}_k[0] = \begin{bmatrix}
 & \mathbf{0}_{\tau_k \times 4} & & & & \mathbf{0}_{\tau_k \times 4} & \cdots & & \mathbf{0}_{\tau_k \times 4} & \\
P_{k1}^0 & P_{k2}^0 & c_{k1}^0 & c_{k2}^0 & 0 & 0 & \cdots & 0 & \cdots & 0 \\
P_{k1}^1 & P_{k2}^1 & c_{k1}^1 & c_{k2}^1 & P_{k1}^0 & P_{k2}^0 & \cdots & 0 & \cdots & 0 \\
\vdots & \cdots & \cdots & \vdots & \vdots & \cdots & \ddots & \vdots & \ddots & \vdots \\
\vdots & \cdots & \cdots & \vdots & \vdots & \cdots & \ddots & P_{k1}^0 & \cdots & c_{k2}^0 \\
\vdots & \cdots & \cdots & \vdots & \vdots & \cdots & \ddots & \vdots & \ddots & \vdots \\
P_{k1}^{2N-1} & P_{k2}^{2N-1} & c_{k1}^{2N-1} & c_{k2}^{2N-1} & P_{k1}^{2N-2} & P_{k2}^{2N-2} & \cdots & P_{k1}^{2N-L} & \cdots & c_{k2}^{2N-L} \\
0 & 0 & 0 & 0 & P_{k1}^{2N-1} & P_{k2}^{2N-1} & \cdots & P_{k1}^{2N-L+1} & \cdots & c_{k2}^{2N-L+1} \\
0 & 0 & 0 & 0 & 0 & 0 & \cdots & P_{k1}^{2N-L+2} & \cdots & c_{k2}^{2N-L+2} \\
\vdots & \cdots & \cdots & \vdots & \vdots & \cdots & \ddots & \vdots & \ddots & \vdots \\
0 & \cdots & \cdots & 0 & 0 & \cdots & \cdots & P_{k1}^{2N-1} & \cdots & c_{k2}^{2N-1} \\
 & \mathbf{0}_{\Delta\tau_k \times 4} & & & & \mathbf{0}_{\Delta\tau_k \times 4} & \cdots & & \mathbf{0}_{\Delta\tau_k \times 4} &
\end{bmatrix}$$

where $\mathbf{0}$ represents a zero matrix, and $\Delta\tau_k = \tau_{max} - \tau_k$. From Fig. 4.2, the nonzero elements in $\mathbf{C}[1]$ include the periods of the transmitted sequences with downward diagonal background. Hence, $\mathbf{C}_k[1], (k = 1, 2, ..K)$ is given by

$$\mathbf{C}_k[1] = \begin{bmatrix} \mathbf{0}_{(2N+\tau_k)\times 4} & & & & \mathbf{0}_{(2N+\tau_k)\times 4} & & \cdots & \mathbf{0}_{(2N+\tau_k)\times 4} \\ P_{k1}^0 & P_{k2}^0 & c_{k1}^0 & c_{k2}^0 & 0 & 0 & \cdots & 0 \\ P_{k1}^1 & P_{k2}^1 & c_{k1}^1 & c_{k2}^1 & P_{k1}^0 & P_{k2}^0 & \cdots & 0 \\ \vdots & \cdots & \cdots & \vdots & \vdots & \cdots & \ddots & \vdots \\ P_{k1}^{L-1} & P_{k2}^{L-1} & c_{k1}^{L-1} & c_{k2}^{L-1} & P_{k1}^{L-2} & \cdots & \ddots & c_{k2}^0 \\ \vdots & \cdots & \cdots & \vdots & \vdots & \cdots & \ddots & \vdots \\ P_{k1}^{\Delta\tau_k+L-2} & P_{k2}^{\Delta\tau_k+L-2} & c_{k1}^{\Delta\tau_k+L-2} & c_{k2}^{\Delta\tau_k+L-2} & P_{k1}^{\Delta\tau_k+L-3} & \cdots & \cdots & c_{k2}^{\Delta\tau_k-1} \end{bmatrix}.$$

Similarly, during the data detection, $\mathbf{C}'[0]$, is defined by

$$\mathbf{C}'[0] = [\mathbf{C}_1'[0], \mathbf{C}_2'[0], ..., \mathbf{C}_K'[0]],$$

with

$$\mathbf{C}_k'[0] = \begin{bmatrix} \mathbf{0}_{\tau_k\times 2} & & \mathbf{0}_{\tau_k\times 2} & & \cdots & \mathbf{0}_{\tau_k\times 2} & \\ c_{k1}^0 & c_{k2}^0 & 0 & 0 & \cdots & 0 & 0 \\ c_{k1}^1 & c_{k2}^1 & c_{k1}^0 & c_{k2}^0 & \cdots & 0 & 0 \\ c_{k1}^2 & c_{k2}^2 & c_{k1}^1 & c_{k2}^1 & \cdots & 0 & 0 \\ \vdots & \vdots & \vdots & \vdots & \ddots & \vdots & \vdots \\ \vdots & \vdots & \vdots & \vdots & \ddots & c_{k1}^0 & c_{k2}^0 \\ \vdots & \vdots & \vdots & \vdots & \ddots & \vdots & \vdots \\ c_{k1}^{2N-1} & c_{k2}^{2N-1} & c_{k1}^{2N-2} & c_{k2}^{2N-2} & \cdots & c_{k1}^{2N-L} & c_{k2}^{2N-L} \\ 0 & 0 & c_{k1}^{2N-1} & c_{k2}^{2N-1} & \cdots & c_{k1}^{2N-L+1} & c_{k2}^{2N-L+1} \\ 0 & 0 & 0 & 0 & \cdots & c_{k1}^{2N-L+2} & c_{k2}^{2N-L+2} \\ \vdots & \vdots & \vdots & \vdots & \ddots & \vdots & \vdots \\ 0 & 0 & 0 & 0 & \cdots & c_{k1}^{2N-1} & c_{k2}^{2N-1} \\ \mathbf{0}_{\Delta\tau_k\times 2} & & \mathbf{0}_{\Delta\tau_k\times 2} & & \cdots & \mathbf{0}_{\Delta\tau_k\times 2} & \end{bmatrix},$$

and

$$\mathbf{C}'[1] = [\mathbf{C}_1'[1], \mathbf{C}_2'[1], ..., \mathbf{C}_K'[1]],$$

where

$$\mathbf{C}_k^{'}[1] = \begin{bmatrix} \mathbf{0}_{(2N+\tau_k)\times 2} & & \mathbf{0}_{(2N+\tau_k)\times 2} & & \cdots & \mathbf{0}_{(2N+\tau_k)\times 2} & \\ c_{k1}^0 & c_{k2}^0 & 0 & 0 & \cdots & 0 & 0 \\ c_{k1}^1 & c_{k2}^1 & c_{k1}^0 & c_{k2}^0 & \cdots & 0 & 0 \\ c_{k1}^2 & c_{k2}^2 & c_{k1}^1 & c_{k2}^1 & \cdots & 0 & 0 \\ \vdots & \vdots & \vdots & \vdots & \ddots & \vdots & \vdots \\ c_{k1}^{L-1} & c_{k2}^{L-1} & c_{k1}^{L-2} & c_{k2}^{L-2} & \ddots & c_{k1}^0 & c_{k2}^0 \\ \vdots & \vdots & \vdots & \vdots & \ddots & \vdots & \vdots \\ c_{k1}^{\Delta\tau_k+L-2} & c_{k2}^{\Delta\tau_k+L-2} & c_{k1}^{\Delta\tau_k+L-3} & c_{k2}^{\Delta\tau_k+L-3} & \cdots & c_{k1}^{\Delta\tau_k-1} & c_{k2}^{\Delta\tau_k-1} \end{bmatrix}.$$

In (4.9)-(4.11), $\mathbf{C}'[-1]$ is $[(2N + L - 1 + \tau_{max}) \times 2LK]$ data code matrix which includes the data sequences corresponding to the K users of the previous STS symbols within the current observation interval. From Fig. 4.2, the nonzero elements in $\mathbf{C}'[-1]$ includes the periods of the transmitted sequences with small grid background,

$$\mathbf{C}^{'}[-1] = [\mathbf{C}_1^{'}[-1], \mathbf{C}_2^{'}[-1], ..., \mathbf{C}_K^{'}[-1]],$$

where

$$\mathbf{C}_k^{'}[-1] = \begin{bmatrix} c_{k1}^{2N-\tau_k} & c_{k2}^{2N-\tau_k} & c_{k1}^{2N-\tau_k-1} & c_{k2}^{2N-\tau_k-1} & \cdots & c_{k2}^{2N-\tau_k-L+1} \\ c_{k1}^{2N-\tau_k+1} & c_{k2}^{2N-\tau_k+1} & c_{k1}^{2N-\tau_k} & c_{k2}^{2N-\tau_k} & \cdots & c_{k2}^{2N-\tau_k-L+2} \\ \vdots & \vdots & \vdots & \vdots & \ddots & \vdots \\ c_{k1}^{2N-1} & c_{k2}^{2N-1} & c_{k1}^{2N-2} & c_{k2}^{2N-2} & \cdots & c_{k2}^{2N-L} \\ 0 & 0 & c_{k1}^{2N-1} & c_{k2}^{2N-1} & \cdots & c_{k2}^{2N-L+1} \\ 0 & 0 & 0 & 0 & \cdots & c_{k2}^{2N-L+2} \\ \vdots & \vdots & \vdots & \vdots & \ddots & \vdots \\ 0 & 0 & 0 & 0 & \cdots & c_{k2}^{2N-1} \\ \mathbf{0}_{(2N+\Delta_k)\times 2} & & \mathbf{0}_{(2N+\Delta_k)\times 2} & & \cdots & \mathbf{0}_{(2N+\Delta_k)\times 2} \end{bmatrix}.$$

A.2 Covariance Matrix of $\mathbf{X}^v$

In this section, we drive the covariance matrix of $\mathbf{X}^v$ at the v^{th} receive antenna, whose elements are defined in (4.32). The covariance matrix of $\mathbf{X}^v$ is defined as

$$\mathbf{R}_x = E[\mathbf{X}^v \mathbf{X}^{vH}] = \begin{bmatrix} \mathbf{R}_{H-H} & \mathbf{0}_{2L\times 2LK} & \mathbf{0}_{2L\times 2L} \\ \mathbf{0}_{2LK\times 2L} & \mathbf{R}_{E-E} & \mathbf{0}_{2LK\times 2L} \\ \mathbf{0}_{2L\times 2L} & \mathbf{0}_{2L\times 2LK} & \mathbf{R}_{N-N} \end{bmatrix}$$

where $\mathbf{R}_{H-H}$, $\mathbf{R}_{E-E}$ and $\mathbf{R}_{N-N}$ represent the cross-correlation matrices corresponding to the channel coefficients of the first user, the channel estimation errors corresponding to the K-user system, and the noise samples at the data decorrelator output of the first user, respectively.

Let

$$\mathbf{h}^v = [h_{11}^{1,v}, h_{21}^{1,v}, h_{12}^{1,v}, \ldots, h_{2L}^{1,v}]^T,$$

$$\mathbf{E}^{v'} = [e_{11}^{1,v}, e_{21}^{1,v}, \ldots, e_{2L}^{1,v}, \ldots, e_{2L}^{K,v}]^T$$

and

$$\mathbf{N}^v = [(\mathbf{N}_{dd}^v)_{1,1}, (\mathbf{N}_{dd}^v)_{2,1}, \ldots, (\mathbf{N}_{dd}^v)_{2L-1,1}, (\mathbf{N}_{dd}^v)_{2L,1}]^T.$$

Then,

$$\mathbf{R}_{H-H} = E[\mathbf{h}^v \mathbf{h}^{vH}] = \begin{bmatrix} \sigma_h^2 & 0 & \cdots & 0 \\ 0 & \sigma_h^2 & \cdots & 0 \\ \vdots & \cdots & \cdots & \vdots \\ 0 & 0 & \cdots & \sigma_h^2 \end{bmatrix},$$

$$\mathbf{R}_{E-E} = E[\mathbf{E}^{v'}\mathbf{E}^{v'H}]$$

$$= \frac{1}{B'^2} \times \begin{bmatrix} (\mathbf{R}_p^{-H})_{1,1} & (\mathbf{R}_p^{-H})_{1,2} & (\mathbf{R}_p^{-H})_{1,5} & \cdots & (\mathbf{R}_p^{-H})_{1,4LK-2} \\ (\mathbf{R}_p^{-H})_{2,1} & (\mathbf{R}_p^{-H})_{2,2} & (\mathbf{R}_p^{-H})_{2,5} & \cdots & (\mathbf{R}_p^{-H})_{2,4LK-2} \\ \vdots & \cdots & \cdots & \cdots & \vdots \\ (\mathbf{R}_p^{-H})_{4L-2,1} & (\mathbf{R}_p^{-H})_{4L-2,2} & (\mathbf{R}_p^{-H})_{4L-2,5} & \cdots & (\mathbf{R}_p^{-H})_{4L-2,4LK-2} \\ \vdots & \cdots & \cdots & \cdots & \vdots \\ (\mathbf{R}_p^{-H})_{4LK-2,1} & (\mathbf{R}_p^{-H})_{4LK-2,2} & (\mathbf{R}_p^{-H})_{4LK-2,5} & \cdots & (\mathbf{R}_p^{-H})_{4LK-2,4LK-2} \end{bmatrix},$$

and

$$\mathbf{R}_{N-N} = E[\mathbf{N}^{v}\mathbf{N}^{vH}]$$

$$= \begin{bmatrix} (\mathbf{R}_d^{-H})_{1,1} & (\mathbf{R}_d^{-H})_{1,2} & \cdots & (\mathbf{R}_d^{-H})_{1,2L} \\ (\mathbf{R}_d^{-H})_{2,1} & (\mathbf{R}_d^{-H})_{2,2} & \cdots & (\mathbf{R}_d^{-H})_{2,2L} \\ \vdots & \cdots & \cdots & \vdots \\ (\mathbf{R}_d^{-H})_{2L,1} & (\mathbf{R}_d^{-H})_{2L,2} & \cdots & (\mathbf{R}_d^{-H})_{2L,2L} \end{bmatrix}.$$

A.3 Coefficient Matrices $\mathbf{S}_1$ and $\mathbf{S}_2$

In this section, we construct the coefficient matrices $\mathbf{S}_1$ and $\mathbf{S}_2$ of the quadratic form defined in (4.30) and (4.31). $\mathbf{S}_1$ is a square matrix of dimension $[4L + 2LK]$, consisting of the coefficients corresponding to the elements of $\mathbf{X}^v$ in (4.30), and is given by

$$\mathbf{S}_1 = \begin{bmatrix} \mathbf{S}_{H-H} & \mathbf{S}_{H-E} & \mathbf{S}_{H-N} \\ \mathbf{S}_{H-E}^T & \mathbf{S}_{E-E} & \mathbf{S}_{E-N} \\ \mathbf{S}_{H-N}^T & \mathbf{S}_{E-N}^T & \mathbf{0}_{2L\times 2L} \end{bmatrix}$$

where

$$\mathbf{S}_{H-H(2L\times 2L)} = \begin{bmatrix} A' & 0 & \cdots & 0 \\ 0 & A' & \cdots & 0 \\ \vdots & \cdots & \cdots & \vdots \\ 0 & 0 & \cdots & A' \end{bmatrix},$$

$$\mathbf{S}_{H-E(2L\times 2LK)} = \begin{bmatrix} \frac{-B'\mathbf{X}_1(1)+A'}{2} & \frac{-B'\mathbf{X}_1(2)-A'}{2} & \frac{-B'\mathbf{X}_1(3)}{2} & \cdots & \frac{-B'\mathbf{X}_1(2LK)}{2} \\ \frac{B'\mathbf{X}_2(1)+A'}{2} & \frac{B'\mathbf{X}_2(2)+A'}{2} & \frac{B'\mathbf{X}_2(3)}{2} & \cdots & \frac{B'\mathbf{X}_2(2LK)}{2} \\ \frac{-B'\mathbf{X}_3(1)}{2} & \frac{-B'\mathbf{X}_3(2)}{2} & \frac{-B'\mathbf{X}_3(3)+A'}{2} & \cdots & \frac{-B'\mathbf{X}_3(2LK)}{2} \\ \vdots & \cdots & \cdots & \cdots & \vdots \\ \frac{B'\mathbf{X}_{2L}(1)}{2} & \frac{B'\mathbf{X}_{2L}(2)}{2} & \cdots & \cdots & \frac{B'\mathbf{X}_{2L}(2LK)}{2} \end{bmatrix},$$

$$\mathbf{S}_{H-N(2L\times 2L)} = \begin{bmatrix} \frac{1}{2} & 0 & \cdots & 0 \\ 0 & -\frac{1}{2} & \cdots & 0 \\ \vdots & \cdots & \cdots & \vdots \\ 0 & 0 & \cdots & -\frac{1}{2} \end{bmatrix},$$

$$\mathbf{S}_{E-N(2LK\times 2L)} = \begin{bmatrix} \frac{1}{2} & 0 & \cdots & 0 \\ 0 & -\frac{1}{2} & \cdots & 0 \\ \vdots & \cdots & \cdots & \vdots \\ 0 & 0 & \cdots & -\frac{1}{2} \\ 0 & 0 & \cdots & 0 \\ \vdots & \cdots & \cdots & \vdots \\ 0 & 0 & \cdots & 0 \end{bmatrix}.$$

Finally, the square matrix, $\mathbf{S}_{E-E(2LK\times 2LK)}$, is given by

$$\begin{bmatrix}
-B'\mathbf{X}_1(1) & \frac{-B'\mathbf{X}_1(2)+B'\mathbf{X}_2(1)}{2} & \cdots & \frac{-B'\mathbf{X}_1(2L)+B'\mathbf{X}_{2L}(1)}{2} & \cdots & \frac{-B'\mathbf{X}_1(2LK)}{2} \\
\frac{B'\mathbf{X}_2(1)-B'\mathbf{X}_1(2)}{2} & B'\mathbf{X}_2(2) & \cdots & \frac{B'\mathbf{X}_2(2L)+B'\mathbf{X}_{2L}(2)}{2} & \cdots & \frac{B'\mathbf{X}_2(2LK)}{2} \\
\frac{-B'\mathbf{X}_3(1)-B'\mathbf{X}_1(3)}{2} & \frac{-B'\mathbf{X}_3(2)+B'\mathbf{X}_2(3)}{2} & \cdots & \frac{-B'\mathbf{X}_3(2L)+B'\mathbf{X}_{2L}(3)}{2} & \cdots & \frac{-B'\mathbf{X}_3(2LK)}{2} \\
\vdots & \cdots & \cdots & \cdots & \cdots & \vdots \\
\frac{B'\mathbf{X}_{2L}(1)-B'\mathbf{X}_1(2L)}{2} & \frac{B'\mathbf{X}_{2L}(2)+B'\mathbf{X}_2(2L)}{2} & \cdots & B'\mathbf{X}_{2L}(2L) & \cdots & \frac{B'\mathbf{X}_2(2LK)}{2} \\
\frac{-B'\mathbf{X}_1(2L+1)}{2} & \frac{B'\mathbf{X}_2(2L+1)}{2} & \cdots & \frac{B'\mathbf{X}_{2L}(2L+1)}{2} & \cdots & 0 \\
\vdots & \cdots & \cdots & \cdots & \cdots & \vdots \\
\frac{-B'\mathbf{X}_1(2LK)}{2} & \frac{B'\mathbf{X}_2(2LK)}{2} & \cdots & \frac{B'\mathbf{X}_{2L}(2LK)}{2} & \cdots & 0
\end{bmatrix}$$

Similarly, one can find the coefficient matrix $\mathbf{S}_2$.

Appendix B

B.1 Estimation of $\mathcal{Q}_k(\mathbf{b}_k|\mathbf{b}^i)$

In this section, we drive a closed-form expression of $\mathcal{Q}_k(\mathbf{b}_k|\mathbf{b}^i)$, which is defined in (5.14). After some mathematical manipulations, (5.14) can be expressed as

$$\mathcal{Q}_k(\mathbf{b}_k|\mathbf{b}^i) = \sum_{v=1}^{V}\sum_{m=0}^{M-1} 2Re\left\{E\left[A_1^{k,v}(m) + A_2^{k,v}(m) - A_3^{k,v}(m) - A_4^{k,v}(m)|\mathbf{y}_w, \mathbf{b}^i\right]\right\} - E\left[A_5^{k,v}(m)|\mathbf{y}_w, \mathbf{b}^i\right], \tag{B1}$$

where

$$A_1^{k,v}(m) = \mathbf{h}_k^{vH}\mathbf{B}_k(m)\mathbf{F}_k[0]^T\mathbf{g}_k^v(m), \tag{B2}$$

$$A_2^{k,v}(m) = \mathbf{h}_k^{vH}\mathbf{B}_k(m)\mathbf{F}_k[1]^T\mathbf{g}_k^v(m+1), \tag{B3}$$

$$A_3^{k,v}(m) = \mathbf{h}_k^{vH}\mathbf{B}_k(m)\mathbf{R}_{kk}[-1]\mathbf{B}_k(m-1)\mathbf{h}_k^v, \tag{B4}$$

$$A_4^{k,v}(m) = \mathbf{h}_k^{vH}\mathbf{B}_k(m)\mathbf{R}_{kk}[-1]^T\mathbf{B}_k(m+1)\mathbf{h}_k^v, \tag{B5}$$

$$A_5^{k,v}(m) = \mathbf{h}_k^{vH}\mathbf{B}_k(m)\mathbf{R}_{kk}[0]\mathbf{B}_k(m)\mathbf{h}_k^v. \tag{B6}$$

Starting with $A_1^{k,v}(m)$ and $A_2^{k,v}(m)$, and using (5.15), $A_1^{k,v}(m)+A_2^{k,v}(m)$ can be represented as

$$A_1^{k,v}(m) + A_2^{k,v}(m) = \mathbf{h}_k^{vH}\mathbf{B}_k(m)\mathbf{R}_{kk}[-1]\mathbf{B}_k(m-1)^i\mathbf{h}_k^v + \mathbf{h}_k^{vH}\mathbf{B}_k(m)$$
$$\times \mathbf{R}_{kk}[-1]^T\mathbf{B}_k(m+1)^i\mathbf{h}_k^v + \mathbf{h}_k^{vH}\mathbf{B}_k(m)\mathbf{R}_{kk}[0]\mathbf{B}_k(m)^i\mathbf{h}_k^v + \beta_k^v\Bigg(\mathbf{h}_k^{vH}\mathbf{B}_k(m)\mathbf{y}_{c,k}^v[m]$$
$$- \sum_{j=1}^{K}\mathbf{h}_k^{vH}\mathbf{B}_k(m)\mathbf{R}_{kj}[-1]\mathbf{B}_j(m-1)^i\mathbf{h}_j^v + \mathbf{h}_k^{vH}\mathbf{B}_k(m)\mathbf{R}_{kj}[-1]^T\mathbf{B}_j(m+1)^i\mathbf{h}_j^v$$
$$+ \mathbf{h}_k^{vH}\mathbf{B}_k(m)\mathbf{R}_{kj}[0]\mathbf{B}_j[m]^i\mathbf{h}_j^v\Bigg). \quad \text{(B7)}$$

Consider the first term of the right-hand side of (B7). By taking the expectation of this term with respect to $\mathbf{y}_w$ and $\mathbf{b}^i$, we obtain

$$E\left[\mathbf{h}_k^{vH}\mathbf{B}_k(m)\mathbf{R}_{kk}[-1]\mathbf{B}_k(m-1)^i\mathbf{h}_k^v|\mathbf{y}_w,\mathbf{b}^i\right] = \sum_{l=1}^{L}\sum_{l'=1}^{L}\rho_{1,ll',m}^{kk^i}(-1)\left(h_{1l}^{k,v^*}h_{1l'}^{k,v}\right)^i$$
$$+ \rho_{2,ll',m}^{kk^i}(-1)\left(h_{1l}^{k,v^*}h_{2l'}^{k,v}\right)^i + \rho_{3,ll',m}^{kk^i}(-1)\left(h_{2l}^{k,v^*}h_{1l'}^{k,v}\right)^i + \rho_{4,ll',m}^{kk^i}(-1)\left(h_{2l}^{k,v^*}h_{2l'}^{k,v}\right)^i, \quad \text{(B8)}$$

where

$$\rho_{1,ll',m}^{kk^i}(-1) = \left(\rho_{11,ll'}^{kk}(-1)b_{k1}[m] + \rho_{21,ll'}^{kk}(-1)b_{k2}[m]\right)b_{k1}[m-1]^i$$
$$+ \left(\rho_{12,ll'}^{kk}(-1)b_{k1}[m] + \rho_{22,ll'}^{kk}(-1)b_{k2}[m]\right)b_{k2}[m-1]^i, \quad \text{(B9)}$$

$$\rho_{2,ll',m}^{kk^i}(-1) = \left(\rho_{11,ll'}^{kk}(-1)b_{k1}[m] + \rho_{21,ll'}^{kk}(-1)b_{k2}[m]\right)b_{k2}[m-1]^i$$
$$- \left(\rho_{12,ll'}^{kk}(-1)b_{k1}[m] + \rho_{22,ll'}^{kk}(-1)b_{k2}[m]\right)b_{k1}[m-1]^i, \quad \text{(B10)}$$

$$\rho_{3,ll',m}^{kk^i}(-1) = \left(\rho_{11,ll'}^{kk}(-1)b_{k2}[m] - \rho_{21,ll'}^{kk}(-1)b_{k1}[m]\right)b_{k1}[m-1]^i$$
$$+ \left(\rho_{12,ll'}^{kk}(-1)b_{k2}[m] - \rho_{22,ll'}^{kk}(-1)b_{k1}[m]\right)b_{k2}[m-1]^i, \quad \text{(B11)}$$

$$\rho^{kk^i}_{4,ll',m}(-1) = \left(\rho^{kk}_{11,ll'}(-1)b_{k2}[m] - \rho^{kk}_{21,ll'}(-1)b_{k1}[m]\right) b_{k2}[m-1]^i$$
$$- \left(\rho^{kk}_{12,ll'}(-1)b_{k2}[m] - \rho^{kk}_{22,ll'}(-1)b_{k1}[m]\right) b_{k1}[m-1]^i, \quad \text{(B12)}$$

where $\rho^{kk}_{qq',ll'}(-1)$, $q,q' \in \{1,2\}$, $l,l' \in \{1,\ldots,L\}$ represents the cross-correlation between the l^{th} path of the q^{th} code of the k^{th} user which is corresponding to the current STS symbol interval and the l'^{th} path of the q'^{th} code of the same user during the previous STS symbol interval. Similarly, we evaluate the conditional expectation of the second and third terms of (B7) by considering the cross-correlation between the multipath versions of the k^{th} user code sequences during the current STS symbol interval with the multipath versions of the code sequences of the same user during the following and current symbol intervals respectively, as well as replacing the iterative estimates of the k^{th} user's previous data bits $(b_{k1}[m-1]^i, b_{k2}[m-1]^i)$ in (B9)-(B12) by the corresponding iterative estimates of the k^{th} user's following $(b_{k1}[m+1]^i, b_{k2}[m+1]^i)$ and current data bits $(b_{k1}[m]^i, b_{k2}[m]^i)$ respectively. Also, we can evaluate the conditional expectation of the sum term in (B7) as follows. Considering the first term in this sum, we have

$$E\left[\mathbf{h}_k^{vH}\mathbf{B}_k(m)\mathbf{R}_{kj}[-1]\mathbf{B}_j(m-1)^i\mathbf{h}_j^v|\mathbf{y}_w,\mathbf{b}^i\right] = \sum_{l=1}^{L}\sum_{l'=1}^{L}\rho^{kj^i}_{1,ll',m}(-1)\left(h_{1l}^{k,v^*}h_{1l'}^{j,v}\right)^i$$
$$+ \rho^{kj^i}_{2,ll',m}(-1)\left(h_{1l}^{k,v^*}h_{2l'}^{j,v}\right)^i + \rho^{kj^i}_{3,ll',m}(-1)\left(h_{2l}^{k,v^*}h_{1l'}^{j,v}\right)^i + \rho^{kj^i}_{4,ll',m}(-1)$$
$$\times\left(h_{2l}^{k,v^*}h_{2l'}^{j,v}\right)^i, \quad \text{(B13)}$$

where

$$\rho^{kj^i}_{1,ll',m}(-1) = \left(\rho^{kj}_{11,ll'}(-1)b_{k1}[m] + \rho^{kj}_{21,ll'}(-1)b_{k2}[m]\right) b_{j1}[m-1]^i$$
$$+ \left(\rho^{kj}_{12,ll'}(-1)b_{k1}[m] + \rho^{kj}_{22,ll'}(-1)b_{k2}[m]\right) b_{j2}[m-1]^i, \quad \text{(B14)}$$

$$\rho^{kj^i}_{2,ll',m}(-1) = \left(\rho^{kj}_{11,ll'}(-1)b_{k1}[m] + \rho^{kj}_{21,ll'}(-1)b_{k2}[m]\right) b_{j2}[m-1]^i$$
$$- \left(\rho^{kj}_{12,ll'}(-1)b_{k1}[m] + \rho^{kj}_{22,ll'}(-1)b_{k2}[m]\right) b_{j1}[m-1]^i, \qquad \text{(B15)}$$

$$\rho^{kj^i}_{3,ll',m}(-1) = \left(\rho^{kj}_{11,ll'}(-1)b_{k2}[m] - \rho^{kj}_{21,ll'}(-1)b_{k1}[m]\right) b_{j1}[m-1]^i$$
$$+ \left(\rho^{kj}_{12,ll'}(-1)b_{k2}[m] - \rho^{kj}_{22,ll'}(-1)b_{k1}[m]\right) b_{j2}[m-1]^i, \qquad \text{(B16)}$$

$$\rho^{kj^i}_{4,ll',m}(-1) = \left(\rho^{kj}_{11,ll'}(-1)b_{k2}[m] - \rho^{kj}_{21,ll'}(-1)b_{k1}[m]\right) b_{j2}[m-1]^i$$
$$- \left(\rho^{kj}_{12,ll'}(-1)b_{k2}[m] - \rho^{kj}_{22,ll'}(-1)b_{k1}[m]\right) b_{j1}[m-1]^i, \qquad \text{(B17)}$$

where $\rho^{kj}_{qq',ll'}(-1)$, $q,q' \in \{1,2\}$, $l,l' \in \{1,\ldots,L\}$, $k,j \in \{1,\ldots,K\}$ represents the cross-correlation between the l^{th} path of the q^{th} code of the k^{th} user which is corresponding to the current STS symbol interval and the l'^{th} path of the q'^{th} code of the j^{th} user during the previous STS symbol interval. Similarly, we find the conditional expectation of the second and third terms of the sum term in (B7) by considering the cross-correlation between the multipath versions of the k^{th} user code sequences during the current STS symbol interval with the multipath versions of the code sequences of the j^{th} user during the following and current symbol intervals respectively, as well as replacing the iterative estimates of the j^{th} user's previous data bits $(b_{j1}[m-1]^i, b_{j2}[m-1]^i)$ in (B14)-(B17) by the corresponding iterative estimates of the j^{th} user's following $(b_{j1}[m+1]^i, b_{j2}[m+1]^i)$ and current data

bits $(b_{j1}[m]^i, b_{j2}[m]^i)$ respectively. Finally, $E\left[A_1^{k,v}(m) + A_2^{k,v}(m)|\mathbf{y}_w, \mathbf{b}^i\right]$ is reduced to

$$E\left[A_1^{k,v}(m) + A_2^{k,v}(m)|\mathbf{y}_w, \mathbf{b}^i\right] = \sum_{l=1}^{L}\sum_{l'=1}^{L}\left(\rho_{1,ll',m}^{kk^i}(-1) + \rho_{1,ll',m}^{kk^i}(1) + \rho_{1,ll',m}^{kk^i}(0)\right)$$
$$\times\left(h_{1l}^{k,v^*}h_{1l'}^{k,v}\right)^i + \left(\rho_{2,ll',m}^{kk^i}(-1) + \rho_{2,ll',m}^{kk^i}(1) + \rho_{2,ll',m}^{kk^i}(0)\right)\left(h_{1l}^{k,v^*}h_{2l'}^{k,v}\right)^i$$
$$+\left(\rho_{3,ll',m}^{kk^i}(-1) + \rho_{3,ll',m}^{kk^i}(1) + \rho_{3,ll',m}^{kk^i}(0)\right)\left(h_{2l}^{k,v^*}h_{1l'}^{k,v}\right)^i + \left(\rho_{4,ll',m}^{kk^i}(-1) + \rho_{4,ll',m}^{kk^i}(1)\right.$$
$$\left.+\rho_{4,ll',m}^{kk^i}(0)\right)\left(h_{2l}^{k,v^*}h_{2l'}^{k,v}\right)^i + \beta_k^v\left((\mathbf{h}_k^v)^{iH}\mathbf{B}_k(m)\mathbf{y}_{c,k}^v[m] - \sum_{j=1}^{K}\sum_{l=1}^{L}\sum_{l'=1}^{L}\left(\rho_{1,ll',m}^{kj^i}(-1)\right.\right.$$
$$\left.+\rho_{1,ll',m}^{kj^i}(1) + \rho_{1,ll',m}^{kj^i}(0)\right)\left(h_{1l}^{k,v^*}h_{1l'}^{j,v}\right)^i + \left(\rho_{2,ll',m}^{kj^i}(-1) + \rho_{2,ll',m}^{kj^i}(1) + \rho_{2,ll',m}^{kj^i}(0)\right)$$
$$\times\left(h_{1l}^{k,v^*}h_{2l'}^{j,v}\right)^i + \left(\rho_{3,ll',m}^{kj^i}(-1) + \rho_{3,ll',m}^{kj^i}(1) + \rho_{3,ll',m}^{kj^i}(0)\right)\left(h_{2l}^{k,v^*}h_{1l'}^{j,v}\right)^i$$
$$\left.+\left(\rho_{4,ll',m}^{kj^i}(-1) + \rho_{4,ll',m}^{kj^i}(1) + \rho_{4,ll',m}^{kj^i}(0)\right)\left(h_{2l}^{k,v^*}h_{2l'}^{j,v}\right)^i\right). \quad \text{(B18)}$$

From (B4), we find the conditional expectation of $A_3^{k,v}(m)$ given $\mathbf{y}_w$ and $\mathbf{b}^i$ as follows. By replacing the iterative estimates of the previous data matrix, $\mathbf{B}_k(m-1)^i$, with its accurate value, $\mathbf{B}_k(m-1)$, in (B8), we obtain a similar expression for $E\left[A_3^{k,v}(m)|\mathbf{y}_w, \mathbf{b}^i\right]$. The same argument is also applied for $A_4^{k,v}(m)$. Finally, after some mathematical manipulations, we evaluate the conditional expectation of $A_5^{k,v}(m)$ given $\mathbf{y}_w$ and $\mathbf{b}^i$ as follows

$$E\left[A_5^{k,v}(m)|\mathbf{y}_w, \mathbf{b}^i\right] = \sum_{l=1}^{L}\sum_{l'=1,l'>l}^{L} 2Re\left\{\rho_{1,ll',m}^{kk}(0)\left(h_{1l}^{k,v^*}h_{1l'}^{k,v}\right)^i + \rho_{2,ll',m}^{kk}(0)\right.$$
$$\left.\times\left(h_{1l}^{k,v^*}h_{2l'}^{k,v}\right)^i + \rho_{3,ll',m}^{kk}(0)\left(h_{2l}^{k,v^*}h_{1l'}^{k,v}\right)^i + \rho_{4,ll',m}^{kk}(0)\left(h_{2l}^{k,v^*}h_{2l'}^{k,v}\right)^i\right\}, \quad \text{(B19)}$$

where

$$\rho_{1,ll',m}^{kk}(0) = \left(\rho_{12,ll'}^{kk}(0) + \rho_{21,ll'}^{kk}(0)\right)b_{k1}[m]b_{k2}[m], \quad \text{(B20)}$$

$$\rho^{kk}_{2,ll',m}(0) = \left(\rho^{kk}_{11,ll'}(0) - \rho^{kk}_{22,ll'}(0)\right) b_{k1}[m] b_{k2}[m], \tag{B21}$$

$$\rho^{kk}_{3,ll',m}(0) = \left(\rho^{kk}_{11,ll'}(0) - \rho^{kk}_{22,ll'}(0)\right) b_{k1}[m] b_{k2}[m], \tag{B22}$$

$$\rho^{kk}_{4,ll',m}(0) = \left(-\rho^{kk}_{12,ll'}(0) - \rho^{kk}_{21,ll'}(0)\right) b_{k1}[m] b_{k2}[m]. \tag{B23}$$

Now, using the conditional expectation of (B2)-(B6) given $\mathbf{y}_w$ and $\mathbf{b}^i$, we evaluate $\mathcal{Q}_k(\mathbf{b}_k|\mathbf{b}^i)$ as

$$\begin{aligned}
\mathcal{Q}_k(\mathbf{b}_k|\mathbf{b}^i) = \sum_{v=1}^{V}\sum_{m=1}^{M} Re\Bigg\{ & \sum_{l=1}^{L}\sum_{l'=1}^{L}\Bigg(\rho^{kk^i}_{1,ll',m}(-1) + \rho^{kk^i}_{1,ll',m}(1) + \rho^{kk^i}_{1,ll',m}(0) \\
& - \rho^{kk}_{1,ll',m}(-1) - \rho^{kk}_{1,ll',m}(1)\Bigg)\left(h^{k,v^*}_{1l} h^{k,v}_{1l'}\right)^i + \Bigg(\rho^{kk^i}_{2,ll',m}(-1) + \rho^{kk^i}_{2,ll',m}(1) + \rho^{kk^i}_{2,ll',m}(0) \\
& - \rho^{kk}_{2,ll',m}(-1) - \rho^{kk}_{2,ll',m}(1)\Bigg)\left(h^{k,v^*}_{1l} h^{k,v}_{2l'}\right)^i + \Bigg(\rho^{kk^i}_{3,ll',m}(-1) + \rho^{kk^i}_{3,ll',m}(1) + \rho^{kk^i}_{3,ll',m}(0) \\
& - \rho^{kk}_{3,ll',m}(-1) - \rho^{kk}_{3,ll',m}(1)\Bigg)\left(h^{k,v^*}_{2l} h^{k,v}_{1l'}\right)^i + \Bigg(\rho^{kk^i}_{4,ll',m}(-1) + \rho^{kk^i}_{4,ll',m}(1) + \rho^{kk^i}_{4,ll',m}(0) \\
& - \rho^{kk}_{4,ll',m}(-1) - \rho^{kk}_{4,ll',m}(1)\Bigg)\left(h^{k,v^*}_{2l} h^{k,v}_{2l'}\right)^i + \beta^v_k \left((\mathbf{h}^v_k)^{iH} \mathbf{B}_k(m) \mathbf{y}^v_{c,k}[m]\right. \\
& - \sum_{j=1}^{K}\sum_{l=1}^{L}\sum_{l'=1}^{L}\Bigg(\rho^{kj^i}_{1,ll',m}(-1) + \rho^{kj^i}_{1,ll',m}(1) + \rho^{kj^i}_{1,ll',m}(0)\Bigg)\left(h^{k,v^*}_{1l} h^{j,v}_{1l'}\right)^i + \Bigg(\rho^{kj^i}_{2,ll',m}(-1) \\
& + \rho^{kj^i}_{2,ll',m}(1) + \rho^{kj^i}_{2,ll',m}(0)\Bigg)\left(h^{k,v^*}_{1l} h^{j,v}_{2l'}\right)^i + \Bigg(\rho^{kj^i}_{3,ll',m}(-1) + \rho^{kj^i}_{3,ll',m}(1) + \rho^{kj^i}_{3,ll',m}(0)\Bigg) \\
& \times \left(h^{k,v^*}_{2l} h^{j,v}_{1l'}\right)^i + \Bigg(\rho^{kj^i}_{4,ll',m}(-1) + \rho^{kj^i}_{4,ll',m}(1) + \rho^{kj^i}_{4,ll',m}(0)\Bigg)\left(h^{k,v^*}_{2l} h^{j,v}_{2l'}\right)^i\Bigg) \\
& - \sum_{l=1}^{L}\sum_{l'=1,l'>l}^{L} \rho^{kk}_{1,ll',m}(0)\left(h^{k,v^*}_{1l} h^{k,v}_{1l'}\right)^i + \rho^{kk}_{2,ll',m}(0)\left(h^{k,v^*}_{1l} h^{k,v}_{2l'}\right)^i + \rho^{kk}_{3,ll',m}(0) \\
& \times \left(h^{k,v^*}_{2l} h^{k,v}_{1l'}\right)^i + \rho^{kk}_{4,ll',m}(0)\left(h^{k,v^*}_{2l} h^{k,v}_{2l'}\right)^i\Bigg\}
\end{aligned} \tag{B24}$$

Considering a large frame M, the second summand in the right-hand side of (5.18) can be neglected (see Appendix B.4). Thus (B24) is reduced to (5.16).

B.2 Derivation of $E\left[\| E_g \|^2\right]$

In this section, we derive a closed-form expression of the error between the true signal vector and its estimate according to (5.26). After some mathematical manipulations, (5.31) can be expressed as

$$\| E_g \|^2 = D_1 - D_2 - D_3 + D_4 + D_5, \tag{B25}$$

where

$$D_1 = 2\sqrt{\beta_k^v} Re\left\{\mathbf{h}_k^{vH}\left(\left(\mathbf{B}_k(m) - \mathbf{B}_k(m)^i\right)^T \mathbf{R}_{kk}[0]^T + \left(\mathbf{B}_k(m-1) - \mathbf{B}_k(m-1)^i\right)^T \mathbf{R}_{kk}[-1]^T + \left(\mathbf{B}_k(m+1) - \mathbf{B}_k(m+1)^i\right)^T \mathbf{R}_{kk}[-1]\right) \times \mathbf{n}_{c,k}^v[m]\right\}, \tag{B26}$$

$$D_2 = 2\beta_k^v Re\left\{\mathbf{h}_k^{vH}\left(\left(\mathbf{B}_k(m) - \mathbf{B}_k(m)^i\right)^T \mathbf{R}_{kk}[0]^T + \left(\mathbf{B}_k(m-1) - \mathbf{B}_k(m-1)^i\right)^T \times \mathbf{R}_{kk}[-1]^T + \left(\mathbf{B}_k(m+1) - \mathbf{B}_k(m+1)^i\right)^T \mathbf{R}_{kk}[-1]\right)\left(\sum_{j=1}^{K}\left(\mathbf{R}_{kj}[0]\left(\mathbf{B}_j(m) - \mathbf{B}_j(m)^i\right) + \mathbf{R}_{kj}[-1]\left(\mathbf{B}_j(m-1) - \mathbf{B}_j(m-1)^i\right) + \mathbf{R}_{kj}[-1]^T\left(\mathbf{B}_j(m+1) - \mathbf{B}_j(m+1)^i\right)\right)\mathbf{h}_j^v + \mathbf{n}_{c,k}^v[m]\right)\right\}, \tag{B27}$$

$$D_3 = 2\beta_k^v\sqrt{\beta_k^v} Re\left\{\mathbf{n}_{c,k}^v[m]^H\left(\sum_{j=1}^{K}\left(\mathbf{R}_{kj}[0]\left(\mathbf{B}_j(m) - \mathbf{B}_j(m)^i\right) + \mathbf{R}_{kj}[-1] \times \left(\mathbf{B}_j(m-1) - \mathbf{B}_j(m-1)^i\right) + \mathbf{R}_{kj}[-1]^T\left(\mathbf{B}_j(m+1) - \mathbf{B}_j(m+1)^i\right)\right)\mathbf{h}_j^v + \mathbf{n}_{c,k}^v[m]\right)\right\}, \tag{B28}$$

$$D_4 = \beta_k^{v2} \parallel \sum_{j=1}^{K} \left(\mathbf{R}_{kj}[0] \left(\mathbf{B}_j(m) - \mathbf{B}_j(m)^i \right) + \mathbf{R}_{kj}[-1] \left(\mathbf{B}_j(m-1) \right. \right.$$
$$\left. \left. - \mathbf{B}_j(m-1)^i \right) + \mathbf{R}_{kj}[-1]^T \left(\mathbf{B}_j(m+1) - \mathbf{B}_j(m+1)^i \right) \right) \mathbf{h}_j^v + \mathbf{n}_{c,k}^v[m] \parallel^2, \quad \text{(B29)}$$

$$D_5 = \beta_k^v \mathbf{n}_{c,k}^v[m]^H \mathbf{n}_{c,k}^v[m], \quad \text{(B30)}$$

In our system model we assume that the noise samples and the channel coefficients are mutually independent. Using (5.32)-(5.33), we can find the expectation of D_1, D_3, and D_5 as follows

$$E[D_1] = 0, \quad \text{(B31)}$$

$$E[D_3] = 2\beta_k^{v\frac{3}{2}} \alpha_k, \quad \text{(B32)}$$

$$E[D_5] = \beta_k^v \alpha_k. \quad \text{(B33)}$$

From (B27), and using (5.32)-(5.33), the expectation of D_2 is reduced to

$$E[D_2] = 2\beta_k^v Re \left\{ E \left[\mathbf{h}_k^{vH} \left(\left(\mathbf{B}_k(m) - \mathbf{B}_k(m)^i \right)^T \mathbf{R}_{kk}[0]^T + \left(\mathbf{B}_k(m-1) \right. \right. \right.$$
$$\left. - \mathbf{B}_k(m-1)^i \right)^T \mathbf{R}_{kk}[-1]^T + \left(\mathbf{B}_k(m+1) - \mathbf{B}_k(m+1)^i \right)^T \mathbf{R}_{kk}[-1] \Big) \left(\mathbf{R}_{kk}[0] \right.$$
$$\times \left(\mathbf{B}_k(m) - \mathbf{B}_k(m)^i \right) + \mathbf{R}_{kk}[-1] \left(\mathbf{B}_k(m-1) - \mathbf{B}_k(m-1)^i \right) + \mathbf{R}_{kk}[-1]^T$$
$$\left. \left. \times \left(\mathbf{B}_k(m+1) - \mathbf{B}_k(m+1)^i \right) \right) \mathbf{h}_k^v \right] \Big\}, \quad \text{(B34)}$$

Starting with the first term in the expectation form of (B34), $E\left[\mathbf{h}_k^{vH} \left(\mathbf{B}_k(m) \right.\right.$
$\left.\left. - \mathbf{B}_k(m)^i \right)^T \mathbf{R}_{kk}[0]^T \mathbf{R}_{kk}[0] \left(\mathbf{B}_k(m) - \mathbf{B}_k(m)^i \right) \mathbf{h}_k^v \right]$, and using (5.32), this term is reduced

to

$$E\left[\mathbf{h}_k^{vH}\left(\mathbf{B}_k(m)-\mathbf{B}_k(m)^i\right)^T\mathbf{R}_{kk}[0]^T\mathbf{R}_{kk}[0]\left(\mathbf{B}_k(m)-\mathbf{B}_k(m)^i\right)\mathbf{h}_k^v\right]=2\sigma_k^2$$
$$\times\sum_{l=1}^{L}\left(r_{kk,0}(2l-1,2l-1)+r_{kk,0}(2l,2l)\right)\left(\left(1-E\left[b_{k1}[m]b_{k1}[m]^i\right]\right)\right.$$
$$\left.+\left(1-E\left[b_{k2}[m]b_{k2}[m]^i\right]\right)\right), \quad \text{(B35)}$$

Similarly, we can evaluate $E\left[\mathbf{h}_k^{vH}\left(\mathbf{B}_k(m-1)-\mathbf{B}_k(m-1)^i\right)^T\mathbf{R}_{kk}[-1]^T\mathbf{R}_{kk}[-1]\right.$
$\left.\times\left(\mathbf{B}_k(m-1)-\mathbf{B}_k(m-1)^i\right)\mathbf{h}_k^v\right]$ and $E\left[\mathbf{h}_k^{vH}\left(\mathbf{B}_k(m+1)-\mathbf{B}_k(m+1)^i\right)^T\mathbf{R}_{kk}[-1]\right.$
$\left.\times\,\mathbf{R}_{kk}[-1]^T\left(\mathbf{B}_k(m+1)-\mathbf{B}_k(m+1)^i\right)\mathbf{h}_k^v\right]$ as follows

$$E\left[\mathbf{h}_k^{vH}\left(\mathbf{B}_k(m-1)-\mathbf{B}_k(m-1)^i\right)^T\mathbf{R}_{kk}[-1]^T\mathbf{R}_{kk}[-1]\right.$$
$$\left.\times\left(\mathbf{B}_k(m-1)-\mathbf{B}_k(m-1)^i\right)\mathbf{h}_k^v\right]$$
$$=2\sigma_k^2\sum_{l=1}^{L}\left(r_{kk,-1}(2l-1,2l-1)+r_{kk,-1}(2l,2l)\right)\left(\left(1-E\left[b_{k1}[m-1]b_{k1}[m-1]^i\right]\right)\right.$$
$$\left.+\left(1-E\left[b_{k2}[m-1]b_{k2}[m-1]^i\right]\right)\right), \quad \text{(B36)}$$

$$E\left[\mathbf{h}_k^{vH}\left(\mathbf{B}_k(m+1)-\mathbf{B}_k(m+1)^i\right)^T\mathbf{R}_{kk}[-1]\mathbf{R}_{kk}[-1]^T\right.$$
$$\left.\times\left(\mathbf{B}_k(m+1)-\mathbf{B}_k(m+1)^i\right)\mathbf{h}_k^v\right]$$
$$=2\sigma_k^2\sum_{l=1}^{L}\left(r_{kk,1}(2l-1,2l-1)+r_{kk,1}(2l,2l)\right)\left(\left(1-E\left[b_{k1}[m+1]b_{k1}[m+1]^i\right]\right)\right.$$
$$\left.+\left(1-E\left[b_{k2}[m+1]b_{k2}[m+1]^i\right]\right)\right), \quad \text{(B37)}$$

In (B34), the rest of terms take the form, $E\left[\mathbf{h}_k^{vH}\left(\mathbf{B}_k(m+m_p)-\mathbf{B}_k(m+m_p)^i\right)^T\right.$
$\left.\times\mathbf{R}_{kk}[m_p]^T\mathbf{R}_{kk}[m_{p'}]\left(\mathbf{B}_k(m+m_{p'})-\mathbf{B}_k(m+m_{p'})^i\right)\mathbf{h}_k^v\right]$, $m_p, m_{p'}\in\{-1,0,1\}$, $m_p\neq m_{m_p'}$, where $\mathbf{R}_{kk}[1]=\mathbf{R}_{kk}[-1]^T$, and $\mathbf{R}_{kk}[1]\mathbf{R}_{kk}[-1]^T=\mathbf{0}$ (see Appendix A.1). After some

mathematical manipulations, we find

$$E\Bigg[\mathbf{h}_k^{vH}\left(\mathbf{B}_k(m+m_p)-\mathbf{B}_k(m+m_p)^i\right)^T\mathbf{R}_{kk}[m_p]^T\mathbf{R}_{kk}[m_{p'}]\left(\mathbf{B}_k(m+m_{p'})\right.$$
$$\left.-\mathbf{B}_k(m+m_{p'})^i\right)\mathbf{h}_k^v\Bigg]=\sigma_k^2\sum_{l=1}^{L}\Big(r_{kk,m_pm_{p'}}(2l-1,2l-1)+r_{kk,m_pm_{p'}}(2l,2l)\Big)$$
$$\times E\left[\left(b_{k1}[m-m_p]-b_{k1}[m-m_p]^i\right)\left(b_{k1}[m-m_{p'}]-b_{k1}[m-m_{p'}]^i\right)\right.$$
$$\left.+\left(b_{k2}[m-m_p]-b_{k2}[m-m_p]^i\right)\left(b_{k2}[m-m_{p'}]-b_{k2}[m-m_{p'}]^i\right)\right]$$
$$+\Big(r_{kk,m_pm_{p'}}(2l,2l-1)+r_{kk,m_pm_{p'}}(2l-1,2l)\Big)E\left[\left(b_{k2}[m-m_p]-b_{k2}[m-m_p]^i\right)\right.$$
$$\times\left(b_{k1}[m-m_{p'}]-b_{k1}[m-m_{p'}]^i\right)+\left(b_{k1}[m-m_p]-b_{k1}[m-m_p]^i\right)$$
$$\left.\times\left(b_{k2}[m-m_{p'}]-b_{k2}[m-m_{p'}]^i\right)\right],m_p\neq m_{m'_p},\quad\text{(B38)}$$

where $r_{kk,m_pm_{p'}}(\zeta,\zeta'),\zeta,\zeta'\in\{1,\ldots,2L\},m_p,m_{p'}\in\{-1,0,1\}$, $m_p\neq m_{m'_p}$, represent the elements of $\mathbf{R}_{kk}[m_p]^T\mathbf{R}_{kk}[m_{p'}]$. We found experimentally that $r_{kk,m_pm_{p'}}(\zeta,\zeta'),\zeta,\zeta'\in\{1,\ldots,2L\},m_p,m_{p'}\in\{-1,0,1\}$, either have zero values or cancel each other in the same bracket. Therefore, we assume the expectation in (B38) has a zero value. Using (B35)-(B38), we can evaluate D_2 as follows

$$E[D_2]=4\sigma_k^2\beta_k^v\sum_{l=1}^{L}\left(r_{kk,0}(2l-1,2l-1)+r_{kk,0}(2l,2l)\right)\left(\left(1-E\left[b_{k1}[m]b_{k1}[m]^i\right]\right)\right.$$
$$\left.+\left(1-E\left[b_{k2}[m]b_{k2}[m]^i\right]\right)\right)+\left(r_{kk,-1}(2l-1,2l-1)+r_{kk,-1}(2l,2l)\right)$$
$$\times\left(\left(1-E\left[b_{k1}[m-1]b_{k1}[m-1]^i\right]\right)+\left(1-E\left[b_{k2}[m-1]b_{k2}[m-1]^i\right]\right)\right)$$
$$+\left(r_{kk,1}(2l-1,2l-1)+r_{kk,1}(2l,2l)\right)\left(\left(1-E\left[b_{k1}[m+1]b_{k1}[m+1]^i\right]\right)\right.$$
$$\left.+\left(1-E\left[b_{k2}[m+1]b_{k2}[m+1]^i\right]\right)\right),\quad\text{(B39)}$$

In (B29), following the same procedure, we can evaluate $E[D_4]$ as follows

$$E[D_4] = 2\beta_k^{v2}\Bigg(\sum_{j=1}^{K}\sigma_j^2\sum_{l=1}^{L}(r_{jj,0}(2l-1,2l-1)+r_{jj,0}(2l,2l))\left((1-E\left[b_{j1}[m]\right.\right.$$
$$\left.\times b_{j1}[m]^i\right]\big)+\big(1-E\left[b_{j2}[m]b_{j2}[m]^i\right]\big)\big)+(r_{jj,-1}(2l-1,2l-1)+r_{jj,-1}(2l,2l))$$
$$\times\left(\left(1-E\left[b_{j1}[m-1]b_{j1}[m-1]^i\right]\right)+\left(1-E\left[b_{j2}[m-1]b_{j2}[m-1]^i\right]\right)\right)$$
$$+(r_{jj,1}(2l-1,2l-1)+r_{jj,1}(2l,2l))\left(\left(1-E\left[b_{j1}[m+1]b_{j1}[m+1]^i\right]\right)\right.$$
$$\left.+\left(1-E\left[b_{j2}[m+1]b_{j2}[m+1]^i\right]\right)\right)+\alpha_k\Bigg) \quad \text{(B40)}$$

Finally, substituting (B31)-(B33), (B39), and (B40), in the expectation of (B25), we get $E[\parallel E_g \parallel^2]$.

B.3 Distribution of $\mathbf{h}^v|\mathbf{y}_w, \mathbf{b}^i$:

In this section, we derive the pdf of the channel vector at the v^{th} receive antenna conditioned on the observed data vector, $\mathbf{y}_w$, and the current data estimates,$\mathbf{b}^i$. Let

$$\mathbf{n}_w = [\mathbf{n}_w^1, \mathbf{n}_w^2, \ldots, \mathbf{n}_w^V],$$

where

$$\mathbf{n}_w^v = [\mathbf{n}_w^v[1], \mathbf{n}_w^v[2], \ldots, \mathbf{n}_w^v[M]].$$

Then, the distribution of $\mathbf{y}_w|\mathbf{h}, \mathbf{b}^i$ is given by

$$f(\mathbf{y}_w|\mathbf{h}, \mathbf{b}^i) = \prod_{v=1}^{V} f\left(\mathbf{y}_w^v|\mathbf{h}^v, \mathbf{b}^i\right), \quad \text{(B41)}$$

where

$$f(\mathbf{y}_w^v|\mathbf{h}^v,\mathbf{b}^i) = \frac{1}{\pi^{2MLK}\left(\det\boldsymbol{\Sigma}_{wl}\right)^M} e^{\frac{-1}{No}\left(\sum_{m=0}^{M-1}\left(\mathbf{y}_w^v[m]-\sum_{\Delta m=0}^{1}\mathbf{F}[\Delta m]\mathbf{B}(m-\Delta m)^i\mathbf{h}^v\right)^H\right)}$$
$$\times\, e^{\frac{-1}{No}\left(\mathbf{y}_w^v[m]-\sum_{\Delta m=0}^{1}\mathbf{F}[\Delta m]\mathbf{B}(m-\Delta m)^i\mathbf{h}^v\right)},$$
$$= \frac{1}{\pi^{2MLK}\left(\det\boldsymbol{\Sigma}_{wl}\right)^M} e^{\frac{-1}{No}\left(\left\{\sum_{m=0}^{M-1}\mathbf{y}_w^v[m]^H\mathbf{y}_w^v[m]\right\}-\left\{\sum_{m=0}^{M-1}\mathbf{y}_c^v[m]^H\mathbf{B}(m)^i\right\}\mathbf{h}^v\right)}$$
$$\times\, e^{\frac{1}{No}\left(\mathbf{h}^{vH}\left\{\sum_{m=0}^{M-1}\mathbf{B}(m)^i\mathbf{y}_c^v(m)\right\}\right)}$$
$$\times\, e^{\frac{-1}{No}\left(\mathbf{h}^{vH}\left\{\sum_{m=0}^{M-1}\mathbf{B}(m)^i\left(\mathbf{R}[0]\mathbf{B}(m)^i+\mathbf{R}[-1]\mathbf{B}(m-1)^i+\mathbf{R}[1]\mathbf{B}(m+1)^i\right)\right\}\mathbf{h}^v\right)}, \quad \text{(B42)}$$

where $\mathbf{y}_c^v[m] = \mathbf{F}[0]^T\mathbf{y}_w^v[m] + \mathbf{F}_k[1]\mathbf{y}_w^v[m+1]$, $\boldsymbol{\Sigma}_{wl} = N_o\mathbf{I}_{2LK}$, and det denotes matrix determinant. The channel vector $\mathbf{h}$ has a multivariate Gaussian distribution defined as

$$f(\mathbf{h}) = \prod_{v=1}^{V} f(\mathbf{h}^v), \quad \text{(B43)}$$

where

$$f(\mathbf{h}^v) = \frac{1}{\pi^{2LK}\det\boldsymbol{\Sigma}_{hh}} e^{-\mathbf{h}^{vH}\boldsymbol{\Sigma}_{hh}^{-1}\mathbf{h}^v}. \quad \text{(B44)}$$

Using (B41) and (B43), the joint distribution

$$f(\mathbf{y}_w,\mathbf{h}|\mathbf{b}^i) = \prod_{v=1}^{V} f(\mathbf{y}_w^v,\mathbf{h}^v|\mathbf{b}^i), \quad \text{(B45)}$$

where

$$f(\mathbf{y}_w^v,\mathbf{h}^v|\mathbf{b}^i) = \frac{1}{\pi^{2LK(M+1)}\left(\det\boldsymbol{\Sigma}_{wl}\right)^M\det\boldsymbol{\Sigma}_{hh}} e^{\frac{-1}{No}\{\sum_{m=0}^{M-1}\mathbf{y}_w^v[m]^H\mathbf{y}_w^v[m]\}}$$
$$\times\, e^{\{N_o^{-1}\{\sum_{m=0}^{M-1}\mathbf{y}_c^v[m]^H\mathbf{B}(m)^i\}\mathbf{h}^v+N_o^{-1}\mathbf{h}^{vH}\{\sum_{m=0}^{M-1}\mathbf{B}(m)^i\mathbf{y}_c^v[m]\}\}}$$
$$\times\, e^{-\{\mathbf{h}^{vH}\{No^{-1}\sum_{m=0}^{M-1}\mathbf{B}(m)^i\left(\mathbf{R}[0]\mathbf{B}(m)^i+\mathbf{R}[-1]\mathbf{B}(m-1)^i+\mathbf{R}[1]\mathbf{B}(m+1)^i\right)+\boldsymbol{\Sigma}_{hh}^{-1}\}\mathbf{h}^v\}}. \quad \text{(B46)}$$

In (B45), we can notice that the pairs $(\mathbf{y}_w^v, \mathbf{h}^v|\mathbf{b}^i)$, $v = 1, \ldots, V$, are mutually independent. Therefore, we will subsequently focus on the individual joint distribution of each pair, $f(\mathbf{y}_w^v, \mathbf{h}^v|\mathbf{b}^i)$. The second and third exponential term in the right-hand side of (B46) can be reformed to take the form of the exponential term of the standard multivariate Gaussian distribution by multiplying (B46) with $\frac{e^{-\mathbf{m}_h^{v\,H}\boldsymbol{\Sigma}_h^{-1}\mathbf{m}_h^v}}{e^{-\mathbf{m}_h^{v\,H}\boldsymbol{\Sigma}_h^{-1}\mathbf{m}_h^v}}$, where

$$\boldsymbol{\Sigma}_h = \Bigg(N_o^{-1} \sum_{m=0}^{M-1} \mathbf{B}(m)^i \left(\mathbf{R}[0]\mathbf{B}(m)^i + \mathbf{R}[-1]\mathbf{B}(m-1)^i + \mathbf{R}[1]\mathbf{B}(m+1)^i \right) + \boldsymbol{\Sigma}_{hh}^{-1} \Bigg)^{-1}, \quad \text{(B47)}$$

$$\mathbf{m}_h^v = \Bigg(\sum_{m=0}^{M-1} \mathbf{B}(m)^i \left(\mathbf{R}[0]\mathbf{B}(m)^i + \mathbf{R}[-1]\mathbf{B}(m-1)^i + \mathbf{R}[1]\mathbf{B}(m+1)^i \right) + N_o \boldsymbol{\Sigma}_{hh}^{-1} \Bigg)^{-1} \times \sum_{m=0}^{M-1} \mathbf{B}(m)^i \mathbf{y}_c^v[m]. \quad \text{(B48)}$$

By integrating (B46) with respect to $\mathbf{h}^v$, we obtain,

$$P(\mathbf{y}_w^v|\mathbf{b}^i) = \frac{\det \boldsymbol{\Sigma}_h}{\pi^{2MLK} \left(\det \boldsymbol{\Sigma}_{wl}\right)^V \det \boldsymbol{\Sigma}_{hh}} e^{\frac{-1}{N_o}\{\sum_{m=0}^{M-1} \mathbf{y}_w^v[m]^H \mathbf{y}_w^v[m]\} + \mathbf{m}_h^{v\,H} \boldsymbol{\Sigma}_h^{-1} \mathbf{m}_h^v}. \quad \text{(B49)}$$

Finally, using (B46) and (B49), we can estimate the conditional distribution of $(\mathbf{h}^v|\mathbf{y}_w^v, \mathbf{b}^i)$ as

$$\begin{aligned} f(\mathbf{h}^v|\mathbf{y}_w^v, \mathbf{b}^i) &= \frac{f(\mathbf{h}^v, \mathbf{y}_w^v|\mathbf{b}^i)}{f(\mathbf{y}_w^v|\mathbf{b}^i)} \\ &= \frac{1}{\pi^{2LK} \det \boldsymbol{\Sigma}_h} e^{-(\mathbf{h}^v - \mathbf{m}_h^v)^H \boldsymbol{\Sigma}_h^{-1} (\mathbf{h}^v - \mathbf{m}_h^v)}, \end{aligned} \quad \text{(B50)}$$

which represents a Gaussian distribution with mean

$$E\left[\mathbf{h}^v|\mathbf{y}_w^v,\mathbf{b}^i\right]=\mathbf{m}_h^v=\Bigg(\sum_{m=0}^{M-1}\mathbf{B}(m)^i\left(\mathbf{R}[0]\mathbf{B}(m)^i+\mathbf{R}[-1]\mathbf{B}(m-1)^i+\mathbf{R}[1]\right.$$
$$\left.\times\mathbf{B}(m+1)^i\right)+N_o\boldsymbol{\Sigma}_{hh}^{-1}\Bigg)^{-1}\times\sum_{m=0}^{M-1}\mathbf{B}(m)^i\mathbf{y}_c^v[m],\quad\text{(B51)}$$

and covariance

$$E\left[(\mathbf{h}^v-(\mathbf{h}^v)^i)(\mathbf{h}^v-(\mathbf{h}^v)^i)^H|\mathbf{y}_w^v,\mathbf{b}^i\right]=\boldsymbol{\Sigma}_h=\Bigg(N_o^{-1}\sum_{m=0}^{M-1}\mathbf{B}(m)^i\left(\mathbf{R}[0]\mathbf{B}(m)^i\right.$$
$$\left.+\mathbf{R}[-1]\mathbf{B}(m-1)^i+\mathbf{R}[1]\mathbf{B}(m+1)^i\right)+\boldsymbol{\Sigma}_{hh}^{-1}\Bigg)^{-1}.\quad\text{(B52)}$$

B.4 Consistency of Channel Estimates

In this part, we show that the channel estimate $(\mathbf{h}^v)^i$ is consistent. First, we prove that the estimate $(\mathbf{h}^v)^i$ is asymptotically unbiased. In other words,

$$\lim_{M\to\infty}E\left[(\mathbf{h}^v)^i|\mathbf{h},\mathbf{b}^i\right]=\mathbf{h}^v.\quad\text{(B53)}$$

We start by the expectation of (5.20) given $\mathbf{h}^v$ and $\mathbf{b}^i$, we have

$$E\left[(\mathbf{h}^v)^i|\mathbf{h}^v,\mathbf{b}^i\right]=\Bigg(\sum_{m=0}^{M-1}\mathbf{B}(m)^i\left(\mathbf{R}[0]\mathbf{B}(m)^i+\mathbf{R}[-1]\mathbf{B}(m-1)^i+\mathbf{R}[1]\right.$$
$$\left.\times\mathbf{B}(m+1)^i\right)+N_o\boldsymbol{\Sigma}_{hh}^{-1}\Bigg)^{-1}\times\sum_{m=0}^{M-1}\mathbf{B}(m)^iE\left[\mathbf{y}_c^v[m]|\mathbf{h}^v,\mathbf{b}^i\right],\quad\text{(B54)}$$

Substituting (5.3) in (B54) and inserting the factor M^{-1}, we obtain

$$E\left[(\mathbf{h}^v)^i\,|\mathbf{h}^v,\mathbf{b}^i\right] = \Bigg(\sum_{m=0}^{M-1} M^{-1}\mathbf{B}(m)^i\left(\mathbf{R}[0]\mathbf{B}(m)^i + \mathbf{R}[-1]\mathbf{B}(m-1)^i + \mathbf{R}[1]\right.$$
$$\left.\times\mathbf{B}(m+1)^i\right) + M^{-1}N_o\Sigma_{hh}^{-1}\Bigg)^{-1} M^{-1}\sum_{m=0}^{M-1}\mathbf{B}(m)^i\left(\mathbf{R}[0]\mathbf{B}(m)^i + \mathbf{R}[-1]\mathbf{B}(m-1)^i\right.$$
$$\left.+\mathbf{R}[1]\mathbf{B}(m+1)^i\right)\mathbf{h}^v, \quad \text{(B55)}$$

Invoking the strong law of large numbers, $M^{-1}\sum_{m=0}^{M-1}\mathbf{B}(m)^i\mathbf{R}[m_p]\mathbf{B}(m+m_p)^i$, $m_p \in \{-1,0,1\}$, converges to $E[\mathbf{B}(m)^i\mathbf{R}[m_p]\mathbf{B}(m+m_p)^i]$, as $M \to \infty$. Since $E[\mathbf{B}(m)^i \times \mathbf{R}[m_p]\mathbf{B}(m+m_p)^i]$ is only defined in terms of the cross-correlation values in $\mathbf{R}[m_p]$, i.e. independent of M, (B53) is proven. Finally, we show that the error covariance matrix of the channel estimates Ω_{hh}^i, in (5.21), converges to $\mathbf{0}$ as $M \to \infty$, i.e.,

$$\lim_{M\to\infty}\Omega_{hh}^i = \mathbf{0}. \quad \text{(B56)}$$

Starting from (5.21), we have

$$M\Omega_{hh}^i = \Bigg(M^{-1}N_o\sum_{m=0}^{M-1}\mathbf{B}(m)^i\left(\mathbf{R}[0]\mathbf{B}(m)^i + \mathbf{R}[-1]\mathbf{B}(m-1)^i + \mathbf{R}[1]\mathbf{B}(m+1)^i\right)$$
$$+ M^{-1}\Sigma_{hh}^{-1}\Bigg)^{-1}. \quad \text{(B57)}$$

Employing the same argument as above, it is easy to show that $M\Omega_{hh}^i$ converges to a matrix with constant elements as $M \to \infty$. Consequently, Ω_{hh}^i converges to $\mathbf{0}$ with rate $\frac{1}{M}$, hence proving (B56).

Bibliography

[1] P. W. Wolniansky, G. J. Foschini, G. D. Golden, and R. A. Valenzuela, "V-BLAST: An architecture for realizing very high data rates over the rich-scattering wireless channel", in *Proc. International Symposium on signals, systems, and electronics (ISSSE-98)*, Sep. 1998.

[2] H Holma and A Toskala, *W-CDAM for UMTS-Radio access for third generation mobile communication*, John Wiley and Sons, 2001.

[3] D. Gesbert, M. Shafi, D. Shiu, P. J. Smith, and A. Naguib, "From theory to practice: An overview of MIMO space-time coded wireless systems", *IEEE J. Select. Areas Commun.*, vol. 21, no. 3, pp. 281–302, Apr. 2003.

[4] G. Raleigh and J. M Cioffi, "Spatio-temporal coding for wireless communication", *IEEE Trans. Commun.*, vol. 46, pp. 357–366, Mar. 1998.

[5] E.Telatar, "Capacity of multi-antenna Gaussian channels", *European Trans. on Telecomm.*, vol. 10, no. 6, pp. 585–595, 1999.

[6] B. A. Bjerke and J. G. Proakis, "Multiple transmit and receive antenna diversity techniques for wireless communications", in *IEEE Adaptive Sys. for Signal Processing, Commun. and Control symposium (AS-SPCC)*, 2000, pp. 70–75.

[7] G. J. Foschini and M. J. Gans, "Layered space-time architecture for wireless com-

munications in a fading environment when using multi-element antennas", *Bell Labs Tech J.*, vol. 1, no. 2, pp. 41–59, 1996.

[8] G. J. Foschini, G. D. Golden, R. A. Valenzuela, and P. W. Wolniansky, "Simplified processing for high spectral efficiency wireless communication employing multi-element arrays", *IEEE J. Select. Areas Commun.*, vol. 17, no. 11, pp. 1841–1852, Nov. 1999.

[9] V. Tarokh, N. Seshadri, and A. R. Calderbank, "Space-time codes for high data rate wireless communication: Performance criterion and code construction", *IEEE Trans. Inform. Theory*, vol. 44, pp. 744–765, Mar. 1998.

[10] V. Tarokh, H. Jafarkhani, and A. R. Calderbank, "Space-time block codes from orthogonal designs", *IEEE Trans. Inform. Theory*, vol. 45, pp. 1456–1467, July 1999.

[11] S. M. Alamouti, V. Tarokh, and P. Poon, "Trellis-coded modulation and transmit diversity: design criteria and performance evaluation", in *Proc. ICUCP*, 1998.

[12] S. M. Alamouti, "A simple transmit diversity technique for wireless communications", *IEEE J. Select. Areas Commun.*, vol. 16, no. 8, pp. 1451–1458, Oct. 1998.

[13] V. Tarokh, A. Naguib, N. Seshadri, and A. R. Calderbank, "Combined array processing and space-time coding", *IEEE Trans. Inform. Theory*, vol. 45, pp. 1121–1128, May 1999.

[14] X. Lin and R. S. Blum, "Improved space-time codes using serial concatenation", *IEEE Commun. Letters*, vol. 4, no. 7, pp. 221–223, July. 2000.

[15] M. J. Juntti and M. Latva-aho, "Multiuser receivers for CDMA systems in Rayleigh fading channels", *IEEE Trans. Veh. Technol.*, vol. 49, no. 3, pp. 885–899, May 2000.

[16] B. Hochwald, T. Marzetta, and C. Papadias, "A transmitter diversity scheme for wideband CDMA systems based on space-time spreading", *IEEE J. Select. Areas Commun.*, vol. 19, no. 1, pp. 1451–1458, Jan. 2001.

[17] "Physical Layer Standard for cdma2000 Spread Spectrum Systems Release C. 3gpp2", May 2002.

[18] S. Verdu, "Wireless bandwidth in the making", *IEEE Commun. Mag.*, vol. 38, no. 7, pp. 53–58, Jul. 2000.

[19] L. Chong and L. Milstein, "The effects of channel-estimation errors on a space-time spreading CDMA system with dual transmit and dual receive diversity", *IEEE Trans. Commun.*, vol. 52, no. 7, pp. 1145–1151, July 2004.

[20] S. Verdu, *Multiuser Detection*, Cambridge University Press, 1998.

[21] G. V. V. Sharma and A. Chockalingam, "Performance analysis of maximum-likelihood multiuser detection in space-time-coded CDMA with imperfect channel estimation", *IEEE Trans. Veh. Techn.*, vol. 55, no. 6, pp. 1824–1837, Nov. 2006.

[22] H. Shuangchi, J. K. Tugnait, and M. Xiaohong, "On superimposed training for MIMO channel estimation and symbol detection", *IEEE Trans. Signal Processing*, vol. 55, no. 6, pp. 3007–3021, June 2007.

[23] A. L. Swindlehurst and G. Leus, "Blind and semi-blind equalization for generalized space-time block codes", *IEEE Trans. Signal Processing*, vol. 50, no. 10, pp. 2489–2498, Oct. 2002.

[24] Y. Sung, L. Tong, and A. Swami, "Blind channel estimation for space-time coded WCDMA", *EURASIP J. on Wireless Comm. and Net.*, pp. 322–334, Dec. 2004.

[25] X. Gao, B. Jiang, X. You, Z. Pan, and Y. Xue, "Efficient channel estimation for

MIMO single-carrier block transmission with dual cyclic time slot structure", *IEEE Trans. Comm.*, vol. 55, pp. 2210–2223, Nov. 2007.

[26] E. de Carvalho and D. T. M. Slock, "Maximum-likelihood blind FIR multi-channel estimation with Gaussian prior for the symbols", in *Proc. IEEE Int. Conf. Acoust. Speech, Signal processing*, Apr. 1997, vol. 5, pp. 3593–3596.

[27] E. de Carvalho and D. T. M. Slock, "Cramér-rao bounds for semi blind, blind and training sequence based channel estimation", in *Proc. 1st IEEE Signal Processing Workshop Signal Processing Advances in Wireless Communication*, Apr. 1997, vol. 1, pp. 129–132.

[28] D. Gore, S. Sandhu, and J. Paulraj, "Blind channel identification and projection receiver determination for multicode and multirate situations in DS-CDMA systems", in *Proc. IEEE International Conference on Communications(ICC'02)*, April-May 2002, vol. 3, pp. 1949–1953.

[29] X. Meng, J. K. Tugnait, and S. He, "Iterative joint channel estimation and data detection using superimposed training: Algorithms and performance analysis", *IEEE Trans. Vehicular Technology*, vol. 56, pp. 1873–1880, Jul. 2007.

[30] Y. Huang and J. A. Ritcey, "Joint iterative channel estimation and decoding for bit-interleaved coded modualtion over correlated fading channels", *IEEE Trans. Wireless Comm.*, vol. 4, no. 5, pp. 2549–2558, Sep. 2005.

[31] D. K. Chun So and R. S. Cheng, "Iterative EM receiver for space-time coded systems in MIMO frequency-selective fading channels with channel gain and order estimation", *IEEE Trans. Wireless Comm.*, vol. 3, no. 6, pp. 1928–1935, Nov. 2004.

[32] T. K. Moon, "The expectation-maximization algorithm", *IEEE Signal Processing Mag.*, pp. 45–59, Nov. 1996.

[33] A. P. Dempster, N. M. Laird, and D. B. Rubin, "Maximum likelihood from incomplete data via EM algorithm", *J. Royal Statist Soc.*, vol. 39, pp. 1–38, Jan. 1977.

[34] C. N. Georghiades and J. C. Han, "Sequence estimation in the presence of random parameters via the EM algorithm", *IEEE Trans. Comm.*, vol. 45, pp. 300–308, Mar. 1997.

[35] M. J. Borran and M. Nasiri-Kenari, "An efficient detection technique for synchronous CDMA communication systems based on the expectation maximization algorithm", *IEEE Trans. Vehicular Technology*, vol. 49, pp. 1663–1668, Sep. 2000.

[36] M. Feder and E. Weinstein, "Parameter estimation of superimposed signals using the EM algorithm", *IEEE Trans. Acoustic, Speech and Signal Process.*, vol. 36, pp. 477–489, Apr. 1988.

[37] A. Kocian and B. H. Fleury, "EM-based joint data detection and channel estimation of DS-CDMA signals", *IEEE Trans. Comm.*, vol. 51, no. 10, pp. 1709–1720, Oct. 2003.

[38] C. Cozzo and B. Hughes, "Joint channel estimation and data detection in space-time communications", *IEEE Trans. Comm.*, vol. 51, no. 8, pp. 1266–1270, Aug. 2003.

[39] Ayman Assra, Walaa Hamouda, and Amr M. Youssef, "Space-time spreading and diversity in asynchronous CDMA systems over frequency-selective fading channels", in *IEEE International Symposium on Signal Process. and its Applications (ISSPA 2007)*, Feb. 2007, pp. 1–4.

[40] Ayman Assra, Walaa Hamouda, and Amr M. Youssef, "Performance of space-time diversity in CDMA over frequency-selective fading channels", in *Proc. IEEE Global Telecommunications Conference (GLOBECOM 2007)*, Nov. 2007, pp. 1514–1518.

[41] Ayman Assra, Walaa Hamouda, and Amr M. Youssef, "Joint decorrelating channel and data estimation for space-time spreading systems", in *Proc. IEEE Vehicular Technology Conference (VTC'2008)*, May 2008, pp. 1399–1403.

[42] Ayman Assra, Walaa Hamouda, and Amr M. Youssef, "BER analysis of space-time diversity in CDMA systems over frequency-selective fading channels", *IET Trans. Commun.*, vol. 3, no. 7, pp. 1216–1226, Jul. 2009.

[43] Ayman Assra, Walaa Hamouda, and Amr M. Youssef, "Performance of superimposed training-based channel estimation in MIMO-CDMA systems", in *Proc. IEEE Global Telecommun. Conf. (GLOBECOM 2009)*, Dec. 2009.

[44] Ayman Assra, Walaa Hamouda, and Amr M. Youssef, "A channel estimation and data detection scheme for multiuser MIMO-CDMA systems in fading channels", *IEEE Trans. Vehicular Technology*, Accepted.

[45] Ayman Assra, Walaa Hamouda, and Amr M. Youssef, "EM-based joint channel estimation and data detection for MIMO-CDMA systems", *IEEE Trans. Vehicular Technology*, vol. 56, no. 3, pp. 1205–1216, Mar. 2010.

[46] Ayman Assra, Walaa Hamouda, and Amr M. Youssef, "Joint channel estimation and data detection using the EM algorithm for MIMO-CDMA systems over frequency-selective fading channels", Submitted.

[47] R. Doostnejad, T. Lim, and E. Sousa, "Space-time spreading codes for a multiuser MIMO system", in *Proc. Asilomar Conf. Signals, Syst.,Comput.*, Nov. 2002, pp. 1374–1378.

[48] L.-L. Yang, "MIMO-assisted space-code-division multiple-access: Linear detectors and performance over multipath fading channels", *IEEE J. Select. Areas Commun.*, vol. 24, no. 1, pp. 121–131, Jan. 2006.

[49] W. Hamouda and M. Aljerjawi, "A transmit diversity scheme using space-time spreading for DS-CDMA systems in fast fading channels", in *Proc. IEEE Vehicular Technology Conference*, Sep. 2005.

[50] M. Aljerjawi and W. Hamouda, "Performance of space-time spreading in multiuser DS-CDMA systems over fast fading channels", in *Proc. IEEE Global Telecommunications Conference*, Nov./Dec. 2005, vol. 3, pp. 1525–1529.

[51] M. Aljerjawi and W. Hamouda, "Performance analysis of space-time diversity in multiuser CDMA systems over rayleigh fading channels", in *Proc. IEEE International Conference on Communications(ICC 2006)*, June 2006.

[52] B. Vucetic and J. Yuan, *Space-Time Coding*, John Wiley and Sons, 2003.

[53] J. G. Proakis, *Digital Communications 4th Ed.*, McGraw Hill, 2001.

[54] T. S. Rappaport, *Wireless Communications: Principles and Practice 2nd Ed.*, Prentice Hall, 2002.

[55] Y. Gong and K. B. Letaief, "Performance evaluation and analysis of space-time coding in unequalized multipath fading links", *IEEE Trans. Commun.*, vol. 48, no. 11, pp. 1778–1782, Nov. 2000.

[56] T. S. Rappaport, *Wireless Communications: Principles and Practice*, Upper Saddle River, NJ: Prentice-Hall, 1996.

[57] S. Haykin, *Array Signal Processing*, Englewood Cliffs, NJ:Prentice-Hall, 1984.

[58] L. E. Baum, T. Petrie, G. Soules, , and N. Weiss., "A maximization technique occurring in the statistical analysis of probabilistic functions in Markov chains", *Ann. Math. Stat.*, vol. 41, pp. 164–171, 1970.

[59] N. Seshadri, "Joint data and channel estimation using fast blind trellis search techniques", in *Proc. IEEE Global Telecommunications Conference (GLOBECOM'90)*, Dec. 1990, pp. 1659–1663.

[60] L. Tong and S. Perreau, "Multichannel blind channel estimation: From subspace to maximum likelihood methods", *Proc. IEEE*, vol. 86, pp. 1951–1968, Oct. 1998.

[61] C. F. J. Wu, "On the convergence properties of the EM algorithm", *Ann. Math. Stat.*, vol. 11, pp. 95–103, 1983.

[62] S.-H. Wu, U. Mitra, and C.-C. J. Kuo, "Iterative joint channel estimation and multiuser detection for DS-CDMA in frequency-selective fading channels", *IEEE Trans. Signal Process.*, vol. 56, no. 7, pp. 3261–3277, Jul. 2008.

[63] E. Bjornson and B. Ottersten, "A framework for training-based estimation in arbitrarily correlated Rician MIMO channels with Rician disturbance", *IEEE Trans. Signal Processing*, vol. 58, no. 3, pp. 1807–1820, Mar. 2010.

[64] X. Dai, H. Zhang, and D. Li, "Linearly time-varying channel estimation for MIMO/OFDM systems using superimposed training", *IEEE Trans. Comm.*, vol. 58, no. 2, pp. 681–695, Feb. 2010.

[65] A. Soysal and S. Ulukus, "Joint channel estimation and resource allocation for MIMO systems part II: Multi-user and numerical analysis", *IEEE Trans. Wireless Comm.*, vol. 9, no. 2, pp. 632–640, Feb. 2010.

[66] J. K. Tugnait and S. He, "Multiuser/MIMO doubly selective fading channel estimation using superimposed training and slepian sequences", *IEEE Trans. Vehicular Technology*, vol. 59, no. 3, pp. 1341–1354, Mar. 2010.

[67] J. Ylioinas and M. Juntti, "Iterative joint detection, decoding, and channel estimation

in turbo-coded MIMO-OFDM", *IEEE Trans. Vehicular Technology*, vol. 58, no. 4, pp. 1784–1796, May 2009.

[68] T.-H. Pham, Y.-C. Liang, and A. Nallanathan, "A joint channel estimation and data detection receiver for multiuser MIMO IFDMA systems", *IEEE Trans. Comm.*, vol. 57, no. 6, pp. 1857–1865, Jun. 2009.

[69] T. Routtenberg and J. Tabrikian, "Blind MIMO-AR system identification and source separation with finite-alphabet", *IEEE Trans. Signal Processing*, vol. 58, no. 3, pp. 990–1000, Mar. 2010.

[70] X. Wautelet, C. Herzet, A. Dejonghe, J. Louveaux, and L. Vandendorpe, "Comparison of EM-based algorithms for MIMO channel estimation", *IEEE Trans. Commun.*, vol. 55, no. 1, pp. 216–226, Jan. 2007.

[71] J. Choi, "An EM based joint data detection and channel estimation incorporating with initial channel estimate", *IEEE Commun. Letters.*, vol. 12, no. 9, pp. 654–656, Sep. 2008.

[72] J. Zhang and J. S. Lehnert, "Space-time coded asynchronous DS-CDMA with decentralized mai suppression: Performance and spectral efficiency", *IEEE Trans. Wireless Comm.*, vol. 7, no. 5, pp. 1550–1559, May 2008.

[73] R. Lupas and S. Verdu, "Near-far resistance of multiuser detectors in asynchronous channels", *IEEE Trans. Commun.*, vol. 38, no. 4, pp. 496–508, April 1990.

[74] H. V. Poor and S. Verdú, "Probability of error in MMSE multiuser detection", *IEEE Trans. on Info. Theory*, vol. 53, no. 3, pp. 858–871, May 1997.

[75] A. Papoulis and S.U. Pillai, *Probability, Random Variables and Stochastic Processes*, McGraw Hill, 2002.

[76] Odoardo Brugia, "A noniterative method for the partial fraction expansion of a rational function with high order poles", *Society for Industrial and Applied Mathematics (SIAM)*, vol. 7, no. 3, pp. 381–387, Jul. 1965.

[77] M. Abramowitz and I. A. Stegun, *Handbook of Mathematical Functions with Formulas, Graphs and Mathematical Tables*, New York:Dover, 1964.

[78] M. K. Simon and M. Alouini, "A unified approach to the performance analysis of digital communication over generalized fading channels", *Proc. of the IEEE*, vol. 86, pp. 1860–1877, Sep. 1998.

[79] I. S. Gradshteyn and I. M. Ryzhik, *Table of Integrals, Series and Products*, New York:Academic, 1995.

[80] Y.-P. Cheng, K.-Y. Zhang, and Z. Xu, *Matrix Theory*, China: Northwesten Polytechnical Univ. Press, 2002.

[81] G. Golub and A. V. Loan, *Matrix Computations*, John Hopkins U. Press, 1996.

[82] R. A. Soni and R. M. Buehre, "On the performance of open-loop transmit diversity techniques for IS-2000 systems: comparative study", *IEEE Trans. Wireless Comm.*, vol. 3, pp. 1602–1615, Sept. 2004.

[83] G. L. Turin, "The characteristic function of Hermitian quadratic forms in complex normal variables", *Biometrika*, vol. 47, pp. 199–201, Jun. 1960.

[84] M. J. Barrett, "Error probability for optimal and suboptimal quadratic receivers in rapid Rayleigh fading channels", *IEEE J. Select. Areas Commun.*, vol. 5, pp. 302–304, Feb. 1987.

[85] D. G. Zill and M. R. Cullen, *Advanced Engineering Mathematics*, Sudbury, MA: Jones and Bartlett Publishers, 2006.

[86] L. L. Chong and L. B. Milstein, "Convolutionally coded multicarrier DS-CDMA with imperfect channel estimation", in *Proc. 39th Allerton Conf. Communications, Control, Computing*, Oct. 2001, pp. 543–552.

[87] A. Russ and M. K. Varanasi, "Noncoherent multiuser detection for nonlinear modulation over the Rayleigh fading channel", *IEEE Trans. Inform. Theory*, vol. 47, pp. 295–307, Jan. 2001.

[88] M. Brehler and M. K. Varanasi, "Asymptotic error probability analysis of quadratic receivers in Rayleigh-fading channels with applications to a unified analysis of coherent and noncoherent space-time receivers", *IEEE Trans. Inform. Theory*, vol. 47, no. 6, pp. 2383–2399, Sep. 2001.

[89] A. Kocian, I. Land, and B. H. Fleury, "Joint channel estimation, partial successive interference cancellation, and data decoding for DS-CDMA based on the SAGE algorithm", *IEEE trans. Commun.*, vol. 55, no. 6, pp. 1231–1241, Jun. 2007.

[90] A. Kocian and B. H. Fleury, "EM-based joint data detection and channel estimation in asynchronous multi-rate DS/CDMA", in *Proc. IEEE Global Telecomm. Conf.*, Dec. 2003, vol. 5, pp. 2458–2462.

[91] A. Kocian, I. Land, and B. H. Fleury, "Optimal weighting of soft-information in a SAGE-based iterative receiver for coded CDMA", in *Proc. IEEE Global Telecomm. Conf.*, Nov./Dec. 2005, vol. 3, pp. 1555–1559.

[92] D. Divsalar, M. K. Simon, and D. Raphaeli, "Improved parallel interference cancellation for CDMA", *IEEE Trans. on Comm.*, vol. 46, no. 2, pp. 258–268, Feb. 1998.

[93] A. Klein, G. K. Kaleh, and P. W. Baier, "Zero forcing and minimum mean-square error equalization of multiuser detection in code-division multiple-access channels", *IEEE Trans. Vehicular Technology*, vol. 45, pp. 276–287, May 1996.

[94] H. V. Poor, *An Introduction to Signal Detection and Estimation*, New York: Springer, 1994.

[95] M. T. Ivriac, W. Utschick, and I A. Nossek, "Fading correlation in wireless MIMO communication systems", *IEEE J. Select. Areas Commun.*, vol. 21, no. 5, pp. 819–828, Jun. 2003.